1993

The Interaction of Sickle Hemoglobin with Phosphatidylserine Vesicles ; Fourier Transform Infrared Spectroscopic Studies of Human Erythrocyte Spectrin

Cynthia C. LaBrake
Loyola University Chicago

PART I

THE INTERACTION OF SICKLE HEMOGLOBIN WITH PHOSPHATIDYLSERINE VESICLES

PART II

FOURIER TRANSFORM INFRARED SPECTROSCOPIC STUDIES OF HUMAN ERYTHROCYTE SPECTRIN

by

Cynthia C. LaBrake

A Dissertation Submitted to The Faculty of the Graduate School of Loyola University of Chicago in Partial Fulfillment of the Requirements for the Degree of Doctor of Philosophy

January 1993

ACKNOWLEDGEMENT

I would like to acknowledge my advisor, Professor Leslie W.-M. Fung, for her guidance and perseverance in my graduate education. Dr. Fung has served a role as an advisor, a mentor and a friend. Her enthusiasm for research and her consistency in pursuing goals have, by example, helped to mold me as a scientist.

In addition, I would like to thank those persons with whom we have collaborated, especially Dr. A. Steve Benight and Donna Budzynski from University of Illinois, Chicago for the dynamic light scattering work, and Dr. Timothy Keiderling and Lijang Wang from University of Illinois, Chicago and Dr. Rina Dukor from Amoco Technology for the Fourier transform infrared work.

I would also like to thank the many people who have worked in the lab from whom I have learned and shared time and space with.

For financial assistance, I would like to express my gratitude to Loyola University of Chicago, The National Institutes of Health, The American Heart Association of Metropolitan Chicago and The Schmidt Foundation.

Special thanks to my parents and parents-in-law for their support, both moral and financial, throughout my graduate career. Thanks to my husband for his never ending support of my research and for his helpful and attentive discussions of my work.

Finally, a very special thank you to my son to whom this thesis is dedicated, for adding a new dimension and bringing countless joy to my life by just being himself.

TABLE OF CONTENTS

LIST OF TABLES

PART I

PART II

LIST OF FIGURES

PART I

PART II

LIST OF ABBREVIATIONS

0.3P7.6	0.3 mM sodium phosphate, pH 7.6
5P7.4	5 mM sodium phosphate, pH 7.4
5P8	5mM sodium phosphate, pH 8.0
A_{700}	absorbance at 700 nm
BHT	butylated hydroxytoluene
BPS	bovine brain phosphatidylserine
CD	circular dichroism
COHb	carbon-monoxy hemoglobin
EDTA	ethylenediaminetetraacetic acid
FSD	Fourier self deconvolution
FTIR	Fourier transform infrared
FWHH	full width at half height
Hb	hemoglobin molecule
HbS	sickle hemoglobin
HbA	normal adult hemoglobin
K_{av}	partition coefficient
LUVs	large unilamellar vesicles
metHbS	oxidized sickle hemoglobin
NMR	nuclear magnetic resonance
oxyHbS	oxygenated sickle hemoglobin
oxyHbA	oxygenated normal hemoglobin

P7.2	100 mM sodium phosphate, pH 7.2
PBS7.4	5 mM sodium phosphate, 150 mM NaCl, pH 7.4
PBS8	5 mM sodium phosphate, 150 mM NaCl, pH 8.0
PEN7.4	23 mM sodium phosphate, 127 mM sodium chloride, 2 mM EDTA, pH 7.4
PLS	partial least squares
R_s	Stokes radius
SDS	sodium dodecylsulfate
SUBH2O	array basic program used to do background subtraction from spectrin absorbance spectrum
SUVs	small unilamellar vesicles
TE8.3	50 mM Tris, 0.1 mM EDTA, pH 8.3
V_e^x	elution volume of protein x
V_o	void volume
V_t	total volume of column

PART I

CHAPTER I

INTRODUCTION

Sickle cell anemia is a molecular disease with a mutation producing an amino acid substitution at the $\beta 6$ positions of the hemoglobin molecule (Hb) (Schechter *et al.*, 1987). Sickle hemoglobin (HbS) molecule exhibits 10 times higher mechanical instability than normal hemoglobin (HbA) (Asakura *et al.*, 1974). HbS is denatured faster and differently at the air-water interface than HbA (Elbaum *et al.*, 1976). It has also been found that sickle red blood cells spontaneously generate approximately twice the normal amounts of superoxide, peroxide and hydroxyl radical (Hebbel *et al.*, 1982). Spontaneous hydroxyl radical generation correlates significantly with the amount of membrane-bound hemichrome, suggesting that hemichrome iron might be directly responsible for hydroxyl radical generation through a Haber-Weiss mechanism, and radicals generated in the membrane would be relatively sequestered from the cell's antioxidant mechanism which are largely cytoplasmic (Hebbel and Miller, 1984). Excess heme was found in sickle erythrocyte inside-out membranes (Kuross *et al*, 1988). The amount of hemin is higher in sickle cell membranes than in normal membranes (Shaklai *et al.*, 1985). The hemin content in the hemolysate of fresh red cells from patients with sickle cell disease is increased three- to five-fold as compared with normal individuals (Liu *et al.*, 1988). Recently several articles reported the studies of the effects of heme on red cell membrane properties (Vincent, 1989; Chiu & Lubin, 1989 and Hebbel & Eaton, 1989). It has been shown that the stability of the heme in Hb follows the order (less stable to more stable): oxidized sickle hemoglobin (with the heme iron in the +3 oxidation state) (metHbS), oxygenated sickle hemoglobin (oxyHbS) and oxygenated normal hemoglobin (oxyHbA), with rate constants of

the heme transfer from these species being 0.923 h^{-1}, 0.023 h^{-1} and 0.014 h^{-1}, respectively (Hebbel *et al.*, 1988). Thus work done in the last few years has clearly demonstrated that excessive oxidation and denaturation of sickle hemoglobin resulting in a larger amount of radicals in sickle red blood cells, lead to membrane oxidation and subsequently to serious damage to the functions of cell membranes in sickle cells. It has been suggested that HbS autoxidation might underlie the development of defective membrane properties in sickle cells.

In a brief report, the autoxidation of HbS was shown to be accelerated when compared to HbA (Hebbel *et al.*, 1988). It is not clear whether the accelerated HbS oxidation or the increased instability in HbS plays the significant role in cell oxidation. Therefore, systematic studies of Hb stability, Hb autoxidation and Hb oxidation in the presence of membrane components using controlled conditions are warranted. Due to experimental difficulties, little work had been done on Hb oxidation in the presence of membrane phospholipids. In fact, we developed a method to monitor Hb oxidation in the presence of lipid vesicles (LaBrake & Fung, 1992; Appendix I). In this dissertation, we present the quantitative effect of bovine brain phosphatidylserine (BPS), in the form of small and large unilamellar vesicles (SUVs and LUVs, respectively), on the oxidation of oxyHbS and interactions between Hb and lipid vesicles.

We have found that the oxidation of oxyHbS is enhanced by one order of magnitude in the presence of LUVs and by two orders of magnitude in the presence of SUVs, and the enhanced oxidation is slightly greater for HbS than for HbA.

We also found that vesicle fusion occurred in vesicle-Hb samples incubated at 37 °C, which was in good agreement with the literature (Szebeni, *et al.*, 1988). Our results show that the fusion is about 2 times greater in the presence of HbS than HbA, for both SUVs and LUVs. We have used this Hb-induced vesicle fusion to investigate the mechanism of the interaction of HbS with BPS SUVs and LUVs, and this mechanism is compared with that of HbA. The interaction of Hb with phospholipid surface leads to Hb oxidation. We believe that

these studies are important in furthering the understanding of the pathophysiology of sickle cell disease.

CHAPTER II

MATERIALS AND METHODS

2.1 Materials

Unless stated otherwise, all experimental steps were carried out at 4 °C, and all chemicals were reagent grade from Fisher (Pittsburgh, PA), Sigma (St. Louis, MO) or Aldrich (Milwaukee, WI). HPLC-grade water was used for all buffers. All glassware was acid-washed. Fresh, packed, normal red blood cells (RBCs) were obtained from a local blood bank. Sickle RBCs were obtained from Mt. Sinai Hospital, Chicago, IL and George Washington Hospital, Washington, DC.

2.2 Hemolysate Preparation

Hemolysate from the sickle RBCs was prepared in tandem with normal hemolysate as follows. The RBCs were used within one week of withdrawal and washed with 5 mM sodium phosphate containing 150 mM NaCl, saturated with carbon monoxide (CO), at pH 7.4. The cells were lysed with 2 volumes of deionized water, followed by ammonium sulphate precipitation and desalting with a P6DG column (BioRad, Richmond, CA), equilibrated with 5 mM Tris buffer containing 150 mM NaCl at pH 7.5 to remove ammonium sulphate and other small molecules, including 2,3-bisphosphoglycerate, which affects hemoglobin autoxidation (Mansouri & Winterhalter, 1974; Kikugawa *et al.*, 1981), to give stripped hemolysate. The hemolysate solution was dialyzed against 23 mM sodium phosphate buffer with 2 mM EDTA and 127 mM NaCl at pH 7.4 (PEN7.4), saturated with CO. If not used

immediately, the hemolysate was frozen drop-wise in liquid N_2 and stored at - 80 °C. After thawing, the hemolysate was centrifuged at 38,000 g for 10 min before use.

2.3 Hemoglobin Preparation

HbS was isolated from the stripped hemolysate solution, in tandem with HbA, according to a modified column chromatography procedure (Kawanishi and Caughey, 1985; Watkins *et al.*, 1985; Winterbourn, 1985a). The stripped hemolysates were dialyzed in 50 mM Tris buffer with 0.1 mM EDTA at pH 8.3 (TE8.3), followed by CO gassing. A DEAE-Sephadex A-50 (Pharmacia, Piscataway, NJ) column was used with a linear pH gradient made from buffer TE8.3 and a similar buffer at pH 7.0. The HbS fractions eluted at pH 7.90 and the HbA eluted at pH 7.75. The HbS and HbA fractions were pooled, concentrated, dialyzed against PEN7.4, and CO gassed to give carbon-monoxy Hb (COHb). This procedure removed all minor hemoglobin components, catalase, superoxide dismutase, "adventitious" metals, and other red cell proteins to give "ultra-pure" Hb (Watkins *et al.*, 1985; Winterbourn, 1985a). If not used immediately, the Hb was frozen drop-wise in liquid N_2 and stored at -80 °C.

2.4 Hb Concentration

The total Hb concentrations in the hemolysate and Hb solutions were determined by the cyano-met method (Riggs, 1981). In addition, at the beginning of each oxidation experiment, the concentration of the oxygenated Hb (oxyHb) solution was determined at 577 nm, using an extinction coefficient of 15.0 mM^{-1} cm^{-1} (Winterbourn, 1985a). No detectable absorbance at 630 nm, and thus no metHb, was observed. The concentrations of oxyHb generally agreed to within 5 % with the values determined by the cyano-met method.

2.5 Lipid Vesicles

Bovine brain phosphatidylserine (BPS) was purchased from Avanti Polar Lipids

(Alabaster, AL) and was used without further purification after verification of purity by thin-layer chromatography. Chloroform in lipid was driven off using N_2 gas followed by pumping under vacuum to remove residual quantities. If necessary, the lipid films were stored, but no longer than 48 h, at -20 °C under a N_2 atmosphere. PEN7.4 buffer solution was saturated with N_2 gas, and added to the lipid film. The solution was hand-swirled in the presence of glass beads to give multilamellar vesicles. For samples containing butylated hydroxytoluene (BHT), 0.5 to 1.5 mM BHT was added to the original lipid-chloroform solution.

2.6 Small Unilamellar Vesicles

Small unilamellar vesicles (SUVs) were prepared from the multilamellar vesicles by slightly modified procedures of Itabe and coworkers (1988). Multilamellar vesicles, with about 13 - 15 mg of BPS in 5 ml PEN7.4, were sonicated using a probe tip sonicator (Heat Systems-Ultrasonics Model W-10), to clearness under N_2 at room temperature for about 20 min, and centrifuged at 38,000 g and 20 °C to remove any large multilamellar vesicles and titanium from the sonicator probe. Sonication conditions were precisely controlled to obtain consistent SUV samples. Otherwise, irreproducible, but generally much faster, oxidation was observed. The SUV samples were used immediately for oxidation studies. Lipid concentrations in these samples were about 2.5 mg/ml, the maximum concentration used for oxidation experiments. At lipid concentrations higher than 2.5 mg/ml, samples remained cloudy after sonication. For studies involving different lipid concentrations, the vesicle samples were prepared either by using different starting lipid concentrations, or by diluting a stock SUV solution at about 2.5 mg/ml with buffer to obtain samples of different lipid concentrations. Freeze fracture electron micrographs of these SUVs showed typical SUVs with vesicle diameters ranging from 10 - 30 nm (LaBrake and Fung, 1992). Some larger vesicles were also seen.

2.7 Large Unilamellar Vesicles

Large unilamellar vesicles (LUVs) were prepared from the multilamellar vesicle solutions (13 mg to 60 mg lipid per 5 ml buffer) by extrusion methods with a lipid extruder (Lipex) (Loughrey *et al.*, 1990) at room temperature. Polycarbonate filters (Nuclepore, Pleasanton, CA) with 50 or 100 nm pore sizes were used. Freeze fracture electron micrographs showed the expected BPS LUVs in solution with vesicle diameters of about 100 nm (LaBrake and Fung, 1992) indicating that these vesicles are much larger than SUVs.

2.8 Lipid Concentration

Lipid concentrations of the vesicle samples were determined by the method of Stewart (1980), following extraction from the aqueous phase (Bligh and Dyer, 1959). An extinction coefficient of 1.99 $mg^{-1}\ cm^{-1}$ for BPS was obtained experimentally, in good agreement with the published value (Stewart, 1980).

2.9 Optical Measurements of Hb and Vesicle Mixtures

COHb was converted to oxyHb on ice under a flood light and O_2 atmosphere immediately before the experiment. Optical spectra were monitored from 500 to 700 nm to insure complete conversion, and to insure that there was no detectable metHb in the samples. Samples with detectable metHb were discarded. The concentration of Hb was adjusted to 17.5 ± 0.3 μM (1.12 ± 0.02 mg/ml). This cold oxyHb solution (120 μl) was introduced to a pre-warmed (37 ± 0.5 °C for about 5 min) solution of lipid vesicles (500 μl) of known concentration in the range from 0.4 to 2.5 mg/ml, to give a final Hb concentration of 0.22 ± 0.02 mg/ml (3.4 ± 0.3 μM). A vesicle solution with the same lipid concentration was used as a blank. The sample cuvettes were covered with parafilm, and maintained at 37 ± 0.5 °C. Spectra were collected from 500 to 700 nm every 2 min for 30 min. In experiments without lipid vesicles, buffer was used as a blank, and spectra were collected every 10 min for the first hour, and then periodically for 24 - 130 hours, if necessary. In some experiments, COHb or

oxygenated hemolysate was used instead of oxyHb.

2.10 Lipid to Hemoglobin Molar Ratios

The lipid to hemoglobin molar ratio's (Lipid/Hb) were calculated using a molecular weight of 64,000 for Hb and 800 for BPS. The ratios ranged from 200 to 1000 for the SUV experiments and 200 to 6000 for the LUV experiments.

2.11 Concentrations of Hb Species during Oxidation

In oxidized samples, oxyHb is oxidized to metHb, hemichrome, and choleglobin, following the definitions of Winterbourn (1985b). Thus the absorbance values at different wavelengths can be analyzed as a four-component (oxyHb, metHb, hemichrome and choleglobin) system at 560, 577, 630 and 700 nm, to determine the concentrations of each Hb species in oxidized samples (Winterbourn, 1985a). The concentration of a component was set to zero if the analysis gave a negative value. The relative concentrations (percentages) for each component were then determined.

2.12 Rate Constant Determination

Rate constants for the disappearance of oxyHb or the appearance of oxidized Hb were obtained from linear regressions (Systat Software, Systat Inc., Evanston, IL) of the linear portions of the logarithmic plots of percent Hb versus time.

2.13 Vesicle Fusion Assay

Purified Hb was mixed with SUVs or LUVs in the same lipid-to-Hb molar ratios used for the oxidation experiments (ranging from 500 - 1000). The samples were allowed to incubate at 37 °C for up to 20 hours. The absorbance at 700 nm (A_{700}) was measured periodically. An increase in A_{700} is used as an index to measure vesicle fusion. At the Hb

concentrations used for this study the maximum absorbance of oxidized Hb at 700 nm is 0.01 (LaBrake and Fung, 1992). Therefore, the absorbance above 0.01 is attributed to vesicle fusion.

For fusion studies under O_2 conditions, the initial state of the Hb is oxyHb. However, through the course of incubation the oxyHb was oxidized to metHb, hemichrome and choleglobin. Therefore, the Hb in the sample is actually a mixture of oxyHb and its oxidation products.

For fusion studies under CO conditions, special care as described below, had to be taken to maintain the CO-Hb ligation. The HbCO samples were added to vesicle dispersions in buffer which had been presaturated with CO gas. The mixture was incubated at 37 °C under an atmosphere of CO gas in test tubes which were sealed with a rubber septum. Each time the test tubes were opened to remove a sample for a reading, the atmosphere was re-equilibrated with CO gas. In this way, the Hb was maintained in the CO state. However, if the atmosphere was not kept under CO conditions and the vesicle dispersion was not purged with CO gas, the HbCO would oxidize to MetHb and hemichrome, thus complicating the experimental condition. The extent of CO saturation was monitored by the visible spectrum of Hb from 700 - 500 nm.

2.14 Analysis of Fusion Data

The amount of fusion in a given sample was analyzed by plotting the A_{700} versus time. Using the Systat linear regression program, it was found that the initial portion of the data (up to 3 hours) was a straight line. The slope of the line was determined and used as a measurement of the vesicle fusion per unit time.

CHAPTER III

RESULTS

3.1 Autoxidation of HbS

The autoxidation of HbS was studied using HbA as a control. The pseudo first order rate constants of Hb autoxidation were obtained from a fit of the linear portion of the semilogarithmic plot of % oxyHb versus time. The rate constants of the autoxidation in buffers with either 23 mM $NaP0_4$, 127 mM NaCl, 2 mM EDTA, at pH 7.4 (PEN7.4) or 100 mM $NaPO_4$, at pH 7.2 (P7.2) were obtained at 37 °C. In PEN7.4 HbS exhibits an average autoxidation of $0.030 \pm 0.004\ h^{-1}$ (n = 4), compared to $0.025 \pm 0.003\ h^{-1}$ for HbA. The ratio of the paired rate constants of HbS and HbA was 1.2 ± 0.1 (n = 4). Thus HbS autoxidizes about 1.2 times faster than HbA in PEN7.4. A paired Students t-test of the data indicates that the difference is statistically significant with $0.025 < P < 0.01$.

Our rate constants in P7.2, a buffer similar to that used in the literature (Hebbel *et al.*, 1988) were $0.053 \pm 0.019\ h^{-1}$ (n = 4) for HbA and $0.046 \pm 0.012\ h^{-1}$ for HbS. Our standard deviations of the rate constants in the absence of EDTA were much greater than the standard deviations for those rate constants obtained in the presence of EDTA. Due to the large fluctuations in the rate constants, we consider the data obtained in P7.2 to be not as reliable as those in PEN7.4. Therefore, the remainder of the oxidation experiments in the presence of vesicles were carried out in solution which contained EDTA.

3.2 Quantitation of Oxidized Hb Species in the Presence of Vesicles

The amounts of the four Hb species, oxyHb, metHb, hemichrome and choleglobin were determined as a function of time for HbS in the presence of SUVs and LUVs at a lipid/Hb ratio of about 800, using HbA as a control. Initial pseudo first order rate constants for the formation of these four species were calculated for the HbS-SUV samples as 3.98 ± 0.42 (n = 4), 1.55 ± 0.13, 1.10 ± 0.38 and 0.39 ± 0.16, respectively. The ratios of the rate constants for HbS samples to those for the paired HbA samples were 1.2 ± 0.1, 1.1 ± 0.1, 1.0 ± 0.4 and 1.4 ± 1.2, respectively (Table 1).

The average pseudo first order rate constants for the four species were also calculated for HbS-LUV samples and were 0.38 ± 0.08 (n = 7), 0.15 ± 0.02, 0.07 ± 0.03 and 0.03 ± 0.02, respectively. The ratios of the rate constants for HbS samples to those for the paired HbA samples were 1.4 ± 0.3, 1.4 ± 0.3, 1.4 ± 0.6 and 0.6 ± 0.3, respectively (Table 1).

The rate constants were further analyzed using the paired Students t-test, to determine the significance of the differences of the rate constants for each component. The results are reported in Table 1 under the corresponding ratios, showing the significance of the difference between HbS and HbA. Only paired experiments in which the Lipid/Hb ratios were closely matched were used for the paired Students t-test and for the rate constant ratio calculation. The HbS data are considered significantly different from the HbA data if the confidence level is equal to or greater than 95 % ($P < 0.05$). The 1.4 and 1.2 fold differences between HbS and HbA in LUVs and SUVs, respectively, for the disappearance of oxyHb are both considered statistically significant. However, the difference in formation of metHb and hemichrome are only considered significant in the case of LUVs. The other rate constants for the formation of metHb, hemichrome and choleglobin in the presence of SUVs and the formation of choleglobin in the presence of LUVs are not considered significantly different as determined by the paired Students t-test and the ratios are presented in parenthesis (Table 1).

Table 1 Rate Constant Ratios [k(HbS)/k(HbA)][a] for the Oxidation of Hb in the Presence of BPS SUVs and LUVs

	oxyHb	metHb	hemichrome	choleglobin
Hb + LUVs	1.4 ± 0.3	1.4 ± 0.2	1.4 ± 0.5	(0.6 ± 0.3)[b]
	.01<P<.025	.0001<P<.0005	.025<P<.05	.5<P
Hb + SUVs	1.2 ± 0.1	(1.1 ± 0.1)[b]	(1.0 ± 0.4)[b]	(1.4 ± 1.2)[b]
	.01<P<.025	.05<P<.1	.5<P	.5<P

a Rate constants were determined for Hb-vesicle systems with a lipid/Hb of ~ 800, in PEN7.4 at 37 °C.

b The rate constant ratio does not reflect a significant difference in rate constants of HbS and HbA since $P > 0.05$.

3.3 Lipid Concentration Effect on the Oxidation of HbS

Figure 1 is a plot of the rate constants of HbS and HbA in the presence of BPS SUVs and LUVs versus Lipid/Hb. A linear regression fit of the data reveals a slight difference between the oxidation behavior of the sickle and normal Hbs in the presence of both SUVs and LUVs. The dependency of oxyHb oxidation on Lipid/Hb ratio for Hb in the presence of SUVs can be quantitated as follows:

$$k_o^{SUV}\ (HbS) = 4.4 \times 10^{-3} \times \text{Lipid/Hb} + k_o^{auto}$$

$$k_o^{SUV}\ (HbA) = 3.7 \times 10^{-3} \times \text{Lipid/Hb} + k_o^{auto}$$

Where k_o^{SUV} (HbS), k_o^{SUV} (HbA), and k_o^{auto} are the initial rate constants for HbS in the presence of SUVs, HbA in the presence of SUVs and autoxidation, respectively. The ratio of the slopes of HbS and HbA data is 1.2. A similar relationship can be written for the oxyHb oxidation in the presence of LUVs:

$$k_o^{LUV}\ (HbS) = 0.21 \times 10^{-3} \times \text{Lipid/Hb} + k_o^{auto}$$

$$k_o^{LUV}\ (HbA) = 0.18 \times 10^{-3} \times \text{Lipid/Hb} + k_o^{auto}$$

Where k_o^{LUV} (HbS) and k_o^{LUV} (HbA) are the initial rate constants in the presence of LUVs for HbS and HbA, respectively. The ratio of the slopes is again 1.2. Thus the order of the rate constants of oxyHb oxidation is:

HbS + SUVs > HbA + SUVs > HbS + LUVs > HbA + LUVs > HbS > HbA

3.4 Physical Significance of A_{700} Measurement

Generally, the intensity of scattered light is a function of particle size, as well as particle concentration. In our samples the lipid concentration is constant, and the vesicle concentration decreases as the vesicle size increases. Thus increased scattering is likely to be due to the formation of larger vesicles. The theoretical relationship between absorbance at 700 nm and size or amount of fused vesicles is not delineated at this time. We are using the increase in A_{700} per unit time as an index of vesicle fusion.

Figure 1 **Rate constant of Hb oxidation versus Lipid/Hb ratio.** Pseudo first-order rate constants for the disappearance of oxyHbS (filled symbols) or oxyHbA (open symbols) in the presence of BPS SUVs (○) or LUVs (□ 100 nm, ◊ 50 nm, ◊ 30 nm) versus Lipid/Hb in PEN7.4 buffer. The lines are linear fits through each data type (HbS + SUVs, HbA + SUVs, HbS + LUVs, HbA + LUVs).

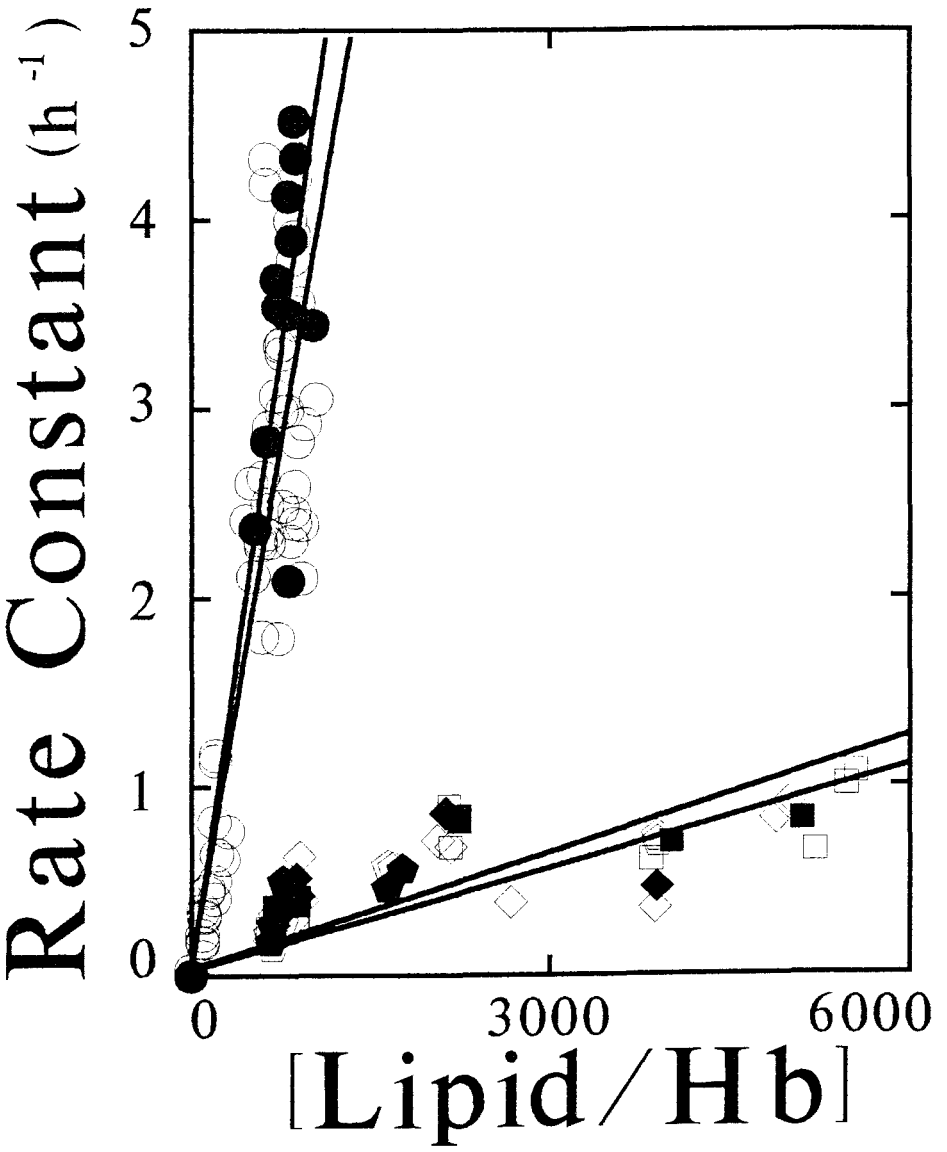
Rate Constant (h-1)
5
4
3
2
1
0
0
3000
6000
[Lipid/Hb]

3.5 Vesicle fusion in the Presence of HbS

We have shown that both SUVs and LUVs fuse when incubated with oxyHb at 37 °C (LaBrake and Fung, 1992). Figure 2 is a plot of average A_{700} (n = 6) for samples of SUVs (lipid concentration of 2.2 mg/ml) incubated with HbS (0.2 mg/ml) versus time. HbA was used as a control. The error bars are the standard deviations of the absorbance. The absorbance values for the HbS samples were always greater than the control HbA samples. The fusions were relatively rapid during the first 5 hours for both HbA and HbS, then it leveled off after about 10 hours, to absorbance values of about 0.11 for HbS and 0.09 for HbA at about 20 hours.

Figure 3 is for the samples containing LUVs (n = 4). Lipid and Hb concentrations were similar to the SUV samples discussed above. The A_{700} also increased as a function of time similar to those in the SUV samples, with A_{700} reaching 0.09 for HbS and 0.08 for HbA at about 20 h. During the first 5 hours, the absorbance values of LUV samples lagged behind those for the SUV samples.

The absorbance data obtained during the first 3 hours in the SUV and LUV samples were further analyzed, compared and shown on an expanded scale in Figure 4. The absorbance values for all four systems (HbS-SUV, HbA-SUV, HbS-LUV and HbA-LUV) exhibit excellent linear time dependence, with the slopes of 17.3 x 10^{-3}, 8.5 x 10^{-3}, 6.7 x 10^{-3}, and 3.9 x 10^{-3} A_{700}*h^{-1}, respectively, for the four systems (Table 2). Thus the vesicle fusion followed the order of: HbS + SUVs > HbA + SUVs > HbS + LUVs > HbA + LUVs. The ratios of these fusion indices for HbS and HbA were calculated as 2.0 for SUVs and 1.7 for LUVs (Table 2). Thus, for both the SUV and LUV systems, the fusion induced by HbS are about 2 times greater than the fusion induced by HbA.

The roles of Hb with different oxidation states in the fusion process were investigated in paired experiments (same SUV stock sample, different Hb conditions) by monitoring the fusion under CO conditions using purified HbCO and under O_2 conditions using hemolysate

Figure 2 **Plot of absorbance at 700 nm of BPS SUVs in the presence of HbS (●) and HbA (○) incubated at 37 °C versus time.** The vesicles were prepared by sonication with a lipid concentration of 2.2 mg/ml and a Hb concentration of 0.2 mg/ml and a Hb concentration of 0.2 mg/ml. Average data, from 6 experiments, are plotted. Error bars are the standard deviation of the average.

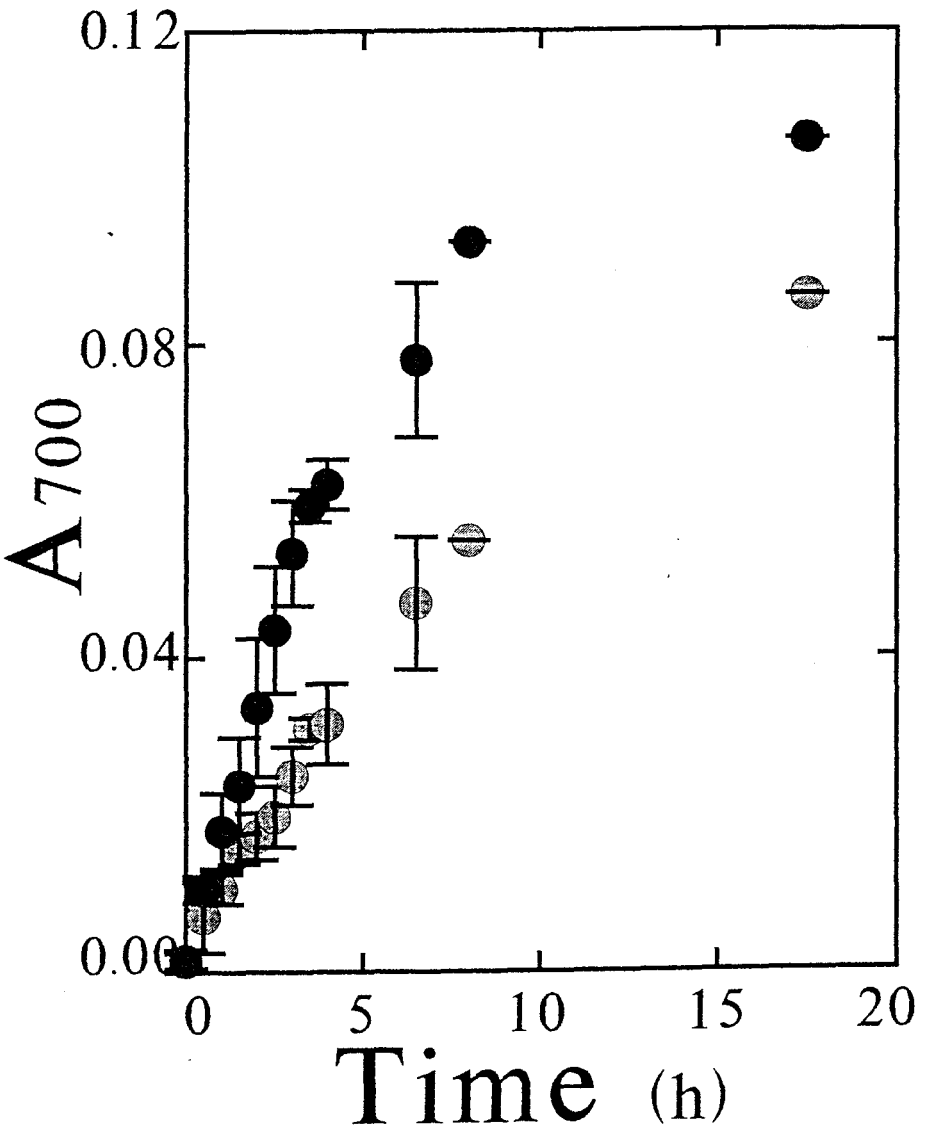
0.12
0.08
0.04
0.00
A 700
0
5
10
15
20
Time (h)

Figure 3 **Plot of absorbance at 700 nm of BPS LUVs in the presence of HbS (□) and HbA (□) incubated at 37 °C versus time.** The vesicles were prepared by extrusion through a 50 nm polycarbonate filter with a lipid concentration of 2.2 mg/ml and a Hb concentration of 0.2 mg/ml. Average data, from 6 experiments, are plotted. Error bars are the standard deviation of the average.

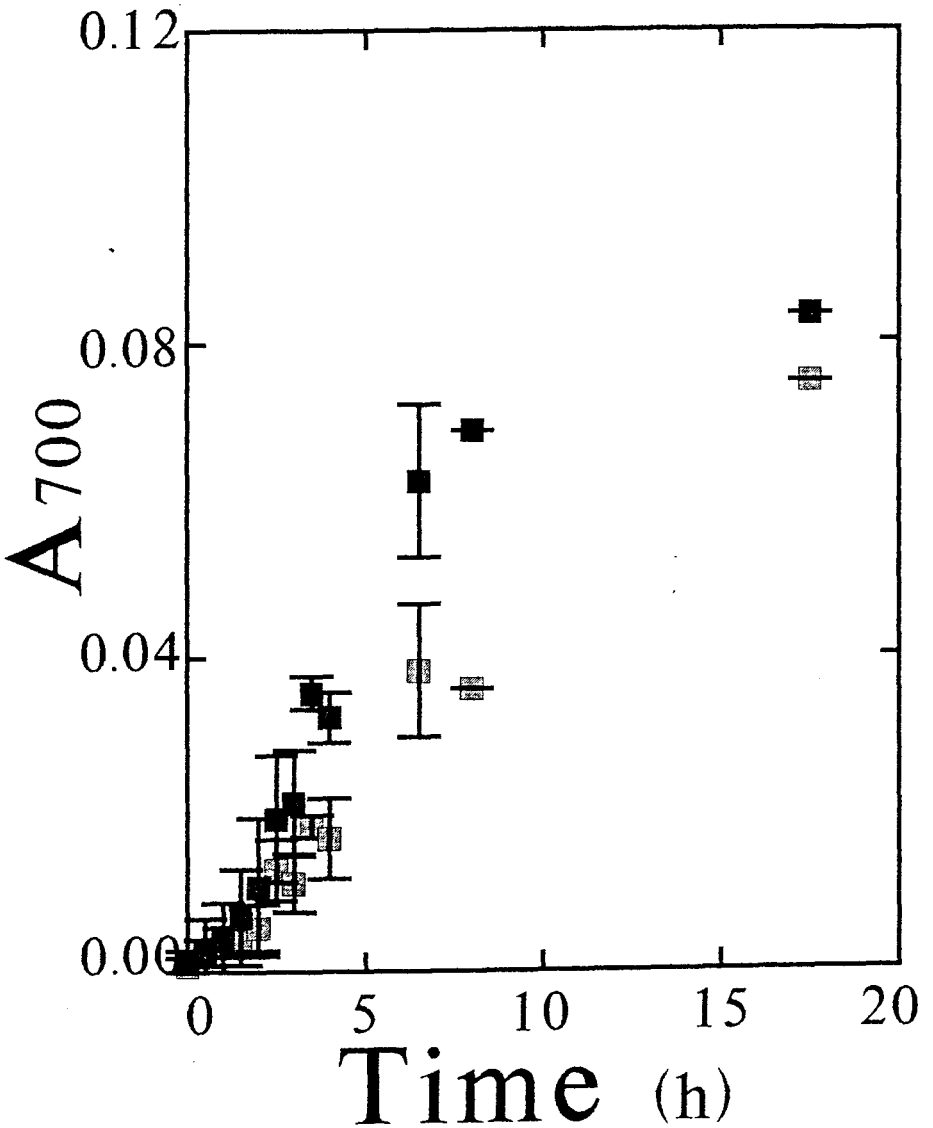
0.12
0.08
0.04
0.00
A700
0
5
10
15
20
Time (h)

Figure 4 **Replot of absorbance at 700 nm versus time for BPS SUVs and LUVs in the presence of HbA and HbS on an expanded scale.** Data are replotted from figures 2 and 3 on an expanded scale. The circles are data from figure 2 and the squares are from figure 3. The closed symbols are with HbS and the shaded symbols with HbA. The initial data (up to 3 hrs incubation time) were fit with linear regression to obtain and index of fusion for quantitative measure of fusion. The slopes of the lines are HbS + SUVs, 17.3×10^{-3}; HbA + SUVs, 8.5×10^{-3}; HbS + LUVs, 3.9×10^{-3}; HbA + LUVs, 6.7×10^{-3}.

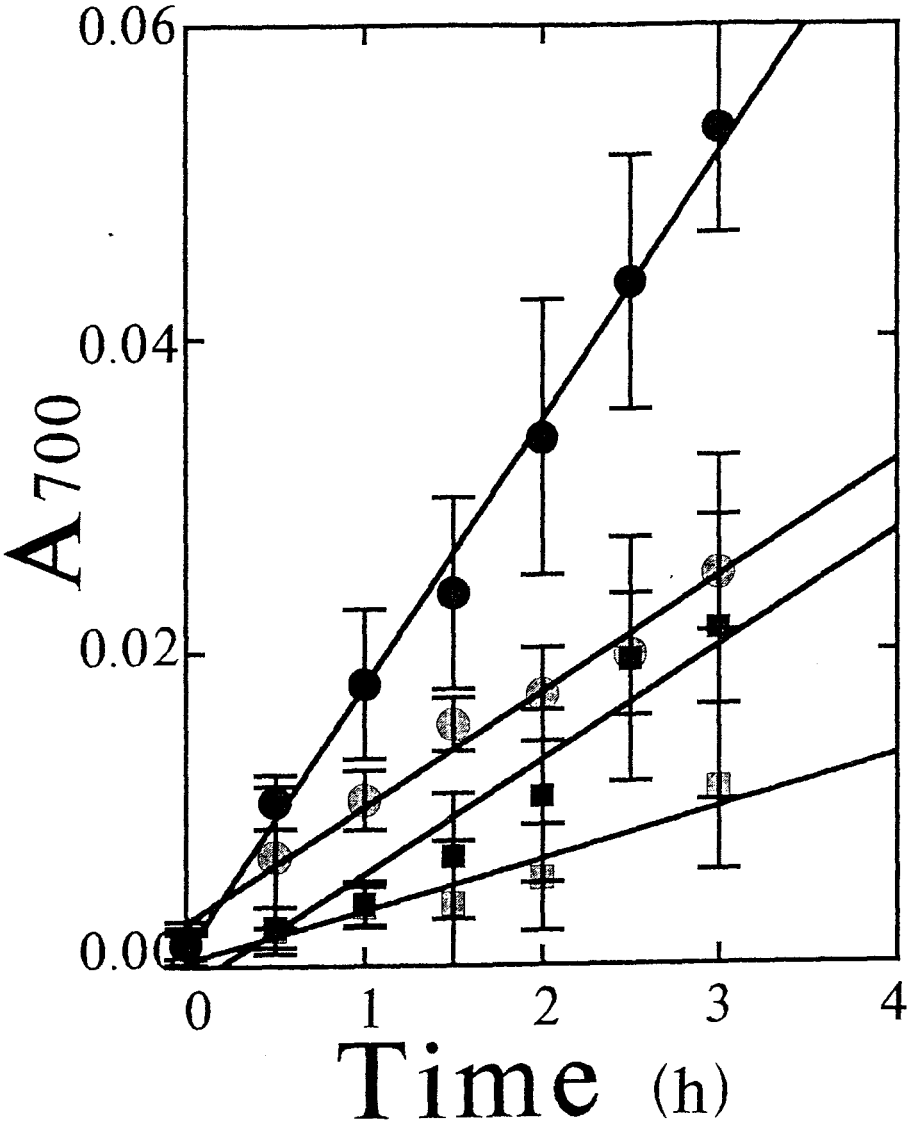
0.06
0.04
0.02
0.00
A700
0
1
2
3
4
Time (h)

Table 2 Indices of Vesicle Fusion for SUVs and LUVs in the Presence of HbS and HbA.

System[a]	Index (A_{700}*h^{-1})		Ratio[b]
	HbS	HbA	HbS/HbA
oxyHb + SUVs[c]	17.3×10^{-3}	8.5×10^{-3}	2.0
COHb + SUVs[d]	9.5×10^{-3}	3.9×10^{-3}	2.4
oxyHs + SUVs[e]	5.5×10^{-3}	3.4×10^{-3}	1.6
oxyHb + LUVs	6.7×10^{-3}	3.9×10^{-3}	1.7
COHB + LUVs	3.7×10^{-3}	2.8×10^{-3}	1.3

a The Hb (oxy- and CO- of HbS or HbA) + vesicle (SUVs or LUVs) solutions were incubated at 37 °C for upto 25 hours, the rate constants were calculated for the initial 3 hours of incubation as described in the text.

b Ratio of indices for HbS divided by that for HbA.

c Lipid concentration 2.2 mg/ml, Hb concentration 0.2 mg/ml.

d Lipid concentration 2.3 mg/ml, Hb concentration 0.2 mg/ml.

e Lipid concentration 1.2 mg/ml, Hb concentration 0.2 mg/ml.

for comparison with those under O_2 condition using purified oxyHb. The samples containing SUVs with a lipid concentration of 2.3 mg/ml were incubated with purified Hb (COHbS, COHbA) at 0.2 mg/ml concentration. The absorbance values of the systems were monitored for 10 hours and are shown in figure 5. The absorbance values for the CO samples with HbS were again larger than those with HbA, similar to the O_2 samples, shown in Figure 2. Although, there is significant fusion under CO conditions, the fusion for the CO samples was generally less than the O_2 samples, for both HbS and HbA. For example, the A_{700} value at 8 hours for HbS was 0.078 for CO samples and 0.093 for O_2 samples, and for HbA was 0.039 for CO samples and 0.055 for O_2 samples. The fusion indices for the CO data were calculated similar to those shown in Figure 4. Again the slope for the COHbS (9.5×10^{-3} $A_{700}*h^{-1}$) was about 2 times greater than that for COHbA (3.9×10^{-3} $A_{700}*h^{-1}$) (Table 2). In addition, the slope for the COHb-SUV was about 2 times slower than that for the oxyHb-SUV, for both HbS and HbA.

Fusion data for LUVs under CO conditions were also collected similar to those for the SUV system and are shown in figure 6. The lipid and Hb concentrations of these LUV samples were similar to those used for the SUV samples. The absorbance values of the LUV samples were generally smaller than those of SUV samples at similar time periods during the first three hours. However, the fusion in the COHbS sample remained higher than the COHbA sample, with fusion indices as 3.7×10^{-3} $A_{700}*h^{-1}$ for COHbS and 2.8×10^{-3} $A_{700}*h^{-1}$ for COHbA (Table 2).

For hemolysate samples, SUVs (1.2 mg/ml) were incubated in the presence of HbS or HbA hemolysates (0.2 mg/ml) under O_2 conditions. The fusion indices were 5.5×10^{-3} $A_{700}*h^{-1}$ for HbS and 3.4×10^{-3} $A_{700}*h^{-1}$ for the HbA, which were more similar to the pure Hb under CO condition (9.5×10^{-3} $A_{700}*h^{-1}$ and 3.9×10^{-3} $A_{700}*h^{-1}$, respectively) than to the pure Hb under O_2 condition (17.3×10^{-3} $A_{700}*h^{-1}$ and 8.5×10^{-3} $A_{700}*h^{-1}$, respectively) (Table 2).

Figure 5 **Plot of absorbance at 700 nm of BPS SUVs in the presence of oxy- and COHb incubated at 37 °C versus time.** HbS (filled symbols) or HbA (shaded symbols) at 0.2 mg/ml were incubated at 37 °C in the presence of BPS SUVs (2.3 mg/ml) under O_2 (O) or CO (◊) conditions.

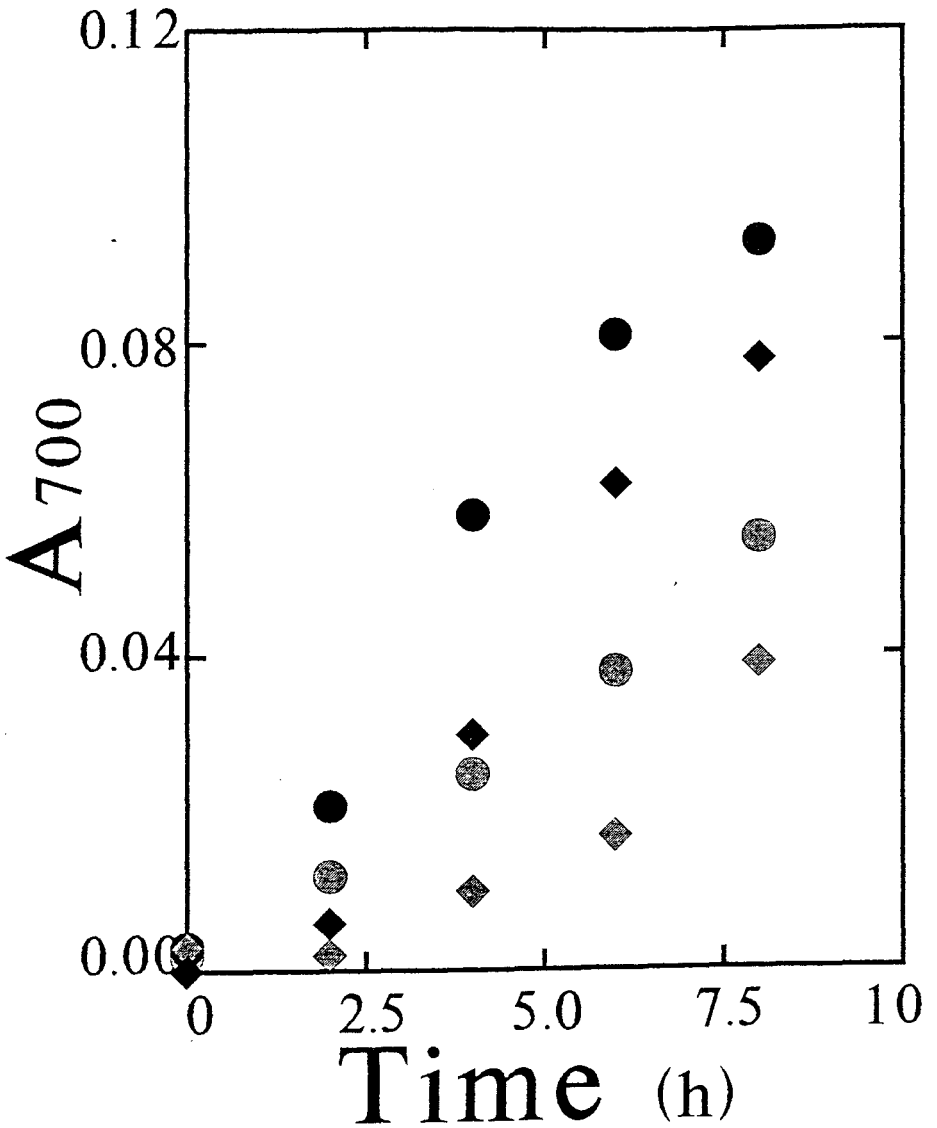
0.12
0.08
0.04
0.00
A700
0
2.5
5.0
7.5
10
Time (h)

Figure 6 **Plot of absorbance at 700 nm of BPS SUVs in the presence of oxy- and COHb incubated at 37 °C versus time.** HbS (filled symbols) or HbA (shaded symbols) at 0.2 mg/ml were incubated at 37 °C in the presence of BPS LUVs (2.3 mg/ml) under O_2 (□) or CO (◊) conditions.

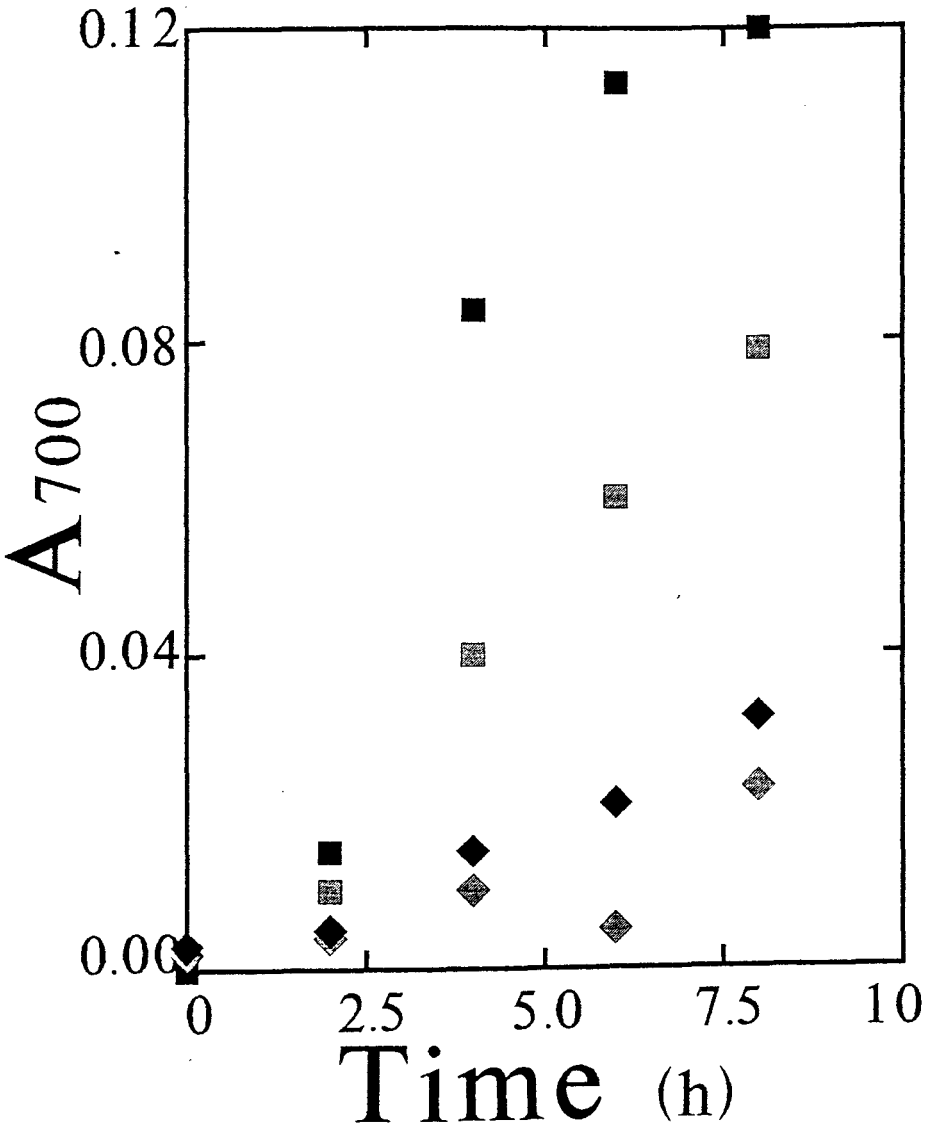
0.12
0.08
0.04
0.00
A 700
0
2.5
5.0
7.5
10
Time (h)

CHAPTER IV

DISCUSSION

4.1 Oxidation of HbS in the Presence and Absence of Vesicles

The initial pseudo first order rate constant for the autoxidation of HbS in PEN7.4, a buffer containing EDTA, at 37 °C was determined to be 0.030 ± 0.004 h^{-1} (n = 4) which was larger than that for HbA (0.025 ± .003 h^{-1}). The 1.2 ± 0.1 fold increase in autoxidation of HbS over that of HbA was shown to be statistically significant. These values are generally in agreement with those presented in a brief report (Hebbel *et al.*, 1988), in which a solution of HbS was shown to autoxidize with a rate constant 0.050 h^{-1}, in P7.2, without EDTA, and HbA with a rate constant of 0.029 h^{-1}. Their ratio of the rate constants is higher than ours. However, no standard deviations were given for their rate constants. The same authors later reported that the autoxidation rates of HbS varied somewhat (Hebbel, 1990), presumably from run to run. We found that the rate of autoxidation in the absence of EDTA was more variable, and thus less reliable, than those in the presence of EDTA. Similar findings that, in the absence of EDTA, the rate of autoxidation was substantially faster and quite variable were reported. (Winterbourn, 1976, Antonini and Brunori, 1971). Thus the determination of the rate constant of autoxidation is more reliable when measured in the presence of EDTA than in the absence of EDTA. In our hands, we are unable to conclude whether the autoxidation for HbS is faster or slower than HbA in buffer without EDTA. However, in the presence of EDTA, as stated above, HbS autoxidizes about 1.2 times faster than HbA.

Although it is not clear how the HbS mutation causes enhanced autoxidation, two

suggestions have appeared in the literature: 1) due to the innate instability of the HbS molecule (Hebbel, 1990), or 2) due to an altered folding/unfolding equilibrium at the N-terminal end of the β6 position (personal communication between Perutz and Hebbel and cited by Hebbel, 1990). Whatever the causes may be, the enhanced autoxidation has been suggested to underlie the membrane damage and hemolysis in sickle cells.

Since Hb oxidation is enhanced by lipid vesicles (LaBrake and Fung, 1992), an understanding of HbS oxidation in the presence of lipid vesicles is crucial. We chose BPS as the lipid for preparing vesicles because PS is one of the major phospholipid components found in the inner leaflet of the erythrocyte membrane bilayer (Marinetti and Crain, 1978). We quantitatively determined the rate constants of the disappearance of oxyHb, and the appearance of metHb, hemichrome and choleglobin for HbS in the presence of SUVs and LUVs. We found that the rate constant for the disappearance of oxyHbS was enhanced one order of magnitude in the presence of LUVs and two orders of magnitude in the presence of SUVs, similar to those results obtained for HbA (LaBrake and Fung, 1992). In our earlier studies, we have shown that the difference in the rate constants between SUVs and LUVs could not be attributed to lipid peroxidation products or artifacts due to the sonication or extrusion processes used in sample preparations, but rather to the different surface energy of the bilayer surface. We have now found that HbS oxidation in the presence of the phospholipid surface is also greatly enhanced. In paired experiments, the ratio of the rate constants of HbS over HbA for the disappearance of oxyHb in the presence of LUVs was 1.4 and of SUVs was 1.2. These ratios were very similar to the 1.2 fold increase in autoxidation. There does not appear to be an antagonistic or synergistic effect on HbS oxidation due to the SUVs or LUVs.

4.2 HbS enhanced Fusion of SUVs and LUVs

Lipid fusion in model membranes can be induced by many different fusogens (species

which promote fusion). The fusion event is preceded by dehydration at the point of close contact between two membranes. This is followed by packing defects among lipid molecules which leads to hydrophobic contact and thus initiation of fusion (Papahadjopoulos, 1991). Understanding the mechanism of Hb induced fusion will help to explain the mechanism of the interaction of Hb with a phospholipid surface and further the understanding of the pathological difference between HbS and HbA.

We monitored the fusion of SUVs and LUVs in the presence of HbS and HbA under O_2 and CO conditions. Hb-induced SUV fusion per unit time was a factor of two larger than that for the Hb-induced LUV fusion. This observation was independent of the Hb system studied and is explained by the increased surface tension associated with the SUVs. It has been shown that, under the same fusion promoting conditions, SUVs fuse more rapidly than LUVs (Ohki, 1984).

Since the behavior of lipid fusion between the LUVs and SUVs was similar for each Hb system (HbS and HbA under O_2 and CO conditions), only the data associated with SUVs in different Hb systems will be discussed.

HbS promoted more fusion compared to HbA under CO conditions, where no Hb oxidation was detected. Fusion induced by hemolysate, which has little detectable Hb oxidation due to the antioxidants in the hemolysate, was similar to fusion induced by COHb.

Although the HbS and HbA molecules are isomorphous at crystallographic resolution (Hebbel, 1990), subtle conformational differences do exist which may, in part, explain the fusion phenomenon. First, during mechanical agitation of Hb solutions, oxyHbS or COHbS precipitate faster than oxyHbA or COHbA, suggesting a conformational difference between HbS and HbA when ligated in the Fe^{+2} oxidation state (Asakura *et al.*, 1973). Surface conformational differences between HbS and HbA were also detected by NMR (Fung *et al.*, 1975). In addition, HbS was found to unfold to a greater extent than HbA at the air water interface, and this difference in surface activity may be due to destabilization of hydrophobic

interactions on the hydrophobic surface (air) (Elbaum *et al.*, 1976).

The fusogenic behavior of the Hb molecule itself is not well understood. In another study of Hb vesicle interaction, when HbA was incubated for 15 h with SUVs, only 11-18 % of the total heme cosedimented with lipid vesicles (Szebini *et al.*, 1988), indicating the Hb molecule is not adhering with a high affinity to the lipid surface. It is possible that the weak Hb-lipid interaction causes increased surface hydrophobicity in lipid vesicles, initiating fusion. Our results demonstrate different surface activities between HbS and HbA to cause increased vesicle fusion of HbS compared to HbA under CO conditions.

The results of Hb under O_2 conditions promoting more vesicle fusion than Hb under CO conditions and hemolysate under O_2 conditions suggest that products of Hb oxidation further promote vesicle fusion, in good agreement with the results showing vesicles fuse more rapidly in the presence of metHb as compared to oxyHb (Szebeni *et al.*, 1988). In addition, lipid peroxidation products are expected to be present in the later stages of Hb-vesicle incubation (> 1 h) (Itabe *et al.*, 1988). The presence of lipid peroxidation products such as lipid hydroperoxides of the fatty acid components of phospholipids, cyclic peroxides and epoxides, are known to promote vesicle fusion (Gast *et al.*, 1982). This is not so for the COHb system where little or no oxidation products are present even in the later stages of incubation (i.e. > 30 min). Therefore, the presence of metHb and other Hb oxidative products as well as other lipid peroxidation products are believed responsible for the much greater initial rate of fusion in the Hb under O_2 conditions as compared to the Hb under CO conditions and hemolysate under O_2 condition systems.

These data support the hypothesis that there are several additive factors in the system contributing to the vesicle fusion. They include the type of vesicle used (SUV or LUV), the oxidation state and ligation of the heme in the molecule, and the surface conformation of the Hb molecule.

The oxidation of HbS in the presence of vesicles is enhanced as compared to HbA.

Therefore, the differences in the HbS compared to HbA under O_2 condition are additive effects of different Hb surface conformations and oxidative products.

4.3 Summary

The known differences between oxyHbS and oxyHbA are the increased mechanical instability and surface activity of HbS as compared to HbA. There also appears to be a slight increase in autoxidation rate for HbS. The mechanism which causes the enhanced oxidation of Hb in the presence of vesicles has been attributed to an interaction of oxyHb with the lipid surface, largely due to hydrophobic interaction. This is indicated by the order of magnitude enhancement of oxidation due to the presence of the more curved SUVs as compared to LUVs. However, the difference in the initial rate of oxidation in the presence of SUVs and LUVs for HbS compared to HbA is no greater than the difference in autoxidation. Therefore, the effect of vesicle surface on Hb oxidation appeared to be similar in HbS and HbA. However, there is a marked difference between the amounts of vesicle fusion for the HbS as compared to the HbA system. This difference is also evident under CO conditions and Hb hemolysate under O_2 conditions. This suggests that HbS is less stable at the lipid-water interface than HbA. It is likely that the excessive oxidation found in sickle red blood cells is due to intrinsic surface conformation difference between HbA and HbS, and not due to the intrinsic oxidative properties in HbA and HbS. Further studies of HbS-lipid surface interaction may provide molecular understanding toward pathophysiology of sickle cells.

REFERENCES

Antonini, A. & Brunori, T. (1971) Hemoglobin and Myoglobin in their Reactions with Ligands; Frontiers in Biology (Neuberger, A. & Tatum, E.L., eds) Vol. 71, North Holland Publishing, Amsterdam.

Asakura, T.; Ohnishi, T.; Friedman, S. & Schwartz, E. (1974) Proc. Natl. Acad. Sci. USA 71, 1594-1598.

Bligh, E.G. & Dyer, W.J. (1959) Can. J. Biochem. Physiol. 37, 911-917.

Chiu, D. & Lubin, B. (1989) Sem. Hemat. 26, 128-135.

Elbaum, D.; Harrington, J.; Roth, E.F. & Nagel, R.L. (1976) Biochim. Biophys. Acta 427, 57-69.

Fung, L.W.-M.; Lin, K.-L.C. & Ho, C. (1975) Biochemistry 14, 3424-3428.

Gast, K.; Zirwer, D.; Ladhoff, A.-M.; Schreiber, J.; Koelsch, R.; Kretschmer, K. & Lasch, J. (1982) Biochim. Biophys. Acta 686, 99-109.

Hebbel, R.P.; Eaton, J.W.; Balasingam, M. & Steinberg, M.H. (1982) J. Clin. Invest. 70, 1253-1259.

Hebbel, R.P. & Miller, W.J. (1984) Blood 64, 733-741.

Hebbel, R.P.; Morgan, W.T.; Eaton, J.W. & Hedlund, B.E. (1988) Proc. Natl. Acad. Sci. USA 85, 237-241.

Hebbel, R.P. & Eaton, J.W. (1989) Sem. Hemat. 26, 136-149.

Hebbel, R.P. (1990) Semin. Hemat. 27, 51-69.

Itabe, H.; Kobayashi, T. & Inoue, K. (1988) Biochim. Biophys. Acta 961, 13-21.

Kawanishi, S. & Caughey, W.S. (1985) J. Biol. Chem. 260, 4622-4631.

Keelung, H.; Meers, P.R. & Duzgunes, N. (1991) in Membrane Fusion (J.Wilschut and D. Howkstra eds.) pp 195-208, Marcel Dekker, New York.

Kikugawa, K.; Sasahara, T.; Sasaki, T. & Kurechi, T. (1981) Chem. Pharm. Bull. 29, 1382-1389.

Kuross, S.A.; Rank, B.H. & Hebbel, R.P. (1988) Blood 71, 876-882.

LaBrake, C.C. & Fung, L. W.-M. (1992) J. Biol. Chem. *in press*

Liu, S.C.; Zhai, S. & Palek, J. (1988) Blood 71, 1755-1758.

Loughrey, H.C.; Wong, K.F.; Choi, L.S.; Cullis, P.R.; & Bally, M.B. (1990) Biochim. Biophys. Acta 1028, 73-81.

Mansouri, A & Winterhalter, K.H. (1974) Biochemistry 13, 3311-3314.

Marinetti, G.V. & Crain, R.C. (1978) J. Supramolecular Structure 8, 191-213.

Ohki, S. (1984) J. Memb. Biol. 77, 265-274.

Papahadjopoulos, D. (1991) in Membrane Fusion (J.Wilschut and D. Howkstra eds.) pp xv-xvii, Marcel Dekker, New York.

Riggs, A. (1981) Methods in Enzymology 76, 5-29.

Schecter, A.N.; Noguchi, C.T. & Rodgers, G.P. (1987) in The Molecular Basis of Blood Diseases (Stamatoyannopoulos, G., Nienhuis, A.W., Leder, P., Majerus, P.W., Eds.) pp 179-218, W.B. Saunders, Philadelphia.

Shaklai, N.; Shviro, Y.; Rabizadeh, E. & Kirschner-Zilber, I. (1985) Biochim. Biophys. Acta 821, 355-366.

Stewart, J.C. (1980) Anal. Biochemistry 104, 10-14.

Szebeni, J.; Hauser, H.; Eskeleson, C.D.; Watson, R.R. & Winterhalter, K.H. (1988) Biochemistry 27, 6425-6433.

Vincent, S.H. (1989) Sem. Hemat. 26, 105-113.

Watkins, J.A.; Kawanishi, S. & Caughey, W.S. (1985) Biochem. Biophys. Res. Commun. 132, 742-748.

Winterbourn, C.C.; McGrath, B.M. & Carrell, R.W. (1976) Biochem. J. 155, 493-502.

Winterbourn, C.C. (1985a) in CRC Handbook of Methods for Oxygen Radical Research (Greenwald, R.A. Ed.) pp 137-141, CRC Press, Boca Raton, FL.

Winterbourn, C.C. (1985b) Environmental Health Perspectives 64, 321-330.

PART II

CHAPTER I

INTRODUCTION

Spectrin, a major protein in the human erythrocyte membrane skeleton, was first isolated in 1971 in the low ionic strength extract of the membrane (Clarke, 1971; Fairbanks *et al.*, 1971). The name "spectrin" was based on the fact that hemoglobin-free erythrocyte membranes are referred to as "ghosts" (ghost = specter) (Bennett, 1990). Its function is to play a role in determining the mechanical properties and maintaining the unique biconcave shape of the erythrocyte. Spectrin consists of two subunits, defined as α with a molecular weight of about 285,000 (Sahr *et al.*, 1990) and β with a molecular weight of about 246,000 (Winkelmann *et al.*, 1990), arranged as a heterodimer with the two subunits associated side-to-side in an anti-parallel orientation to give a flexible rod approximately 1,000 Å long, as visualized by electron microscopy (Shotton *et al.*, 1979). The dimers associate head-to-head to form tetramers. Amino acid sequence (Speicher *et al*, 1983) and cDNA sequence (Curtis *et al.*, 1985; Winkelmann *et al.*, 1988) analyses reveal that about 90 % of spectrin, by mass, is comprised of repetitive structural units of 106 amino acid residues. The dimensions of the 106-residue segment, ~55 x 30 Å, based on electron microscopy (EM) data of the intact spectrin (Shotton *et al.*, 1979), are similar to the dimensions of other globular proteins. A simple and attractive triple helical structure has been proposed for the 106-residue segment (Speicher, 1983), and refinements of the original triple helical model have also been published (Dubreuil *et al.*, 1989; Parry *et al.*, 1992). A more detailed five-fold structure has also been suggested (Xu, *et al.*, 1990).

Since spectrin plays a role in the dynamics of the highly flexible erythrocyte membrane, several studies have been used to probe the dynamic nature of the molecule. Saturation transfer (ST) EPR studies of spin-labeled spectrin-actin complex provided quantitative information on the motion of the molecule, and revealed that the spectrin-actin complex appears to exhibit multiple classes or rates of motion over a wide time range, from 10^{-9} to 10^{-3} s (Fung & Johnson, 1983). Proton nuclear magnetic resonance studies suggested some internal motions within the spectrin molecule with about 15 % of the molecules exhibiting motions about 10^{-9} - 10^{-10} s at 37 °C (Fung *et al.*, 1986), and the remaining motions being slower than 10^{-6} s (Fung *et al.*, 1989). Transient dichroism studies reveal motions of about 10^{-4} s at 4 °C (Clague *et al.*, 1990). Dynamic light scattering measurements have detected segmental motion on the order of 23 μs at 20 °C (Budzynski *et al.*, 1992). Together these studies suggest multiple classes of segmental motions in spectrin molecules.

Structural studies have also been performed on spectrin. Electric birefringence relaxation studies (Mikkelsen & Elgsaeter, 1978), measurements of the rotational relaxation time and intrinsic viscosity studies of spectrin dimers (Mikkelsen, 1984) support the description of spectrin as a flexible and extended molecule in solution. Light scattering experiments (Elgsaeter, 1978) have revealed that the radius of gyration nearly doubles upon decreasing the ionic strength from 100 mM NaCl to 1 mM NaCl. Circular dichroism (CD) data estimate the α-helix content to range from ~60-75 % (Ralston, 1978; Calvert *et al.*, 1980), and secondary structure prediction programs predict the secondary structure to have 62 % α-helix, 16 % β-sheet and 22 % other structural components such as random coils and turns (Xu *et al.*, 1990). Due to its large molecular weight, it has been difficult to apply multidimensional NMR techniques to study structural components of spectrin, and since spectrin has not been crystallized there is no x-ray information.

We have used Fourier transform infrared spectroscopy (FTIR) to investigate the secondary structure of spectrin under different ionic strength, denaturing conditions and in

the presence of lipid vesicles. Recent developments in infrared spectroscopy using Fourier transform instrumentation have eliminated the problems of low sensitivity and interfering absorbances by solvents such as water (Surewicz & Mantsch, 1988). IR spectroscopy is sensitive to the C=O stretching (1600 - 1700 cm^{-1}, amide I) and the N - H bending (1500 - 1600 cm^{-1}, amide II, for samples in H_2O; and N-D bending at 1400 - 1500 cm^{-1}, amide II', for samples in D_2O) arising from the molecular bonds in the protein backbone (Cantor & Shimmel, 1980). Changes in the frequencies of these characteristic IR absorbances also reveal the strength of the H-bonding in the backbone. Thus, each type of secondary structure (α-helix, β-sheet, random coil and turns) has a characteristic IR spectrum. A protein is assumed to be a linear combination of the above mentioned secondary structural components. Thus, by examining the spectrum in the amide I and II regions, one can obtain the percentage of secondary structural components in a protein. FTIR methods have proven superior to circular dichroism (CD) methods in the prediction of β-sheet (Sarver & Kreuger, 1991), and the secondary structure can also be probed under conditions of high concentration and in the presence of vesicles which would cause absorbance and light scattering problems in a CD experiment.

In this thesis, the secondary structure of spectrin under denaturing conditions of high pH, SDS treatment and heat treatment was probed to determine the sensitivity of the FTIR technique to structural changes in spectrin. This technique was then applied to study the secondary structural changes under different ionic strength and in the presence of large unilamellar vesicles. We found that FTIR is a sensitive and reliable technique to study the secondary structure of spectrin. Since the overall dimension of spectrin has been shown to be sensitive to ionic strength (Elgsaeter, 1978), we used gel filtration chromatography to determine the effect of ionic strength on the Stokes radius of our spectrin sample. We have shown that the Stokes radius of spectrin is sensitive to changes in sodium chloride concentration in buffer. However, using FTIR, we found no secondary structural differences

in spectrin in buffers of different ionic strength. Finally, we use our experimental results to support a proposed model of the tertiary structure of spectrin.

CHAPTER II

MATERIALS AND METHODS

2.1 Spectrin Preparation

Human red blood cells (RBCs) were obtained from the local blood bank and used within one week of withdrawal. All steps were carried out at 4 °C unless specified otherwise. RBCs were washed 3 times with 5 mM sodium phosphate buffer with 150 mM NaCl at pH 8.0 (PBS8). White membrane ghosts were prepared by lysing the washed RBCs with 20 volumes of 5 mM phosphate buffer at pH 8.0 (5P8) and then washing the membrane 3 times with the same buffer, according to the method of Dodge *et al.* (1963). The spectrin dimer and tetramer preparations were done according to published methods (Ungewickell & Gratzer, 1978; Budzynski *et al.*, 1992). For spectrin dimer preparation, the membrane ghosts were washed once with 0.3 mM phosphate buffer at pH 7.6 (0.3P7.6), followed by incubation with 2-3 volumes of 0.3P7.6 for 30 min at 37 °C. For spectrin tetramer preparation, the membrane ghosts were dialyzed against 0.3P7.6 buffer overnight. After incubation at 37 °C or overnight dialysis, the membranous solution was centrifuged at 400,000 g in an ultracentrifuge for 20 min. The supernatant containing the spectrin-actin complex was pooled and concentrated with an ultrafiltration cell (Amicon, Danvers, MA) to a concentration of about 1.5 mg/ml. The spectrin concentrations for the experiments were determined using an extinction coefficient of $\epsilon^{1\%}_{280}$=10 (Marchesi *et al.*, 1969; Clarke, 1971). The spectrin-actin solution was loaded onto a gel filtration column (Sepharose 4B-CL, Pharmacia, Piscataway, NJ) equilibrated with 25 mM Tris, 5 mM EDTA and 100 mM NaCl at pH 7.6 and eluted at a flow rate of 22 ml/hr

for about 16 hours. The spectrin fractions, either dimer or tetramer, were pooled and concentrated (Amicon CF-25 cones) to a concentration of 5 - 10 mg/ml and dialyzed overnight against either PBS7.4 (same as PBS8 except at pH 7.4) or 5P7.4 (same as 5P8 except at pH 7.4). The spectrin was then concentrated (Amicon Centricon-30 Microconcentrators) to about 35 mg/ml.

2.2 Spectrin in D_2O Buffer

Spectrin dimer sample was subjected to D_2O exchange, using PBS7.4/D_2O buffer (PBS7.4 made with 99.9 % D_2O, Norell, Inc, Landisville, NJ). The D_2O exchange was carried out by adding about 1.5 ml of the D_2O buffer to about 500 μl of the concentrated spectrin (35 ± 5 mg/ml). The solution was concentrated for about 1.5 h (Amicon Centricon-30 Microconcentrator). The cycle was repeated 4 times. The filtrate from the last exchange was saved and used as the background for the FTIR measurements, to account for the residual HOD or H_2O in the sample. The final spectrin concentration was 35 ± 5 mg/ml.

2.3 SDS treated Spectrin

50 μl of a 10 % sodium dodecyl sulphate (SDS) (Bio-Rad, Richmond, CA) in PBS7.4/H_2O was added at room temperature to 450 μl of spectrin dimer (35 ± 5 mg/ml) in PBS7.4/H_2O to give a final concentration of 1 % SDS. The mixture was allowed to equilibrate for about 1 hour before the FTIR measurement. A 1 % SDS solution in PBS7.4 was used as a blank.

2.4 Heat denatured Spectrin

Dilute spectrin dimer (about 5 mg/ml) in 5P7.4/H_2O was heated to 80 °C for 10 min, then cooled to room temperature. The sample was then concentrated to 35 ± 5 mg/ml. The low salt 5P7.4 buffer was used because spectrin precipitated out of solution when heated in

high ionic strength PBS7.4.

2.5 NaOH treated Spectrin

Concentrated sodium hydroxide (NaOH) was added to the spectrin dimer sample (35 ± 5 mg/ml) in PBS7.4/H_2O) to yield a final concentration of 2 M NaOH. Buffer with 2 M NaOH was used as a blank.

2.6 Spectrin and Lipid Vesicles

Large unilamellar vesicles (LUVs) of bovine brain phosphatidylserine (BPS) were prepared by dispersing a film of BPS in PBS7.4/H_2O (LaBrake & Fung, 1992). The dispersion was subjected to a freeze/thaw cycle five times by submerging the flask in liquid N_2 followed by a 37 °C water bath, then passed through an Extruder (Lipex, Vancouver, B.C. Canada), equipped with two 100 nm pore size polycarbonate filters (Nuclepore, Pleasanton, CA), ten times at high N_2 pressure (about 250 psi) to form LUVs. The average diameter of these LUVs is 130 nm (LaBrake & Fung, 1992). The LUVs were mixed with the pure spectrin dimer to yield a final concentration of 28 mg/ml BPS LUVs and 20 mg/ml spectrin. A blank composed of BPS LUVs at the same concentration was used.

2.7 Stokes Radius

The Stokes radius (R_s) of spectrin under different buffer conditions was estimated using a gel filtration column (Sepharose 4B-CL, 81 x 1.5 cm) with a flow rate of 22 ml/h. The column was equilibrated with PBS7.4. A gel filtration calibration kit (Pharmacia) including the proteins, hemoglobin (R_s = 31 Å), bovine serum albumin (R_s = 37 Å), catalase (R_s = 52 Å), ferritin (R_s = 60 Å) and thyroglobulin (R_s = 81 Å) were used to calibrate the column. The Stokes radii of the proteins were given with the literature accompanying the kit. Dextran blue was used to calculate the void volume (V_o). The partition coefficient (K_{av})

of each protein was calculated according to the following equation:

$$K_{av}^{x} = (V_e^{x} - V_o)/(V_t - V_o)$$

where: V_e^{x} = elution volume of protein x and V_t = total volume of the column. The values of K_{av} vs $\log(R_s)$ are shown in Figure 1, also shown is the linear regression of the data to give a calibration curve. The equation of the line, $\log(R_s) = 2.52 - 1.22 \times K_{av}$, was used to calculate the Stokes radius of the spectrin under different conditions.

For the elution of spectrin under different buffer conditions, the column was first equilibrated with the appropriate buffer.

2.8 Infrared Spectroscopy

Fourier transform infrared (FTIR) spectra were recorded with a Bio-Rad FTS-40 FTIR spectrophotometer with a triglycine sulphate (TGS) detector and processed with the dedicated Digilab computer. Typically, 1048 interferograms were recorded at 20 °C, coadded, triangularly apodized and Fourier transformed to give a single beam spectrum (intensity vs. wavenumber) with a resolution of 2 cm^{-1}. For the measurements of samples in H_2O buffer, a semi-permanent cell equipped with CaF_2 salt plates and a 6 μm tin spacer was used. It is necessary to use 6 μm spacers to insure the H_2O absorbance at 1640 cm^{-1} is less than unity to permit quantitative spectral subtraction of the background (Dousseau & Pezolet, 1990). Although a restriction in resolution to 2 to 3 cm^{-1} results, an open aperture was used to allow maximum signal to reach the detector. For the measurements of samples in D_2O buffer, a standard IR cell equipped with CaF_2 salt plates and a 15 μm teflon spacer was used. A 2 cm^{-1} aperture size was adequate for these measurements. For each spectrin sample run, a single

Figure 1 **Plot of partition coefficient (K_{av}) vs log of the Stokes radius (R_s) for a series of standard proteins.** Points are for the standard proteins hemoglobin, bovine serum albumin, catalase, ferritin and thyroglobulin. The best fit least squares line is the calibration curve for determining the Stokes radius of spectrin.

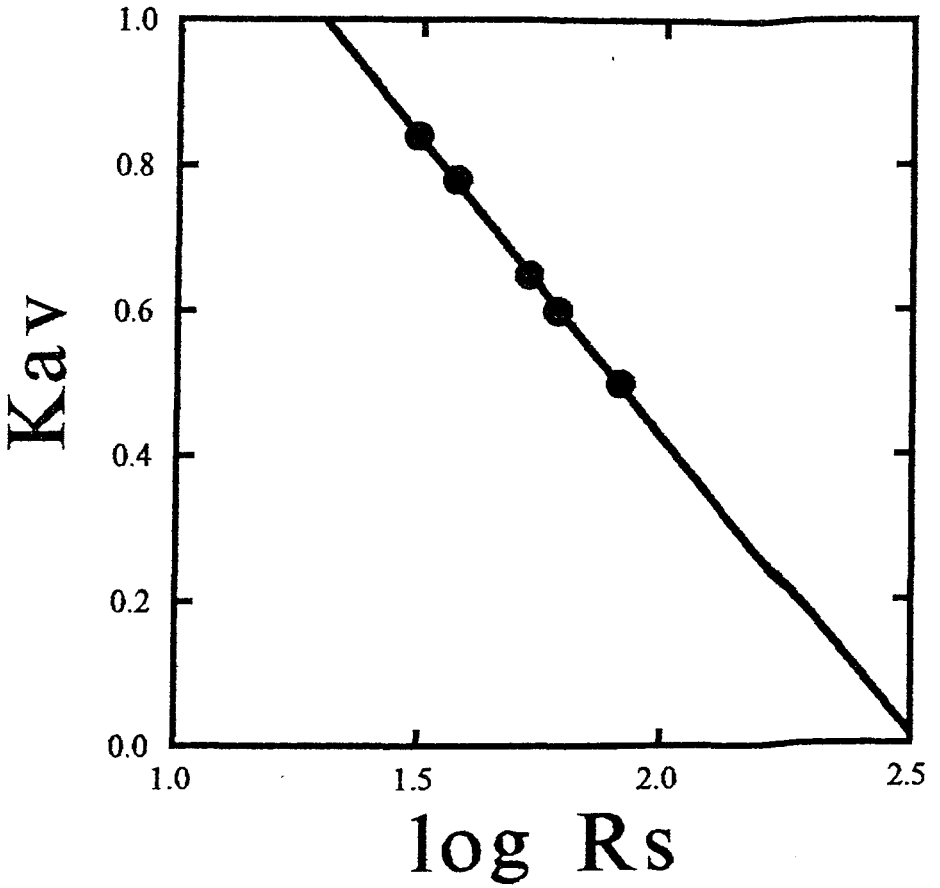
1.0
0.8
0.6
0.4
0.2
0.0
Kav
1.0
1.5
2.0
2.5
log Rs

beam spectrum was collected on the spectrin sample, on the buffer (background) and on a clean empty cell (air).

2.9 Data Analysis

2.9.1 Absorbance Spectra

The absorbance spectra of the samples were calculated from the single beam intensity spectra by taking the log of the ratio of the single beam spectrum of the sample of spectrin to that of air. Similarly, the absorbance of the background referenced to air was determined.

2.9.2 Baseline Subtraction

To obtain the absorbance spectrum of spectrin in solution, the background absorbance spectrum was subtracted from the spectrin absorbance spectrum numerically with an array basic program (SUBH2O) (Dousseau *et al.*, 1989), which was written for Spectra-Calc software (Galactic Ind., Salem, NH) and was generously provided to us by Dr. Pezolet. In order to use this numerical method, the spectra had to be transferred from the Digilab to the IBM computer and imported into the Spectra-Calc software. The algorithm for the array basic program was designed to multiply the background spectrum by a scaling factor (scaled up and down in small increments) and subtract it from the sample spectrum until the difference spectrum in the region of 1750 - 2650 cm^{-1} was flat as determined by a minimum chi^2 for the least squares fit (Dousseau *et al.*, 1989). The subtraction was also performed manually using the Digilab computer, equipped with a joy stick on the keyboard, by "tweaking" the scaler unit of the background spectrum with the joy stick until a flat baseline in the sample spectrum was obtained in the region from 2000 to 1700 cm^{-1}.

2.9.3 Second Derivative Spectra

The second derivative spectra of the absorbance spectra were calculated using

satandard Digilab software (BIO-RAD) to provide the peak positions needed for the band fitting routine (see below).

2.9.4 FSD Deconvolved Spectra

Deconvolution of the absorbance spectrum serves to narrow the broad overlapping IR bands, thereby resolving the bands due to different secondary structure components. Fourier self-deconvolution (FSD), an algorithm which operates on the Fourier transform of the absorbance spectrum (Kauppinen *et al.*, 1981), was used for the deconvolution. A triangular apodization function with a resolution enhancement parameter of K = 2.0 and full width at half height parameter of FWHH = 16 cm^{-1} was used for the spectrin in D_2O spectra and FWHH = 14 cm^{-1} for the spectrin in H_2O spectra.

2.9.5 Band Fitting to the FSD Deconvolved Spectra

The band fitting was performed on the deconvolved spectra using the Spectra-Calc software Curve-fit routine following the guidelines outlined by Byler and Susi (1986). The initial peak positions were obtained from the second derivative spectra. A 100 % Gaussian band shape was assumed. The integrated area under the curve-fit bands was assumed to be proportional to the concentration of secondary structure responsible for that band. Band assignments of secondary structure components were made according to the literature (Cantor & Shimmel, 1980; Byler & Susi, 1986; Dong *et al.*, 1990).

2.9.6 Partial Least Squares Analysis

The data for spectrin in H_2O buffer were also analyzed using the partial least squares analysis (PLS) method as outlined before (Dousseau & Pezolet, 1990). The method can be easily employed by using the PLS-QUANT module in the Spectra-Calc software. A set of 14 spectra of proteins of known secondary structure in H_2O buffer (Dousseau & Pezolet, 1990)

(training set) was obtained from Dr. Pezolet. These protein spectra were then input into the PLS QUANT module of Spectra-Calc, and the calibration spectrum was calculated using a dimension of 25 and four components: ordered α-helix, unordered α-helix, β-sheet and other (includes turns and random coil). For comparison to the band fitting results, the ordered and unordered helix components were added together and presented as total α-helix.

One of the proteins from the calibration set was a 100 % α-helix polylysine. Since polylysine is sometimes unstable at 100 % structure, the calibration spectrum was recalculated without this polypeptide. However, there was no significant difference in the structural prediction in the absence of polylysine, so this polypeptide was left in the training set. The spectrin spectra with the background subtracted using the SUBH2O program mentioned above, were normalized before being analyzed by the PLS method. The spectra were prepared by setting the limits of the spectra from 1480 - 1720 cm^{-1}, adjusting a flat baseline with 2 point baseline correction, setting the baseline to 0 and finally normalizing the total intensity to unity. Thus, using the PLS-QUANT Spectra-Calc program with our calibration spectrum, the secondary structure of the protein could be determined from the spectrin FTIR absorbance spectrum.

CHAPTER III

RESULTS

3.1 Stokes Radius

The Stokes radius of a molecule is defined as its effective hydrated radius (Cantor & Shimmel, 1980). The Stokes radius for spectrin has been determined from gel filtration chromatography (Kam, *et al.*, 1977). We used similar methods to calculate the Stokes radius of spectrin dimers and tetramers in 5 mM sodium phosphate buffer at pH 7.4 with sodium chloride concentrations ranging from 0 to 150 mM (Table 1). The Stokes radius of spectrin dimer increases from 124 Å in buffer with 150 mM NaCl to 178 Å in buffer without NaCl. The radius determined for spectrin tetramer was 250 Å in buffer with 150 mM NaCl. However, the radius in buffer without NaCl was not obtained because the spectrin tetramer eluted with the void volume, but can be estimated to be $\geq$ 330 Å, when K_{av} is 0.

3.2 FTIR Spectra of Spectrin Dimer

3.2.1 Spectrin in PBS7.4/H_2O Buffer

The absorbance spectrum of spectrin dimer (35 ± 5 mg/ml) in PBS7.4/H_2O is shown in figure 2a. The spectrum has two major bands, assigned as the amide I band (1700 - 1600 cm^{-1} region) and the amide II band (1600 - 1500 cm^{-1} region). The amide I band is symmetric and narrow, which is consistent with a protein of high α-helical content (Dousseau & Pezolet, 1990).

The second derivative spectrum of the absorbance spectrum is shown in figure 2b. The

Table 1 Stokes Radii for Spectrin Dimer and Tetramer in Different Ionic Strength Buffers.

Sample	[NaCl] (mM)	R_s (Å)
spectrin dimer	150	124
spectrin dimer	100	155
spectrin dimer	50	160
spectrin dimer	0	178
spectrin tetramer	150	250
spectrin tetramer	0**	-

** eluted with void, unable to calculate Stokes radius

Figure 2 **FTIR absorbance, second derivative, FSD deconvolution and band fit spectra of spectrin in PBS7.4/H_2O.** (a) Absorbance spectrum of spectrin (35 ± 5 mg/ml) in PBS7.4/H_2O buffer. (b) Second derivative spectrum of the absorbance spectrum in (a). (c) Deconvolved spectrum of the absorbance spectrum in (a) using deconvolution parameters FWHH = 14 cm^{-1} and K=2. (d) Band fit of the deconvolved spectrum from the (c). The spectrum was curvefit out to 1500 cm^{-1} to insure minimum error due to overlap between the Amide I and II regions. The five bands in the Amide I region yield 55 % α-helix, 9 % β-sheet and 29 % "other".

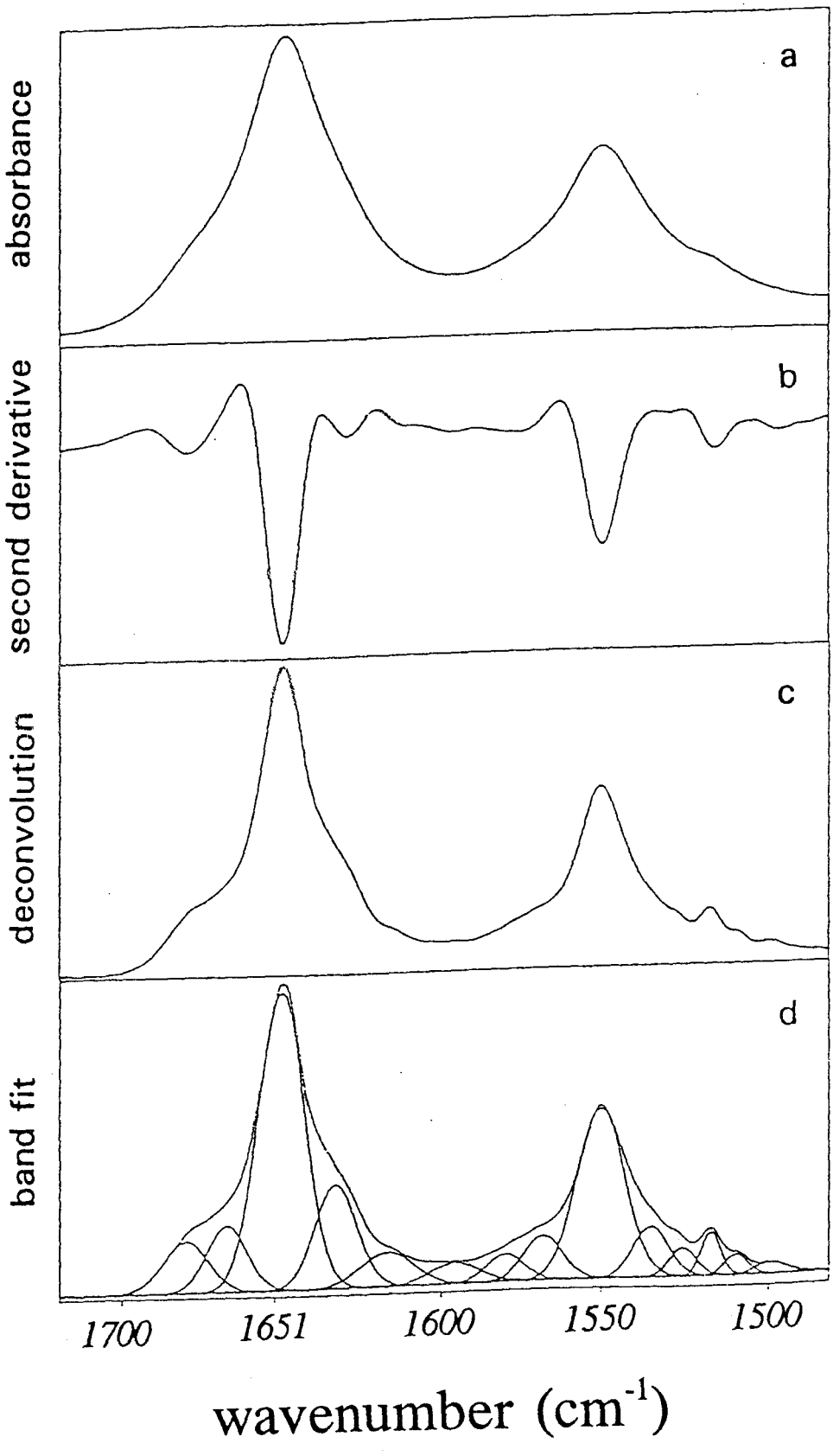
absorbance
a
second derivative
b
deconvolution
c
band fit
d
1700
1651
1600
1550
1500
wavenumber (cm-1)

amide I band is comprised of 3 major bands at 1681 cm^{-1}, 1651 cm^{-1} and 1631 cm^{-1}. The largest peak at 1651 cm^{-1} is assigned to the α-helix component (Dong *et al.*, 1990). It has been reported that the second derivative bands can be assigned and used to quantitate the secondary structure elements by measuring the area of the peaks (Dong *et al.*, 1990). However, in our case there was a large percentage of α-helix which distorts the baseline, and the second derivative spectra were not a reliable method of structure quantitation.

Figure 2c shows the FSD deconvolved spectrum corresponding to the original absorbance spectrum (Figure 2a). Band narrowing by the deconvolution operation allows the decomposition of the amide I band into its underlying components.

Figure 2d is the best band fit to the FSD deconvolved spectrum from figure 2c. Band fitting allows quantitation of the bands arising from the secondary structure elements which are narrowed as a result of the deconvolution procedure (Byler & Susi, 1986). The spectrum was curvefit to 1500 cm^{-1} to insure minimum error due to overlap between the amide I and II regions. However, for quantitation of the secondary structure our attention was focused on the amide I region only. The analysis gave rise to 5 bands under the amide I region. The positions of the bands and their relative areas are shown in Table 2. The band centered at 1651 cm^{-1} was assigned to α-helix and accounted for 55 % of the integrated intensity. The band at 1680 cm^{-1} was assigned to the β-sheet with 9 % of the area, and the bands at 1667 cm^{-1} and 1632 cm^{-1} were assigned to other structural components, including random coil and turns, to comprise the remaining 29 %. Simple analysis has assumed that the extinction for each secondary structural type is the same so that these percentages are proportional to the fraction of that secondary structure type in the protein (Byler & Susi, 1986).

Table 2 Band Fitting Peaks, Assignments and Relative Areas of Amide I and I' Regions.

H_2O buffer[a]			D_2O buffer		
Peak (cm^{-1})	Assignment[b]	Area (%)	Peak (cm^{-1})	Assignment[c]	Area (%)
1680	β-sheet	9	1675	β-sheet	3
1667	other[d]	11	1669	β-sheet	4
1651	α-helix	55	1647	α-helix	60
1632	other	18	1628	other	28
1616	unsure[e]	7	1606	unsure[e]	5

a 5 mM sodium phosphate, 150 mM sodium chloride, pH 7.4

b Assignments made from Dong *et al*, 1990 & Cantor and Shimmel, 1980.

c Assignments made from Byler & Susi, 1986.

d Other includes random coil and turns.

e This band cannot be assigned from the literature.

3.2.2 Spectrin in PBS7.4/D_2O Buffer

The absorbance spectrum of spectrin (35 ± 5 mg/ml) in PBS7.4/D_2O buffer is shown in figure 3a. The one major band is assigned as the amide I' band, which is similar to the amide I band except all absorbances are shifted to lower energy due to the increased mass of the deuterium (^2H) atom. The amide II' band (1500 - 1400 cm^{-1}, not shown) was not analyzed due to HOD absorbance interfering with the protein absorbance in this region. The low broad band between 1600 cm^{-1} and 1500 cm^{-1} is assigned to the glutamate and aspartate absorbances (Venyaminov & Kalnin, 1990). Spectrin is comprised of 10 mole % aspartic acid and 18 mole % glutamic acid (Sahr *et al.*, 1990; Winkelmann *et al.*, 1990).

The second derivative spectrum is shown in figure 3b. Three major peaks are evident at 1677 cm^{-1}, 1648 cm^{-1} and 1602 cm^{-1}. In addition, there is a shoulder at 1629 cm^{-1} on the 1648 cm^{-1} peak. The largest peak in the amide I' region at 1648 cm^{-1} is assigned to α-helix.

The FSD deconvolution spectrum of the absorbance spectrum is shown in figure 3c. The most striking feature is that the amide I' band is much broader than the amide I band. A possible explanation for the amide I' band being broader is that the absorption which arises from the random coil element in the D_2O sample is shifted more to a lower energy than are the transitions arising from the α-helix (Prestrelski, 1992; personal communication).

Figure 3d is the best band fit to the deconvolution spectrum from figure 3c. The amide I' band was used for the quantitation of secondary structure. However, the bands were fit out to the 1500 cm^{-1} for the same reason as with the H_2O spectrum. The spectrum has 5 bands under the amide I' region. The prominent band at 1647 cm^{-1} is assigned to the α-helix, which accounts for 60 % of the secondary structure. The β-sheet assignments were more

Figure 3 **FTIR absorbance, second derivative, FSD deconvolution and band fit spectra of spectrin in PBS7.4/D_2O.** (a) Absorbance spectrum of spectrin (35 ± 5 mg/ml) in PBS7.4/D_2O buffer. (b) Second derivative spectrum of the absorbance spectrum in (a). (c) Deconvolved spectrum of the absorbance spectrum in (a) using deconvolution parameters FWHH = 16 cm^{-1} and K=2. (d) Band fit of the deconvolved spectrum from (c). The spectrin was fit out to 1500 cm^{-1} for the same reason as in Figure 2d. The five bands in the Amide I' region yield 64 % α-helix, 7 % β-sheet, and 28 % "other".

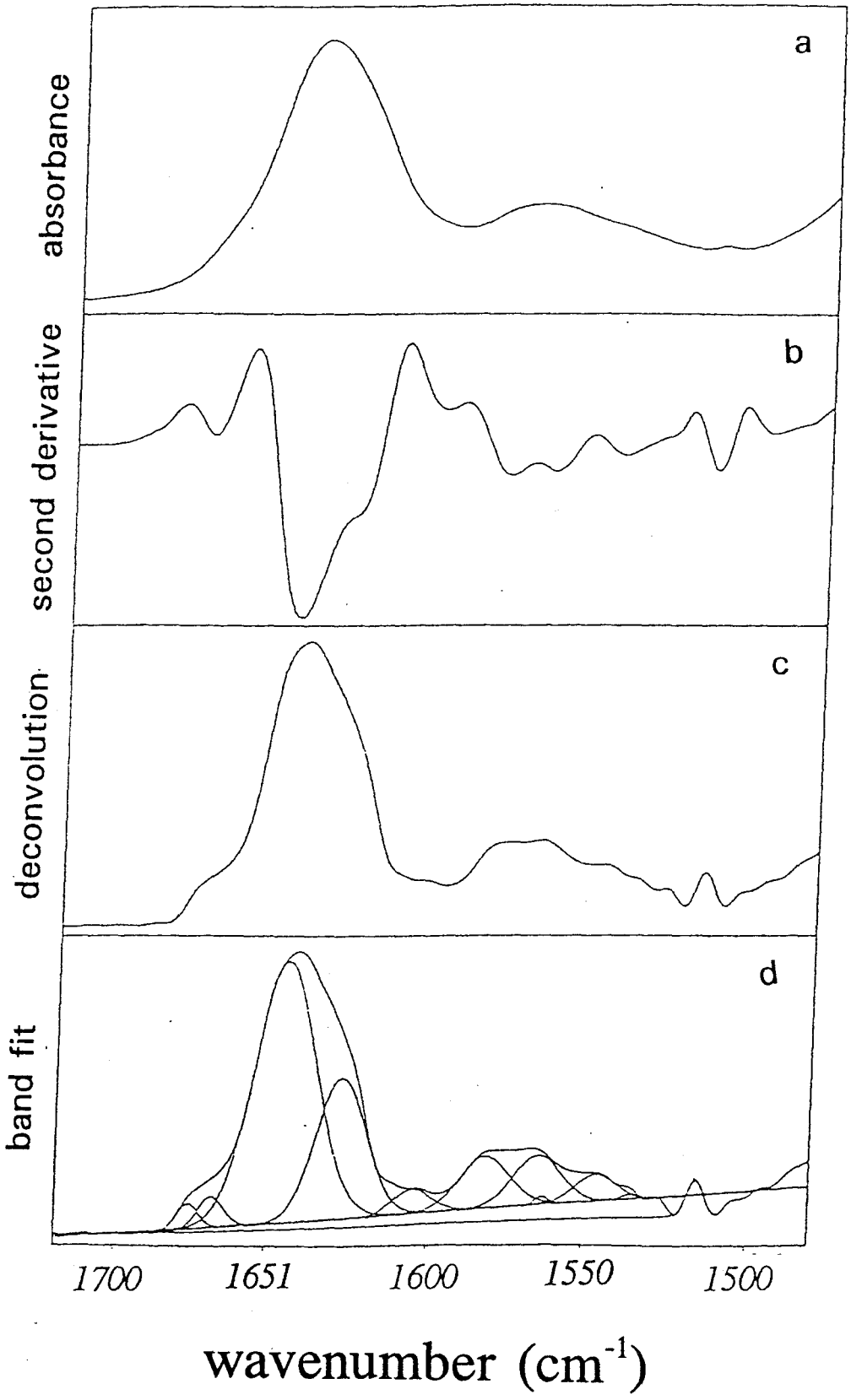
a
absorbance
b
second derivative
c
deconvolution
d
band fit
1700
1651
1600
1550
1500
wavenumber (cm-1)

difficult to assign in this spectrum. They were assigned as 1675 cm^{-1} (3 %) and 1669 cm^{-1} (4 %) for a total of 7 %. The assignment of the 1606 cm^{-1} band is questionable. The band at 1628 cm^{-1} is assigned with confidence to other, which accounts for the remaining 28 %. A summary of the assignments is given in Table 2.

3.2.3 PLS Analysis

Although band fitting provides a basis for the quantitative estimation of the secondary structure of proteins, it is not a routine procedure since there are still difficulties with obtaining artifact free resolution enhanced spectra and with the band fitting procedure (Dousseau and Pezolet, 1990). And more importantly the band assignments are a problem due to their nonuniqueness and partial deuteration of the sample. Therefore, another more robust technique using the partial least squares (PLS) method of spectral analysis was employed. We used a training set of spectra from 14 proteins of known secondary structure in H_2O buffer, recently published (Dousseau & Pezolet, 1990), to calculate a calibration spectrum for the PLS analysis. A similar quality training set of spectra for proteins in D_2O buffer was not available to us, therefore, only spectra recorded in H_2O buffer were analyzed by this method.

PLS analysis of the absorbance spectra of spectrin (35 ± 5 mg/ml) in PBS7.4 similar to that shown in figure 2a yields 59 ± 5 % (n = 5) α-helix, 16 ± 1 % β-sheet and 26 ± 3 % other (Table 3). These values are in good agreement with the band fitting results outlined above with 55 % α-helix, 9 % β-sheet and 29 % other (Table 2). Therefore, due to the objectivity and relative ease of the PLS method of analysis, all the spectra of the modified spectrin in H_2O buffer samples were analyzed with the PLS method.

3.2.4 Spectrin under Denaturing Conditions

The FTIR data of spectrin molecules under denaturing conditions (high pH, high temperature and SDS treatment) are presented in Table 3. In the high pH (2 M NaOH) and

high temperature (80 °C, spectrum recorded at 20 °C, after heating) studies, the percentage of α-helix dropped about 10 %, from 59 % to 47 % and 49 %, respectively. The percentage of β-sheet remained nearly the same (11 % and 16 %, respectively). The structural components defined as other increased to 42 % and 35 %, respectively. The SDS treatment caused an increase in the β-sheet structure to 21 % and a decrease in α-helix structure to 38%.

3.2.5 Spectrin in 5P7.4/H_2O Buffer

The spectra of spectrin in 5P7.4 (no NaCl) were obtained to study the effect on the secondary structure of changing the ionic strength of the buffer. The results of the PLS analysis are 64 ± 4 % (n = 3) α-helix, 16 ± 6 % β-sheet and 20 ± 6 % other (Table 3), similar to the results for spectrin in PBS7.4 with 150 mM NaCl. These results indicate that the secondary structure is not sensitive to ionic strength. If the H bonds, which maintain the secondary structure, are affected by the ionic strength of the buffer, one may expect to see a shift in the absorbance maximum for the α-helix absorbance band. However, the second derivative analysis of the spectra reveal that its positions were the same (1651 cm^{-1}) for spectrin in high salt buffer (PBS7.4) and in low salt buffer (5P7.4). Indeed if the H bonds were to change the helix would probably change and the total amount of helix as well as the position of the center position would change. However, since we see no change we can conclude that the helix is not affected locally by a change in ionic strength.

3.2.6 Spectrin incubated with BPS LUVs

The absorbance spectra of spectrin incubated with BPS LUVs in PBS7.4 were analyzed using the PLS method, and the results are similar to those of spectrin in PBS7.4, with 59 ± 1 % (n = 2) α-helix, 19 ± 1 % β-sheet and 23 ± 1 % other (Table 3).

Table 3 Percentage of Secondary Structure Components from PLS Analyzed Spectra of Spectrin and Modified Spectrin in 5P7.4 with Various Concentrations of NaCl.

[NaCl]	150 mM	0 mM	150 mM	0 mM	150 mM	150 mM
Treatment	-	-	2 M NaOH	80 °C[a]	1 % SDS	BPS LUVs
n	5	3	2	1	2	2
α-helix	59 ± 5	64 ± 6	47 ± 11	49	38 ± 5	59 ± 1
β-sheet	16 ± 1	16 ± 4	11 ± 5	16	21 ± 4	19 ± 1
other	26 ± 3	20 ± 6	42 ± 7	35	41 ± 2	23 ± 1

[a]Sample held at 80 °C for 10 min, spectrum collected at 20 °C.

CHAPTER IV

DISCUSSION

4.1 Validity and Sensitivity of FTIR to Determination of Secondary Structure

To evaluate the validity and reliability of using FTIR as a tool to determine the secondary structure of spectrin, it is important to first discuss the potential problems in using FTIR analysis methods to quantitate secondary structure. Although band fitting methods to FSD deconvolved spectra are widely used in the literature (Byler & Susi, 1986; Wantyghem *et al.*, 1990; He *et al.*, 1991; Prestrelski *et al.*, 1991), they are limited due to the following inherent problems. Care must be taken not to over-deconvolve the spectrum because over deconvolution produces negative side lobes on absorption bands and can result in artificial bands from noise or incomplete compensation of water vapor (Mantsch *et al.*, 1988). However, since we used a relatively low FWHH maximum parameter, we avoided serious band area changes by not over deconvolving, as is evident by the absence of side lobes on our FSD deconvolved spectra. There is also a problem with assignment of the bands, and often a complete assignment cannot always be made. In addition, the helix and random coil band positions overlap greatly in the H_2O spectra, therefore prudence must be used in assigning the proper band size to these bands. We have shown that these bands are better resolved in D_2O solution, but one must still be concerned with incomplete deuteration. Further difficulties in assignment may arise due to noise, water vapor, amino acid side chains or contaminants (Lee *et al.*, 1990). Another problem which has been disputed in the literature is the assumption that the extinction coefficients of the bands assigned to the different structures are identical. Evidence for changes in extinction coefficients as proteins undergo

conformational changes is now emerging (Jackson *et al.*, 1989). However, it appears that variations in cell path length are more important than variations in absorption coefficient (Lee *et al.*, 1990). Therefore, within the experimental error the assumption that the extinction coefficients are the same is valid. Finally, the PLS method we employed uses only the proteins in H_2O buffer which gives rise to very low protein absorptions compared to solvent absorptions. However, we performed careful and systematic subtraction of the background; thus eliminating spectral distortion due to the water absorption.

When the band fitting method is judiciously applied the error in prediction of structure type is about 4 % (Byler & Susi, 1986), and for the PLS method we employed the error in prediction of structure type is reported to be about 5 % (Dousseau & Pezolet, 1990). An awareness of potential pitfalls and careful data collection can lead to an adequate prediction of secondary structure using FTIR. More importantly since the FTIR band fitting and FTIR PLS analysis gave similar values for the secondary structure components as the previous CD studies (Ralston, 1978), we have concluded that the values that we have determined are reliable. Further, since the potential error was less for PLS analysis method than the band fitting method, we decided to use the PLS method for the majority of our analysis.

The secondary structural changes of spectrin treated with heat, 2 M NaOH and 1 % SDS detected by FTIR demonstrate the sensitivity of the FTIR method to structural changes in the molecule. Heat and alkaline treatment denature proteins and cause hydrolysis of the peptide bonds, yielding smaller fragments of the protein molecule (Stryer, 1981). The effects of these treatments were detected as a decrease in α-helix content by about 10 %. SDS treatment had the greatest effect on the α-helix content, which decreased from 59 ± 5 % to

38 ± 5 % and other structural components increased from 26 ± 3 % to 41 ± 2 %. SDS treatment has been shown, using gel filtration chromatography, to cause the spectrin molecule to unfold into a rod-like structure (Nozaki *et al.*, 1976). It is important to note that the trends of change in secondary structure are considered more important than the exact percentage value because they demonstrate the sensitivity of the method.

As a measure of the sensitivity of the α-helix band center position to the strength of H bond, we measured the FTIR spectrum in H_2O and D_2O buffer. The amide I and II band maxima shifted from 1651 cm^{-1} to 1648 cm^{-1} and from 1551 cm^{-1} to 1460 cm^{-1}, respectively, upon changing from H_2O buffer to the D_2O buffer, thus reflecting the decreased strength of deuterium bonds as compared to hydrogen bonds (Jackson *et al.*, 1991). Therefore, the technique is sensitive to the strength of the H bonds in spectrin.

The position of the α-helix center frequency has been shown to vary from about 1640 cm^{-1} to 1656 cm^{-1} depending on the length of the α-helix (Dousseau & Pezolet, 1990). The variation in peak frequency has been correlated with the proportion of distorted helical structures, such as those at the ends of a helix (disordered helix), compared to the standard α-helix (ordered helix). For proteins of high α-helical content, the lower the frequency of the α-helical band center correlates with a larger proportion of ordered helix to disordered helix. The α-helix center frequency at 1651 cm^{-1} for spectrin in PBS7.4/H_2O is lower than that of hemoglobin (1655 cm^{-1}) and higher than that of tropomyosin (1642 cm^{-1}) (Dousseau & Pezolet, 1990), indicating that the proportion of disordered helix to ordered helix is less than that for myoglobin, which is made up of 8 short helical segments about 30 Å long (Stryer, 1981), but lower than that in the fibrous tropomyosin molecule, which is a 2 stranded extended α-helical rod 385 Å long (Stryer, 1981). Therefore, for proteins of high α-helical content, such as spectrin, the relative position of the helix center frequency can be used to get an estimate of the α-helix length. This result, that the length of the α-helix is between 30 Å and 385 Å, supports a recent model of spectrin which predicts the helix length to be 50.5 Å (Parry *et al.*, 1992). In this model, the 106 amino acid structural repeating unit in spectrin

has a triple helical structure with a left handed coiled-coil structure stabilized by maximum ion pairing between the helices. The helices are held together by ionic bonds formed between charged amino acid side chains which are arranged in a heptad manner, *ie.* the periodicity of the amino acid types (polar or apolar) is repeated every seventh amino acid (*a,b,c,d,e,f,g*, where *a* and *d* are apolar and *e* and *g* are polar, Parry *et al.*, 1992). Based on optimum ion pairing, the length of the axial repeat in this model is 50.5 Å.

4.2 Effect of Ionic Strength on Spectrin

Decreasing the salt concentration causes the elution volumes of pure spectrin on agarose gels to decrease (Ralston , 1976) implying that the isolated spectrin molecules swell with decreasing ionic strength. Furthermore, erythrocyte skeletons, which are largely composed of a two-dimensional array of spectrin, reversibly expand and contract upon decreasing and increasing the buffer ionic strength (Shen *et al.*, 1986; Svoboda *et al.*, 1992). Thus, it is important to understand the structural response of spectrin to ionic strength.

The Stokes radius is a convenient parameter to measure the response of a protein dimension in solution to changes in ionic strength. The Stokes radius for the spectrin dimer in 100 mM NaCl was reported to be 102 Å (Kam *et al.*, 1977) and for tetramer in 100 mM NaCl was 200 Å (Ralston, 1978), as determined by hydrodynamic measurements in tris and phosphate buffer, respectively. However, carefully controlled experiments of the Stokes radius of spectrin in buffers of varying ionic strength had not been done previously. The Stokes radius of spectrin calculated by its sedimentation coefficient was shown to correlate with the partition coefficient (K_{av}) of gel filtration column chromatography (Kam *et al.*, 1977). Using gel filtration chromatography, we found that the Stokes radius of spectrin dimer in 150 mM NaCl was 124 Å and increased to 178 Å in buffer without NaCl. The radius for spectrin tetramer in 150 mM NaCl was 250 Å and increased to ≥ 330 Å in buffer without NaCl. The values in high salt buffer were slightly higher than the published values (Ralston, 1978; Kam *et al.*, 1977). Since the FTIR technique has shown to be sensitive to secondary

structural changes in spectrin under denaturing conditions and is sensitive to the strength of the H bonds, we used it to probe the effects of change in ionic strength on the spectrin dimer. The secondary structural components were not affected by NaCl concentrations in the buffer (Table 3), and the α-helix center peak frequency remained the same (1651 cm^{-1}) indicating that the strength of the H bonds in the helix were not affected either.

It is conceivable that the ionic strength in the medium affects the ionic interactions between the heptads as suggested in the coiled coil model (Parry *et al.*, 1992) to change the relative spatial arrangement of the helices. When the helices are lined up to form maximum ion pairing, a shorter overall dimension is obtained. When the helices shift their vertical register, a longer overall dimension is obtained. The difference in the Stokes radius for spectrin dimers between low and high ionic strength buffers was about 54 Å. If the helices, within the repeating unit, shift relative to one another by about 1-2 Å, this could account for the increase in R_s for the molecule, without any apparent or detectable change in secondary structure. Further, since FTIR is a spectral technique sensitve to the short range interactions, if there was a difference in the packing or length of the helix it would have been evident in the FTIR spectrum. A model, explaining our FTIR and Stokes radii data, based on the model presented by Parry *et al.*, (1992) is presented in figure 4.

4.3 Spectrin with BPS LUVs

Spectrin has been shown to have an affinity for negatively charged lipid vesicles with a binding constant of $K_a \sim 10^7$ mol/L and to actually penetrate the lipid bilayer (Sikorski *et al.*, 1987; Cohen *et al.*, 1986). Therefore, we examined the secondary structure of spectrin in the presence of BPS LUVs. No change in secondary structure was detected with FTIR upon binding to BPS LUVs. These results are consistent with the hypothesis that a small positively charged domain on the spectrin molecule is responsible for the binding to negatively charged

Figure 4 **Model of 106 amino acid repeating domain of spectrin in high and low salt buffer.** Model of spectrin 106 amino acid repeating segment as proposed by Parry *et al.* (1992) (left). Modified model in which the proposed α-helices have shifted slightly, by about 2 Å, due to a lowering in ionic strength (right).

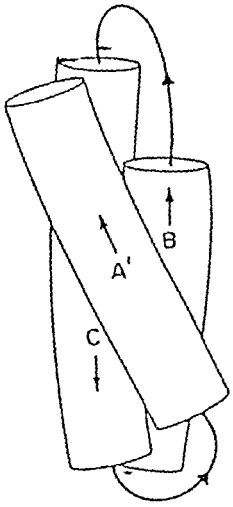
A'
B
C

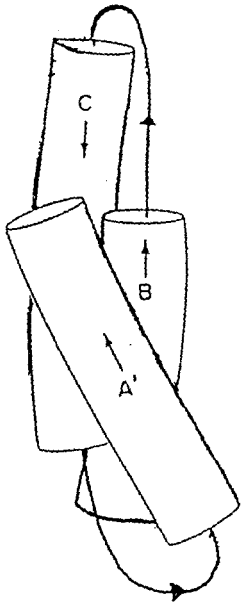
C
B
A'

lipid bilayers (Mombers *et al.*, 1980; Maksymiw *et al.*, 1987). An application of this technique could be to test the spectrin-lipid interaction hypothesis that hydrophobic interaction is responsible for spectrin binding to zwitterionic lipids such as phosphatidylcholine and phosphatidylethanolamine (Mombers *et al.*, 1980). In such cases a structural change would be expected because a greater change in structure would be required in exposing the hydrophobic interior of the spectrin molecule. More experiments must be done to elucidate the change in secondary structure of spectrin in the presence of phospholipid vesicles.

REFERENCES

Bennett, V. (1990) Physiological Reviews 70, 1029-1065.

Budzynski, D.M.; Benight, A.S.; LaBrake, C.C. & Fung, L.W.-M. (1992) Biochemistry 31, 3653-3660.

Byler, D.M. & Susi, H. (1986) Biopolymers 25, 469-487.

Calvert, R.P.; Bennett, V. & Gratzer, W. (1980) Eur. J. Biochem. 107, 355-361.

Cantor, C.R. & Schimmel, P.R. (1980) Biophysical Chemistry, PartII: Techniques for the Study of Biological Structure and Function W.H. Freeman, NY.

Clague, M.J.; Harrison, J.P.; Morrision, I.E.G.; Wyatt, K.J. & Cherry, A.J. (1990) Biochemistry 29, 3898-3904.

Clarke, M. (1971) Biochem. Biophys. Res. Comm. 45, 1063-1070.

Cohen, A.M.; Liu, S.-C.; Derick, L.H. & Palek, J. (1986) Blood 68, 920-926.

Dodge, J.T.; Mitchell, D. & Hanahan, D.J. (1963) Arch. Biochem. Biophys. 100, 119-130.

Dong, A.; Huang, P. & Caughey, W.S. (1990) Biochemistry 29, 3303-3308.

Dousseau, F.; Therrien, M.; & Pezolet, M. (1989) Appl. Spectrosc. 43, 538-542.

Dousseau, F. & Pezolet, M. (1990) Biochemistry 29, 8771-8779.

Dubreuil, R.R.; Byers, T.J.; Sillman, A.L.; Bar-Zvi, D.; Goldstein, L.S.B. & Branton, D. (1989) J. Cell Biol. 109, 2197-2205.

Elgsaeter, A. (1978) Biochim. Biophys. Acta 536, 235-244.

Fairbanks, G.; Steck, T.L. & Wallach, D.F.H. (1971) Biochemistry 10, 2606-2617.

Fung, L.W.-M. & Johnson, M.E. (1983) J. Magn. Reson. 51, 233-244.

Fung, L.W.-M.; Lu, H.-A.; Hjelm, R.P.,Jr. & Johnson, M.E. (1986) FEBS Lett. 105, 379-383.

Fung, L.W.-M.; Lu, H.-A.; Hjelm, R.P.,Jr. & Johnson, M.E. (1989) Life Sci. 44, 735-740.

He, W.-Z.; Newell, W.R.; Haris, P.I.; Chapman, D. & Barber, J. (1991) Biochemistry 30, 4552-4559.

Jackson, M.; Harris, P.I. & Chapman, D. (1991) Biochemistry 30, 9681-9686.

Kam, Z.; Josephs, R.; Eisenberg, H. & Gratzer, W.B. (1977) Biochemistry 16, 5568-5572.

LaBrake, C.C. & Fung, L.W.-M. (1992) J. Biol. Chem. *in the press*

Lee, D.C.; Haris, P.I.; Chapman, D. & Mitchell, R.C. (1990) Biochemistry 29, 9185-9193.

Maksymiw, R.; Sen-Fang, S.; Gaub, H. & Sackmann, E. (1987) Biochemistry 26, 2983-2990.

Mantsch, H.H.; Moffat, D.J. & Casal, H.L. (1988) J. Mol. Struct. 173, 285-298.

Marchesi, S.L.; Steers, E.; Marchesi, V.T. & Tillach, W.T. (1970) Biochemistry 9, 50-57.

Mikkelsen, A. & Elgsaeter, A. (1978) Biochim. Biophys. Acta 536, 245-251.

Mikkelsen, A.; Stokke, B.T. & Elgsaeter, A. (1984) Biochim. Biophys. Acta 786, 95-102.

Mombers, C.; DeGier, J.; Demel, R.A. & BanDeenen, L.L.M. (1980) Biochim. Biohys. Acta 603, 52-62.

Nozaki, Y.; Schecter, N.M.; Reynolds, J.A. & Tanford, C. (1976) Biochemistry 15, 3884-3890.

Parry, D.A.D.; Dixon, T.W. & Cohen, C. (1992) Biophys. J. 61, 858-867

Prestrelski, S.J.; Arakawa, T.; Kenney, W.C. & Byler, D.M. (1991) Arch. Biochem. Biophys. 285, 111-115.

Ralston, G.B. (1976) Biochim. Biophys. Acta 443, 387-393.

Ralston, G.B. (1978) J. Supramol. Struc. 8, 361-373.

Sahr, D.E.; Laurila, P.; Kotula, L.; Scarpa, A.L.; Coupal, E.; Leto, T.L.; Linnenbach, A.J.; Winkelmann, J.C.; Speicher, D.S.; Marchesi, V.T.; Curtis, P.J. & Forget, B.G. (1990) J. Biol. Chem. 265, 4434-4443.

Sarver, R.W.,Jr. & Kreuger, W.C. (1991) Analyt. Biochem. 194, 89-100.

Shen, B.W., Josephs, R. & Steck, T.L. (1986) J. Cell Bio. 102, 997-1006.

Shotton, D.M.; Burke, B.E. & Brank, D. (1979) J. Mol. Biol. 131, 303-329.

Sikorski, A.F., Michalak, K. & Bobrowska, M. (1987) Biochim. Biophys. Acta 904, 55-60.

Speicher, D.V.; GAry, D. & Marchesi, V.T. (1983) J. Biol. Chem. 258, 15938-15947.

Stryer, L. (1981) Biochemistry W.H.Freemen, NY.

Surewicz, W.K. & Mantsch, H.H. (1988) Biochim. Biophys. Acta 952, 115-130.

Svoboda, K.; Schmidt, C.F.; Branton, D. & Block, S.M. (1992) Biophys. J. 61, A523 (abstract).

Ungewickell, E. & Gratzer, W. (1978) Eur. J. Biochem. 88, 379-385.

Venyaminov, S.Y. & Kalnin, N.N. (1990) Biopolymers 30, 1243-1257.

Wantyghem, J.; Baron, M.-H.; Picquart, M. & Lavialle, F. (1990) Biochemistry 29, 6600-6609.

Winkelmann, J.C.; Leto, T.L.; Watkins, P.C.; Eddy, R.; Shows, T.B.; Linnenbach, A.J.; Sahr, K.E.; Kathuria, N.; Marchesi, V.T. & Forget, B.T. (1988) Blood 72, 328-334.

Winkelmann, J.C.; Chang, J.-G.., Tse, W.T.; Scarpa, A.L., Marchesi, V.T. & Forget, B.G. (1990) J. Biol. Chem. 265, 11827-11832..

Xu, Y.; Prabhakaran, M,; Johnson, M.E. & Fung, L.W.-M. (1990) J. Biomol. Struct. & Dynam. 8, 55-62.

APPENDIX

MANUSCRIPT IN THE PRESS

(Journal of Biological Chemistry, August 1992)

PHOSPHOLIPID VESICLES PROMOTE HUMAN HEMOGLOBIN OXIDATION[#]

Cynthia C. LaBrake and Leslie W.-M. Fung[*]

Department of Chemistry, Loyola University of Chicago

Chicago, IL 60626

[#]This work was supported, in part, by USPHS Grants R01-HL38361, S15-HL41756, by the American Heart Association of Metropolitan Chicago and by funds from Loyola University of Chicago.

Running title: lipid vesicles promote Hb oxidation

Send proofs to: Dr. Leslie Fung, Department of Chemistry, Loyola University of Chicago, 6525 N. Sheridan Road, Chicago, IL 60626. Phone: (312) 508-3128. FAX: (312) 508-3086.

SUMMARY

We have studied the heme oxidation kinetics of purified human hemoglobin (Hb) in the presence of lipid vesicles of dipalmitoyl phosphatidylcholine and bovine brain phosphatidylserine that exhibited minimal lipid peroxidation. We showed that the lipid vesicles enhanced Hb oxidation, and that small unilamellar vesicles (SUVs) exerted a larger effect than large unilamellar vesicles (LUVs). We have determined pseudo first-order rate constants for the initial disappearance of oxygenated ferrous Hb (k_O) and for the initial formation of several ferric Hb species (methemoglobin, hemichrome and choleglobin) in the presence of SUVs and LUVs. k_O and other rate constants depended linearly on lipid-to-hemoglobin molar ratio (Lipid/Hb), with $k_O^{SUV}(h^{-1}) = k_O^{auto}(h^{-1}) + 3.7 \times 10^{-3} \times$ Lipid/Hb, and $k_O^{LUV}(h^{-1}) = k_O^{auto}(h^{-1}) + 0.2 \times 10^{-3} \times$ Lipid/Hb, where k_O^{auto} is the rate constant for Hb autoxidation in the absence of vesicles. Thus, in the absence of lipid peroxidation products, lipid vesicles themselves promote Hb oxidation by enhancing the rate of Hb oxidation. The enhanced oxidation was inhibited by catalase, but not by butylated hydroxytoluene. The rate constants were independent of Hb concentration, in the range of about 3.1 μM to 100 μM. We suggest that the lipid surface properties, including surface curvature, surface energy and hydrophobicity, promote hemoglobin oxidation.

Extensive investigations of Hb[1] oxidation using purified Hb in various buffer systems have been carried out (Weiss, 1964; Misra and Fridovich, 1972; Winterbourn, 1985a; Caughey and Watkins, 1985). Although the exact mechanism for heme oxidation in Hb or myoglobin is not clear (Shikama, 1990; Watkins *et al.*, 1985; Shikama, 1984), quantitative studies have demonstrated that Hb autoxidation is mediated by protons, enhanced by anions (Wallace *et al.*, 1974), and may involve heme deoxygenation prior to electron transfer (Wallace *et al.*, 1982). Most of these studies were carried out in the absence of membrane components, whereas *in vivo* Hb oxidation occurs in an environment enclosed by cell membranes. Furthermore, it has been shown that Hb interacts with membrane components on the inner leaflet of the erythrocyte (Kimelberg, 1976; Szundi *et al.*, 1980; Fung, 1981; Shviro *et al.*, 1982; Rauenbuehler *et al.*, 1982; Kaul and Köhler, 1983; Walder *et al.*, 1984). Thus, it is useful to study Hb oxidation in the presence of various lipid and other inner leaflet membrane components.

The study of Hb oxidation in the presence of lipid molecules is also important in developing Hb-containing liposomes as oxygen-carrying fluid (Rabinovici *et al.*, 1990; Ligler *et al.*, 1989; Brandl *et al.*, 1989). It is vital to maintain Hb in the reduced state in the presence of lipid to provide functioning Hb to carry oxygen in liposomes.

Recent studies of lipid vesicle - Hb systems suggested that lipid peroxidation products caused spectral changes in oxyHb (Itabe *et al.*, 1988; Szebeni *et al.*, 1984; Szebeni *et al.*, 1985; Szebeni *et al.*, 1988). No kinetic data were provided in these studies - - probably, in part, due to some of the experimental difficulties that we discuss below. It was not clear whether the lipid bilayer exhibited intrinsic effects on Hb oxidation. In this work, we have monitored Hb oxidation in the presence of small and large unilamellar vesicles prepared from lipids with minimal peroxidation, and developed methods using optical spectroscopy to obtain kinetic information on the *initial* Hb oxidation in the presence of vesicles. Bovine brain phosphatidylserine (BPS), which contains unsaturated fatty acids, and dipalmitoyl

phosphatidylcholine (DPPC), which contains only saturated fatty acids, were used. BPS was selected for detailed studies, because PS is one of the major phospholipid components found in the inner leaflet of the erythrocyte membrane bilayer (Marinetti and Crain, 1978). Furthermore, BPS includes a mixture of saturated and unsaturated acyl chains similar to the chemical composition found in erythrocyte phospholipids (Ways and Hanahan, 1964; Yamamoto *et al.*, 1985). Pseudo-first order rate constants for the initial disappearance of ferrous Hb, and for the formation of several ferric Hb species (methemoglobin, hemichrome and choleglobin) were determined for the Hb oxidation reactions in the presence of vesicles. The kinetic data showed that both SUVs and LUVs enhance Hb oxidation, but to different extents. Control experiments were carried out to ensure that lipid peroxidation products were not responsible for the observed vesicle effects.

MATERIALS AND METHODS[2]

RESULTS

Hb Oxidation

A typical spectrum of partially oxidized oxyHb in the absence of lipid vesicles in 23 mM sodium phosphate buffer with 2 mM EDTA and 127 mM NaCl at pH 7.4 (PEN7.4) showed reduced intensity at 540 and 577 nm, and increased intensity at 630 nm at time (t) = 22 h, when compared with the oxyHb spectrum at t = 0 (Fig 1A). These spectra were similar to published spectra obtained under similar conditions (Antonini and Brunori, 1972; Watkins *et al.*, 1985; Winterbourn, 1985b). The addition of SUVs to Hb dramatically enhanced the reduction in intensity at 540 and 577 nm. Fig 1B shows that the time period to obtain spectra similar to those obtained in Fig 1A was reduced from 22 h to about 30 min in the presence of SUVs at a lipid concentration of 2.3 mg/ml with Hb concentration at 0.21 mg/ml. These SUV-enhanced spectral changes were not observed when oxyHb was replaced with oxygenated hemolysate or COHb (Fig 1C).

The spectral changes observed in Fig 1B suggested lipid-enhanced Hb oxidation. After several potential problems were addressed[3], the data were analyzed quantitatively to give kinetic information on the enhanced oxidation.

Rate Constants

Fig 2A shows the logarithmic values of oxyHb concentration as a function of time (rate constant plot, assuming that the oxidation is a pseudo first-order reaction) for a typical autoxidation experiment. The oxyHb concentrations remained linear for about 50 h in the absence of lipid vesicles. The slope obtained from the linear portion of these data was the pseudo first-order rate constant (k_O) for the initial disappearance of oxyHb. A linear fit of data in Fig 2A yielded an autoxidation rate constant (k_O^{auto}) of 0.018 h^{-1}, with a correlation coefficient (R^2) of 0.998. Data from multiple runs gave an average k_O^{auto} value of 0.030 ±

0.010 h^{-1}, in good agreement with the published value of 0.042 h^{-1} (Watkins *et al.*, 1985).

Since metal ions are known to affect Hb oxidation, we have checked the effectiveness of EDTA for removing metal ions in samples. A Hb sample with 4 μM $CuSO_4$ added in a buffer solution similar to PEN7.4, but without EDTA, exhibited a k_O^{auto} of 0.417 h^{-1}, more than an order of magnitude higher than those without added $CuSO_4$ but in PEN7.4 buffer. The rate constant for the same sample, but treated with Chelex, was 0.031 h^{-1}. The rate constant for a sample without Chelex, but with 2 mM EDTA was 0.022 h^{-1}, and the rate constant for a sample in PEN7.4 buffer and with Chelex treatment was 0.025 h^{-1}. The last three rate constants were in good agreement with the above-mentioned average k_O^{auto} of 0.030 h^{-1}. Thus these data indicated that either Chelex or 2 mM EDTA treatment was sufficient to remove the metal ions in μM concentration in samples. All our samples were prepared in buffer containing 2 mM EDTA (PEN7.4).

For a 0.20 mg/ml Hb samples containing about 2 mg/ml BPS SUVs, the linear portion in the rate constant plot shortened to about 12 min. A typical set of data, as shown in Fig 2B, exhibited an excellent linear fit (R^2 of 0.998), to give a rate constant (k_O^{SUV}) of 3.91 h^{-1}. The excellent linear fit suggests that reliable rate constants for the *initial* disappearance of oxyHb in the presence of lipid vesicles can be obtained optically. Reproducibility of these data was also very good. The average k_O^{SUV} value for six separate runs (with 0.20 ± 0.02 mg/ml Hb and 2.11 ± 0.03 mg/ml lipid) was 3.20 ± 0.52 h^{-1}, with a coefficient of variability of 15.6 %. The average rate constants for the formation of metHb, hemichrome and choleglobin were also obtained from the data as 1.32 ± 0.20 h^{-1}, 1.03 ± 0.23 h^{-1}, and 0.33 ± 0.16 h^{-1}, respectively. These values were also higher than the corresponding values for the autoxidation experiments (0.02 ± 0.01 h^{-1}, < 0.01 h^{-1} and < 0.01 h^{-1}, respectively).

Lipid to Hemoglobin Molar Ratio

For most of the rate constant measurements, we held Hb concentrations constant at about 0.20 mg/ml (3.1 μM) and varied lipid concentrations, ranging from 0.25 mg/ml to 2.5 mg/ml. These concentrations corresponded to lipid-to-Hb molar ratios (Lipid/Hb) ranging from about 100 to 1000, assuming a molecular weight of 64,000 for Hb and 800 for BPS. Fig 3 shows that k_O^{SUV} depended linearly on Lipid/Hb, with a slope of 0.0037, to give the following relationship between k_O^{SUV} and Lipid/Hb. $k_O^{SUV}\ (h^{-1}) = k_O^{auto}\ (h^{-1}) + 3.7 \times 10^{-3}$ x Lipid/Hb.

We also prepared samples with various Hb concentrations, ranging from 0.20 mg/ml (3.1 μM) to 7 mg/ml (109.3 μM), and lipid concentrations ranging from 0.25 mg/ml to 9 mg/ml to maintain Lipid/Hb of 100 or 200. We found that at either Lipid/Hb value, the values of k_O^{SUV} remained similar as the Hb concentrations increased from 12.4 μM to 437 μM in heme (Fig 4). Since we could not prepare SUVs at about 18 mg/ml, we were unable to obtain a sample with Lipid/Hb of 200 and Hb concentration at about 400 μM in heme.

Effects of BPS LUVs on Hb Oxidation Rate Constants

We found that the extruded LUVs enhanced Hb oxidation to a lesser extent than sonicated SUVs, at similar Lipid/Hb. For LUVs at about 2 mg/ml lipid concentration and 0.2 mg/ml Hb (Lipid/Hb = 800), the rate constants (k_O^{LUV}) were about 0.29 ± 0.07 h^{-1} (n = 7), about an order of magnitude higher than k_O^{auto}, but an order of magnitude smaller than k_O^{SUV}. The average values of the rate constants for the formation of metHb, hemichrome and choleglobin were 0.11 ± 0.02 h^{-1} (n = 7), 0.07 ± 0.02 h^{-1} and 0.04 ± 0.07 h^{-1}, respectively. The LUV-enhanced oxidation rate constants also depended linearly on Lipid/Hb, with a slope of 0.0002 (Fig 5) to give $k_O^{LUV}\ (h^{-1}) = k_O^{auto}\ (h^{-1}) + 0.2 \times 10^{-3}$ x Lipid/Hb.

Potential Artifacts in SUV and LUV Sample Preparations

Since it is well known that ultrasonic irradiation of water promotes the production of hydroxyl free radicals and hydrogen peroxide (Lorimer and Mason, 1987; Almog *et al.*, 1991), it is crucial to check whether the different methods used in preparing these vesicles were responsible for the differences discussed above. We prepared LUVs from lipid extracted from SUVs with chloroform, methanol and water (Bligh and Dyer, 1959), and found that the k_O for these SUV-extruded LUVs was similar to those of LUVs, as shown in Fig 5, indicating that sonication did not introduce artifacts in oxidation. We also subjected a sample of LUVs to sonication and centrifugation, similar to the steps used in preparing SUVs. The k_O for these LUV-sonicated SUVs was larger than for the control LUV sample, and was actually similar to those obtained for samples containing SUVs, as shown in Fig 3. Thus the effects observed with SUV and LUV samples were not simply due to artifacts in sample preparations.

Effects of DPPC Vesicles

We also prepared SUVs and LUVs with DPPC, which contains only saturated fatty acids. The k_O^{SUV} and k_O^{LUV} values for DPPC are very similar to the corresponding ones for BPS, as shown in Fig 3 and Fig 5 respectively, indicating that neither the head group nor the degree of fatty acid saturation play a critical role in the enhanced oxidation process.

Effects of BHT on Hb Oxidation Rate Constants

The addition of butylated hydroxytoluene (BHT) (about 0.5 – 1.5 mM) to samples did not eliminate the vesicle-enhanced oxidation. For samples containing BPS SUVs, the average ratio of k_O^{SUV} with and without BHT was 0.93 ± 0.26 (n = 18), with Lipid/Hb ranging from 150 to 1000. For samples containing BPS LUVs, the average ratio of rate constants with and without BHT was 1.09 ± 0.73 (n = 12), with Lipid/Hb ranging from 1000 to 3000.

Catalase Effects on Hb Oxidation Rate Constants

We added various amounts of catalase to purified Hb samples and monitored the oxidation in samples containing SUVs with a Lipid/Hb value ranging from about 100 to 1,000. Addition of low levels of catalase (200 units/gm-Hb) reduced the rate constant by about 30 %, for example, from 2.5 h^{-1} to 1.8 h^{-1} for a Lipid/Hb of 800. Addition of catalase (1,500 units/gm-Hb or more) reduced the rate constant by about 95 %, for example, from 2.4 h^{-1} to 0.1 h^{-1} at a Lipid/Hb value of 930, and from 0.82 h^{-1} to 0.04 h^{-1} at a Lipid/Hb of 200.

The effect of adding catalase to samples with oxidation already in progress was also studied. At t = 7 - 11 min after Hb was incubated with SUVs, the sample consisted of about 70 to 80 % oxyHb and 20 - 30 % oxidized Hb. The oxidation rate decreased substantially upon addition of catalase (39,000 units/gm-Hb) (Fig 6). The rate constant at a Lipid/Hb of about 940 was about 2.2 h^{-1} before the addition of catalase. Upon addition of catalase at t = 7 min the rate constant decreased to about 0.4 h^{-1}. These results demonstrate substantial inhibition of lipid-enhanced Hb oxidation by catalase.

These results also suggest that catalase with a concentration of about 1.6 x 10^4 units/gm-Hb may be responsible, at least in part, for the very slow oxidation observed in hemolysate samples containing SUVs (Fig 1C).

Lipid Peroxidation Products in BPS Vesicles

Lipid peroxidation has been studied extensively in many biological samples. A number of techniques are available for measuring peroxidation. Each technique measures something different, and no one method by itself appears to be very accurate, but a combination of methods can be used to indicate the extent of lipid peroxidation (Gutteridge and Halliwell, 1990). To determine the concentrations of lipid peroxidation products in our vesicle systems we used the following three methods: (1) Conjugated diene assay with A_{233}/A_{215} values, (2) Assay for detecting malondialdehyde (MDA) and the thiobarbituric acid reactive products (TBARP), and (3) GC-mass spectrometry measurements for fatty acid

composition. Table I shows the results of these measurements. Also listed in Table I are literature values from various experiments, with conditions not necessarily the same as ours, to provide reference points for the level of lipid peroxidation as measured by these assay methods. For example, for conjugated diene measurements, a value of 0.08 was considered low, whereas a value of 0.66 was considered to be a high level of lipid peroxidation (Szebeni and Toth, 1986). The values for our SUVs and LUVs in Table I are less than 0.18, which suggest that little lipid peroxidation occurred in both SUV and LUV samples. For TBARP level, values of 4 - 18 nm MDA/μmol lipid (Szebeni and Toth, 1986), or 6 - 23 nm MDA/μmol lipid (Itabe *et al.*, 1988) were observed in the presence of Hb-induced lipid peroxidation. Again, our values of 1.3 - 1.4 nm MDA/μmol lipid in SUVs and LUVs suggested that little lipid peroxidation occurred in the SUV and LUV samples. GC-mass spectrometry results showed that both the SUV and LUV samples consisted of essentially the same fatty acid compositions as those of the stock solution. Thus, our data suggest that both BPS SUVs and BPS LUVs exhibited very similar, i.e. very low levels of, lipid peroxidation. Since it has been reported that Hb is a biologic Fenton reagent (Sadrzadeh *et al.*, 1984), and that Hb induces lipid peroxidation (Itabe *et al.*, 1988; Szebeni *et al.*, 1988), we also examined the vesicle samples after incubation with Hb for 30 min. However, since Hb interferes with the conjugated diene and MDA (Kikugawa *et al.*, 1981) assays, we only carried out the GC-mass spectrometry measurements on these samples. The data show little fatty acid composition change in vesicle samples before and after incubation with Hb for 30 min. Thus during the time period needed for our experiments, minimal Hb-induced lipid peroxidation was observed in all samples.

Heme Concentration in BPS SUVs

We incubated Hb (0.52mg/ml) with BPS SUVs (4.2 mg/ml) (Lipid/Hb = 673) for 2 h at 37 °C to obtain substantially oxidized Hb in the Hb-vesicle samples. The Hb and BPS SUVs

were then separated by column chromatography. We found that the total heme concentration in BPS SUVs was 0.08 ± 0.03 μmoles heme/g lipid (n = 4) in these samples. Since the starting Hb concentration corresponds to about 2 μmoles/g lipid, or 8 μmoles in heme/g lipid, the heme concentration detected in SUVs corresponds to about 1 % of the total heme in Hb. The choleglobin concentration in the sample under similar conditions was about 7 ± 3 %. No heme was detected in the vesicles separated from the column immediately after mixing with Hb (t = 0).

DISCUSSION

The systems containing oxyHb and SUVs, or LUVs, in phosphate buffer were optically complicated, because oxyHb, metHb, hemichrome, choleglobin, and SUVs, or LUVs, as well as large vesicles from Hb-induced fusion of smaller vesicles (Fig 3-S in Miniprint) co-existed at concentrations that varied with time. However, when the process of vesicle fusion induced by Hb was slower than that of oxyHb oxidation, reliable kinetic information for the *initial* oxidation process of Hb in the presence of SUVs, or LUVs, could be obtained optically in the 500 - 700 nm region. We emphasize that this work focused on the *initial* oxidation process. As oxidation proceeds, many additional molecular events, such as vesicle fusion, lipid peroxidation, *etc.* occur, and some of these have been reported (Szebeni and Toth, 1986; Szebeni *et al.*, 1988; Itabe *et al.*, 1988).

Having the oxidation process described quantitatively in terms of pseudo first-order rate constants, we showed clearly that the initial Hb oxidation was enhanced by lipid vesicles. The rate constants for the initial disappearance of oxyHb, or for the appearance of metHb, hemichrome or choleglobin were much larger than those in the system without vesicles. Furthermore, the k values for systems containing SUVs were larger than those containing LUVs, with $k_O^{SUV}\,(h^{-1}) = k_O^{auto}\,(h^{-1}) + 3.7 \times 10^{-3} \times$ Lipid/Hb, and $k_O^{LUV}\,(h^{-1}) = k_O^{auto}\,(h^{-1}) + 0.2 \times 10^{-3} \times$ Lipid/Hb for Hb and vesicles in PEN7.4 buffer at 37 °C.

Assuming a 0.6 nm^2 surface area for the BPS headgroup and a 4 nm bilayer thickness (Cullis and Hope, 1985), the number of vesicles and the number of BPS molecules exposed to the Hb molecules in the outer monolayer could be calculated, if the size of the vesicles was known. Assuming 10 nm and 130 nm diameters in ideal SUV and LUV samples, respectively, we calculated that there were 1.4×10^{15} vesicles in SUV samples (1 mg/ml BPS) and 4×10^{12} in LUV samples. There are 7.2×10^{17} BPS molecules on the outer monolayer of 1 ml SUV samples, compared to 3.6×10^{17} molecules per ml for the LUV samples. Thus, the number

of BPS molecules accessible to Hb molecules was only about two times more in SUV samples than in LUV samples, despite the large differences in the size and number of vesicles in the two samples. Therefore the order of magnitude difference in rate constants seen in SUV- and LUV-containing samples is probably not due to a difference in the accessible lipid molecules to Hb molecules in the two vesicle systems.

The differences in the values of k^{SUV} and k^{LUV} could not be attributed to lipid breakdown products from sonication or extrusion methods, or to different lipid peroxidation products in SUVs and LUVs. The rate constants of sonicated samples prepared from LUVs were the same as those for SUVs. Similarly, the rate constants of extruded samples prepared from SUVs were the same as those for LUVs. Lipid peroxidation assay data for both SUVs and LUVs showed similar, limited lipid peroxidation. Data from samples containing the lipid peroxidation inhibitor BHT were similar to those without BHT. In addition, BPS and DPPC vesicles exhibited similar effects indicating that the degree of fatty acid saturation did not play an important role in this process. It is interesting to note that in a study of Hb-induced lipid peroxidation, BPS was found to have both deleterious and protective effects on lipid peroxidation (Szebeni *et al.*, 1988). In a similar study, it was found that hemoglobin did not induce lipid peroxidation when vesicles were prepared with low conjugated diene/lipid hydroperoxy content (Szebeni and Toth, 1986), in good agreement with our findings in detecting limited lipid peroxidation products in the samples.

BPS and DPPC vesicles exhibited similar effects, indicating that there was little head group specificity in this vesicle-enhanced oxidation.

In our studies, the hemoglobin concentrations were relatively low, ranging from about 3 μM (0.2 mg/ml) to about 100 μM (7 mg/ml). At low Hb concentrations, Hb tetramers dissociate to dimers, which exhibit a much higher rate of heme dissociation than tetramers (Benesch and Kwong, 1990). Consequently, Hb autoxidation is enhanced by dissociation into dimers (Zhang *et al.*, 1991). However, our data show that similar rate constants were obtained

from samples with the same Lipid/Hb but different Hb concentrations (Fig 4). We did not observe increased oxidation upon decreasing Hb concentration. On hydrogen peroxide induced oxidation of oxyHb Titov and coworkers also did not observe a Hb concentration effect, with Hb concentration ranging from 12 μM to 24 μM (Titov *et al.*, 1991). Our Hb concentration range (12 μM to 400 μM in heme) is within the Hb concentration range (3 μM to 1 mM in heme) that exhibit sharp changes in autoxidation due to tetramers dissociation to dimers (Zhang *et al.*, 1991). Thus our results indicate that the enhanced oxidation is not directly related to the concentrations of oxyHb tetramers and dimers.

Hb interacts with erythrocyte membranes at low ionic strength (Kaul and Köhler, 1983), with an equilibrium dissociation constant of about 10^{-4} M in 5 mM phosphate buffer at pH 8 (Fung, 1981). The interactions weakens to about $8.1 \pm 5.6 \times 10^{-5}$ M at physiological ionic strength and temperature (Lilley and Fung, 1987). Hb also interacts with phospholipids. The electrostatic interactions (Szundi *et al.*, 1980) and the hydrophobic interactions (Calissano *et al.*, 1972; Papahadjopoulos *et al.*, 1973) between Hb and PS have been observed. A model has been proposed to suggest that Hb interacts with the lipid surface initially by charge interactions, followed by insertion of the hydrophobic part of the globin into the lipid bilayer (Kimelberg, 1976). Shviro and coworkers suggested that the hydrophobic interactions in the model referred to a transfer of hydrophobic heme groups from Hb to the lipid bilayer, rather than a specific globin moiety interacting hydrophobically with PS (Shviro *et al.*, 1982). Although apomyoglobin and apohemoglobin can extract heme from the lipid bilayer (Rose *et al.*, 1985; Cannon *et al.*, 1988), the affinity between CO-heme and globin (Light and Olson, 1990) is higher than that of hemin and globin (Cannon *et al.*, 1988). In addition, globin denatures at room temperature (Rose *et al.*, 1985). In the presence of PS no interaction was found between globin and hemin (Shviro *et al.*, 1982). The heme transfer rate constant between Hb and hemopexin was not detectable for COHb, whereas it was 0.9 h^{-1} for metHb (Hebbel *et al.*, 1988). We have detected about 1 % of heme in SUVs after 2 h incubation with

oxyHb. Our detection method does not distinguish between reduced and oxidized forms of heme since all hemes are converted to porphyrin in the process of detection. About 7 ± 3 % choleglobin was detected under similar conditions (Fig 4-S in Miniprint). Thus it is plausible that in our samples the oxidized Hb interacts with the lipid surface, facilitating the transfer of oxidized heme to the lipid bilayer. The enhancement of oxidation is probably not due to any specific Hb unfolding reaction at the membrane surface, but due to dissociation of hemin from Hb, resulting in globin and hemin precipitation. The lipid bilayers serve to solubilize the hemin, allowing it to catalyze the production of strong oxidants, particularly hydrogen peroxide and hydroxide radicals, which promote further Hb oxidation. Our catalase results support this hypothesis. Catalase mediates the removal of hydrogen peroxide (Deisseroth and Dounce, 1970). The addition of sufficient catalase arrests the induced oxidation. Our data are in agreement with the finding that the addition of catalase a short time after the addition of hydrogen peroxide arrested further oxidation of Hb (Titov *et al.*, 1991). This hypothesis suggests that the ability of a lipid surface to enhance Hb oxidation depends on its ability to solubilize the hemin generated from oxidized Hb.

The SUVs and LUVs have very different curvatures, calculated as 2/diameter (Protter and Morrey, 1970), and therefore different surface chemistry due to the different intermolecular forces associated with the individual vesicle systems (MacDonald, 1990; Ohki and Duax, 1986; Ohki, 1984). For the strongly curved bilayer in SUVs with diameter of about 10 - 30 nm (Fig 1A-S in Miniprint), the strength of the lateral forces, tending to divide the phospholipid molecules, closely approximates the strength of the hydrophobic interactions holding them together (Gray and Morgan, 1991). Thus SUVs become more susceptible to solubilization by, for example, lipoproteins (Scherpof *et al.*, 1979). Furthermore, SUVs fuse much more readily than LUVs (Szoka, 1987; Düzgünes and Bentz, 1988; MacDonald, 1988). With the high curvature, the hydrophobic (hydrocarbon) moieties of SUVs have a larger exposure to water. Thermodynamic analysis indicates that membrane surface pressure can

account for differential activities of any membrane-penetrating molecules (MacDonald and MacDonald, 1988). LUVs exhibit surface curvatures different from those of SUVs regardless of the size of the filters used to extrude them. The LUVs extruded with 30 nm, 50 nm and 100 nm filters have overlapping size distribution. For example, the mean diameters of extruded PC vesicles prepared with an extruder similar to the one we used in our studies are given as 103 ± 20 nm for 100 nm filter, 68 ± 19 nm for 50 nm filter and 56 ± 17 for 30 nm filter (Mayer *et al.*, 1986). Extrusion may not be capable of giving small vesicles that have significant strain as in sonicated vesicles. Since it seems impossible to make vesicles much smaller than 60 nm with extrusion, it may be that the vesicles choose the smallest strain-free state even when it is larger than the filter pore diameter. It has been reported that vesicles with low curvature are more readily destabilized by proteins like spectrin than vesicles of high curvature (Subbarao *et al.*, 1991). It appears that the SUVs are highly strained, whereas the LUVs are more relaxed. Thus the differences in surface chemistry in SUVs and LUVs may facilitate the transfer of oxidized heme from Hb to vesicles differently, and thereby increase the kinetics of Hb oxidation to different extents.

Whether the lipid effects observed in this study have physiological significance is not clear. The Hb concentrations in erythrocytes are much higher than those used in this study, and thus the lipid-to-Hb molar ratios used in this study may be relatively high compared to those in the erythrocyte. However, Hb molecules and lipid molecules in erythrocytes do not mix. It is not clear whether a simple molar ratio of inner leaflet lipid molecules to total Hb molecules in red blood cells is relevant for our consideration. Within the erythrocyte, a fraction of the Hb molecules closely associated with the inner membrane leaflet at any one time. The membrane-associated Hb molecules exhibit time-dependent exchange with the bulk erythrocyte Hb molecules. With the surface area of a lipid head group being 0.6 nm^2 (Cullis and Hope, 1985), and the projected surface area of Hb being 24 nm^2, one Hb molecule may interact with about 40 lipid head groups at the interface to form a single layer of closely

packed Hb next to the lipid monolayer surface at any moment. At this Lipid/Hb value of 40, k_O^{SUV} would be about 0.2 h^{-1}, an order of magnitude higher than k_O^{auto}. In studying the Hb effect on liposome permeability, Calissano and coworkers found that about 0.4 nmoles of Hb bound to one μmole PS (Calissano *et al.*, 1972; Kimelberg, 1976). Their results suggest a Lipid/Hb of 2500. At this ratio, our studies show that SUVs would increase the oxidation by several orders of magnitude. However, the curvature of the erythrocyte surface is much larger than those of SUVs, and may be more appropriately described by LUVs. Further studies on the spatial distribution of phospholipids (lipid patches) in the inner leaflet of erythrocyte and the physical interactions between lipid and Hb will be useful in determining lipid effects on Hb oxidation in erythrocytes. It is also interesting to note that the inhibitory effect of catalase in red cells. It is possible that the presence of this enzyme prevents much of the lipid enhanced oxidation in erythrocyte.

The overall mechanism for lipid enhanced Hb oxidation is likely to be quite complicated, and its formulation will require further quantitative studies to provide kinetic parameters under experimental conditions that are known to affect (1) oxyHb autoxidation, (2) physical interactions between lipid and oxyHb, metHb or hemichrome molecules, and (3) the interactions of the heme group with the protein moiety in oxyHb, metHb and hemichrome molecules, and with different lipid surfaces to delineate various molecular events in the Hb - lipid mixture. It is also important to study the surface chemistry of lipids on the inner leaflet of erythrocytes to understand how lipid molecules affect Hb oxidation *in vivo*. Our findings suggest that the physiological significance of lipid-enhanced Hb oxidation should be further studied.

The findings also indicate that LUVs are substantially more desirable than SUVs for maintaining Hb stability in liposomes when used as an oxygen-carrying fluid. The SUV and LUV systems may also provide a quantitative means for studying anti-Hb-oxidation in liposomes.

ACKNOWLEDGMENTS

We are most grateful for comments and suggestions provided by Drs. R.C. and R.I. MacDonald of Northwestern University on surface properties of lipid vesicles, and by the reviewers on possible mechanisms for the enhanced oxidation.

REFERENCES

Almog, R., Forward, R. and Samsonoff, C. (1991) *Chem. and Phys. Lipids* **60**, 93-99.

Antonini, E., and Brunori, M. (1971) in *Hemoglobin and Myoglobin in Their Reactions with Ligands*, p. 18, American Elsevier, New York, NY.

Aust, S.D. (1985) in *CRC Handbook of Methods for Oxygen Radical Research* (Greenwald, R.A. Ed.) pp 203-207, CRC Press, Boca Raton, FL.

Benesch, R.E., and Kwong, S. (1990) *J. Biol. Chem.* **265**, 14881-14885.

Bligh, E.G., and Dyer, W.J. (1959) *Can. J. Biochem. Physiol.* **37**, 911-917.

Brandl, M., Becker, D., and Bauer, K.H. (1989) *Drug Develop. Indust. Pharm.* **15**, 655-669.

Buege, J.A., and Aust, S.D. (1978) *Methods in Enzymology* **51**, 302-310.

Calissano, P., Alema, S., and Rusca, G. (1972) *Biochim. Biophys. Acta* **255**, 1009-1013.

Cannon J.B., Kuo F.-S., Pasternack, R.F., Wong, N.M. and Muller-Eberhard, U. (1984) *Biochemistry*, **23**, 3715-3721.

Caughey, W.S., and Watkins, J.A. (1985) in *CRC Handbook of Methods for Oxygen Radical Research* (Greenwald, R.A. Ed.) pp 95-104, CRC Press, Boca Raton, FL.

Chiesi, M., and Inesi, G. (1980) *Biochem.* **19**, 2912-2918.

Claiborne, A. (1985) in *CRC Handbook of Methods for Oxygen Radical Research* (Greenwald, R.A. Ed.) pp 283-284, CRC Press, Boca Raton, FL.

Cullis, P.R., and Hope, M.J. (1985) in *Biochem. of Lipids and Membranes* (Vance, D.E. and Vance, J.E., Eds.) pp 25-70, Benjamen/Cummings Publishing Co., Menlo Park, CA.

Das, S.K., and Nair, R.C. (1980) *British J. Haematology* **44**, 87-92.

Deisseroth, R.G. and Dounce, A.L. (1970) Physiol. Rev. 50, 319.

Dunn, M.F., Pattison, S.E., Storm, M.C., and Quiel, E. (1980) *Biochem.* **19**, 718-725.

Düzgünes, N., and Bentz, J. (1988) in *Spectroscopic Membrane Probes* (Loew, L.M., Ed.) CRC Press, Boca Raton, FL.

Fridovich, I.(1985) in *CRC Handbook of Methods for Oxygen Radical Research* (Greenwald, R.A. Ed.) pp 213-215, CRC Press, Boca Raton, FL.

Fung, L.W.-M. (1981) *Biochem.* **20**, 7162-7166.

Gray, A. and Morgan, J. (1991) *Blood Reviews* **54**, 258-272.

Gutteridge, J.M.C., and Halliwell, B. (1990) *Trends In Biol. Sci.* **15**, 129-135.

Hebbel, R.P., Morgan, W.T., Eaton, J.W., and Hedlund, B.E. (1988) *Proc. Natl. Acad. Sci.USA* **85**, 237-241.

Itabe, H., Kobayashi, T., and Inoue, K. (1988) *Biochim. Biophys. Acta* **961**, 13-21.

Kaul, R.K., and Köhler, H. (1983) *Klin Wochenschr* **61**, 831-837.

Kawanishi, S. and Caughey, W.S. (1985) *J. Biol. Chem.* **260**, 4622-4631.

Kikugawa, K., Sasahara, T., Sasaki, T., and Kurechi, T. (1981) *Chem. Pharm. Bull.* **29**, 1382-1389.

Kimelberg, H.K. (1976) *Molecul. Cell. Biochem.* **10**, 171-190.

Klein, R.A. (1970) *Biochim. Biophys. Acta* **210**, 486-489.

Light, W.R., and Olson, J.S. (1990) *J. Biol. Chem.* **265**, 15623-15631.

Ligler, F.S., Stratton, L.P., and Rudolph, A.S. (1989) in *The Red Cell: Seventh Ann Arbor Conf.* pp. 435-455, Alan R. Liss, Inc, Ann Arbor. MI.

Lilley, G.L. and Fung, L. W.-M. (1987) Life Sciences 41, 2429-2436.

Lorimer, J.P. and Mason, T.J. (1987) *Chem. Soc. Rev.* **16**, 239-274.

Loughrey, H.C., Wong, K.F., Choi, L.S., Cullis, P.R., and Bally, M.B. (1990) *Biochim. Biophys. Acta* **1028**, 73-81.

MacDonald, R.C. (1988) in *Molecular Mechanisms of Membrane Fusion* (Ohki, S., Doyle, D., Flanagan, T.D., Hui, S.W., and Mayhew, E., Eds.) pp. 101-112, Plenum Press, New York, NY.

MacDonald, R.C., and MacDonald, R.I. (1988) *J. Biol. Chem.* **263**, 10052-10055.

MacDonald, R.C. (1990) *Hepatology* **4**, 1-10.

MacDonald, V.W., and Charache, S. (1982) *Biochim. Biophys. Acta* **701**, 39-44.

Mansouri, A., and Winterhalter, K.H. (1974) *Biochem.* **13**, 3311-3314.

Marinetti, G.V., and Crain, R.C. (1978) *J. Supramolecular Structure* **8**, 191-213.

Mayer, L.D., Hope, M.J., and Cullis, P.R. (1986) *Biochim. Biophys. Acta* **858**, 161-168.

Misra, H.P., and Fridovich, I. (1972) *J. Biol. Chem.* **247**, 6960-6962.

Morrison, G.R. (1965) *Anal. Chem.* **37**, 1124-1126.

Ohki, S., and Duax, J. (1986) *Biochim. Biophys. Acta* **861**, 177-186.

Ohki, S. (1984) *J. Memb. Biol.* **77**, 265-274.

Papahadjopoulos, D., Cowden, M., and Kimelberg, H.K. (1973) *Biochim. Biophys. Acta* 330, 8-26.
Protter, M.H., and Morrey, C.B. (1970) *College Calculus with Analytic Geometry*, Addison Wesley Publishing, Reading, MA.

Rabinovici, R., Rudolph, A.S., Ligler, F.S., Yue, T.-L., and Feuerstein (1990) *Circulatory Shock* **32**, 1-17.

Rauenbuehler, P.B., Cordes, K.A. and Salhany, J.M. (1982) *Biochim. Biophys. Acta* **692**, 361-370.

Riggs, A. (1981) *Methods in Enzymology* **76**, 5-29.

Rose, M.Y., Thompson, R.A., Light, R. and Olson, J.S. (1985) *J. Biol. Chem.* **260**, 6632-6640.

Sadrzadeh, S.M.H., Graf, E., Panter, S.S., Hallaway, P.E., and Eaton, J.W. (1984) *J. Biol. Chem.* **259**, 14354-14356.

Scherpof G, Morselt H, Regts J, Wilschu JC (1979) *Biochim. Biophys. Acta* **556**, 196.

Shaklai, N., Shviro, Y., Rabizadeh, E. and I. Kirschner-Zilber (1985) *Biochim. Biophys. Acta* **821**, 355- 366.

Shikama, K. (1984) *Biochem. J.* **233**, 279-280.

Shikama, K. (1990) *Bio. Rev.* **65**, 517-527.

Shviro, Y., Zilber, I., and Shaklai, N. (1982) *Biochim. Biophys. Acta* **687**, 63-70.

Stewart, J.C.M. (1980) *Anal. Biochem.* **104**, 10-14.

Subbarao, N.K., MacDonald, R.I., Takeshita, K. and MacDonald, R.C. (1991) *Biochim. Biophys. Acta* **1063**, 147-154.

Szebeni, J., Winterbourn, C.C., and Carrel, R.W. (1984) *Biochem. J.* **220**, 685-692.

Szebeni, J., DiIorio, E.E., Hauser, H., and Winterhalter, K.H. (1985) *Biochem.* **24**, 2827-2832.

Szebeni, J., and Toth, K. (1986) *Biochim. Biophys. Acta* **857**, 139-145.

Szebeni, J., Hauser, H., Eskelson, C.D., Watson, R.R., and Winterhalter, K.H. (1988) *Biochem.* **27**, 6425-6433.

Szoka F.C. (1987) in *Cell Fusion* (Sowers, A.E., Ed.) Plenum Press, New York, NY.

Szundi, I., Szelenyi, J.G., Breuer, J.H. and Berczi, A. (1980) *Biochim. Biophys. Acta* **595**, 41-46.

Titov, V. Yu., Petrenko, Yu. M., Petrov, V. A. and Vladimirov, Yu. A. (1991) *Bulletin of Experimental Biology and Medicine* **112**, 957-961.

Van den Berg, J.J.M., Kuypers, F.A., Qju, J.H., Chiu, D., Lubin, B., and Roelofsen, B. (1988) *Biochim. Biophys. Acta* **944**, 29-39.

Walder, J.A., Chatterjee, R., Steck, T.L., Low,P.S., Musso, G.F., Kaiser, E.T. Rogers, P.H. and Arnone, A. (1984) *J. Biol. Chem.* **259**, 10238-10246.

Wallace, W.J., Maxwell, J.C., and Caughey, W.S. (1974) *FEBS Lett.* **43**, 33-36.

Wallace, W.J., Houtchens, R.A., Maxwell, J.C., and Caughey, W.S. (1982) *J. Biol. Chem.* **257**, 4966-4977.

Watkins, J.A., Kawanishi, S., and Caughey, W.S. (1985) *Biochem. Biophys. Res. Commun.* **132**, 742-748.

Ways, P., and Hanahan, D.J. (1964) *J. Lipid Res.* **5**, 318-328.

Weiss, J.J. (1964) *Nature* **202**, 83-84.

Wilschut, J., Düzgünes, N., and Papahadjopoulos, D. (1981) *Biochem.* **20**, 3126-3133.

Winterbourn, C.C., Hawkins, R.E., Brian, M., and Carrell, R.W. (1975) *J. Lab. Clin. Med.* **85**, 337-341.

Winterbourn, C.C. (1985a) in *CRC Handbook of Methods for Oxygen Radical Research* (Greenwald, R.A. Ed.) pp 137-141, CRC Press, Boca Raton, FL.

Winterbourn, C.C. (1985b) *Environmental Health Perspectives* **64**, 321-330.

Yamamoto,Y., Niki, E., Eguchi, J., Kamiya, Y., and Shimasaki, H. (1985) *Biochim. Biophys. Acta* **819**, 29-36.

Zhang, L., Levy, A. and Rifkind, J.M. (1991) *J. Biol. Chem.* **266**, 24698-24701.

[1]The abbreviations used are: BHT, butylated hydroxytoluene; BPS, bovine brain phosphatidylserine; CO, carbon monoxide; COHb; carbon-monoxy Hb; DPPC, dipalmitoyl phosphatidylcholine; Hb, human hemoglobin; k_O, pseudo first-order rate constant for the initial disappearance of oxyHb; LUV, large unilamellar vesicles; MDA, malondialdehyde; oxyHb, oxygenated Hb; PEN7.4, 23 mM sodium phosphate buffer with 2 mM EDTA and 127 mM NaCl at pH 7.4; RP, reactive products; SOD, superoxide dismutase; SUV, small unilamellar vesicles; TBA, 2-thiobarbituric acid; TE8.3, 50 mM Tris buffer with 0.1 mM EDTA at pH 8.3.

[2]The "Materials and Methods" section is presented in miniprint at the end of this paper.

[3]The discussions on potential problems are presented in miniprint at the end of this paper.

FIGURE LEGENDS

Fig 1: Spectra from 500 to 700 nm at 37 °C of (A) Hb (0.21 mg/ml) at t = 0 (top) and t = 22 h (bottom), using PEN7.4 buffer as a blank, (B) Hb (0.21 mg/ml) and BPS SUVs (2.3 mg/ml) at t = 0 (top), 12 min (middle) and 30 min (bottom), and (C) hemolysate (0.20 mg/ml) and BPS SUVs (1.2 mg/ml) at t = 0 and 30 min (top two spectra, spectra were offset by 0.1 absorbance unit), and COHb and BPS SUVs (1.5 mg/ml) at t = 0 and 2 h (bottom two spectra). BPS SUVs with matching lipid concentrations were used as blanks for spectra in (B) and (C).

Fig 2: Semilogarithmic plot of percentage of oxyHb as a function of time, for (A) oxyHb in the absence of BPS SUVs and (B) in the presence of BPS SUVs. OxyHb solution (0.19 mg/ml) was incubated at 37 °C in the presence of BPS SUVs (2.1 mg/ml) in PEN7.4 buffer. Spectra were collected every 2 min in the presence of BPS SUVs and every 10 min in the absence of BPS SUVs. In the presence of BPS SUVs the data are linear up to the first 12 min, while in the absence of BPS SUVs the data are linear up to 50 h. The solid lines are a linear fit of the linear portion of the data points, with slope in (A) as 0.018 h^{-1} and in (B) as 3.91 h^{-1}. The correlation coefficients for both linear fits were 0.998.

Fig 3: Pseudo first-order rate constants for the disappearance of oxyHb (k_O^{SUV}) in the presence of BPS SUVs as a function of lipid-to-Hb molar ratio (Lipid/Hb) in PEN7.4 buffer. The Hb concentration was held at about 0.20 mg/ml. The solid line was the linear fit of all data points, with a slope of 0.0037 and a correlation coefficient of 0.850. The data from samples containing DPPC sonicated vesicles are in shaded symbols (●). The rate constant of the SUV sample prepared from LUVs is shown with a star symbol (★).

Fig 4: The average pseudo first-order rate constants (n = 2) for the disappearance of oxyHb (k_O^{SUV}) in the presence of BPS SUVs as a function of Hb concentration, in heme

(mM). The samples were held at a constant Lipid/Hb of about 100 (●) and about 200 (■). The error bars indicate the standard deviations of the average values.

Fig 5: Pseudo first-order rate constants for the disappearance of oxyHb (k_O^{LUV}) in the presence of BPS LUVs vs lipid-to-Hb molar ratios (Lipid/Hb) in PEN7.4 buffer. LUVs were prepared by extrusion methods, either with 100 nm, (■) 50 nm (♦) or 30 nm filters (▲). The line is the linear fit of the data points with a slope of 0.0002 and a correlation coefficient of 0.867. The data from samples containing DPPC LUVs, extruded with 50 nm filter, are in shaded symbols (◊). The star symbol (★) is for the sample in which the lipid was extracted from an SUV sample and made into LUVs. The dotted line is the same line fitted to the data shown in Fig 3 for BPS SUVs, and is re-plotted for comparison.

Fig 6: OxyHb oxidation in the absence (shaded symbols) and in the presence (filled symbols) of catalase (39,000 units/gm-Hb). Catalase was added after Hb was incubated with BPS SUVs at 37 °C for 7 min (●) in one sample and 11 min (■) in another sample. The initial Hb concentration was 0.21 mg/ml and the lipid concentration was 2.4 mg/ml to give a Lipid/Hb of 940.

TABLE I

Lipid Peroxidation Measurements of Various Lipid Samples

Method			Sample		
		BPS Stock[a]	SUVs[b]	LUVs[c]	SUVs + Hb[c]	LUVs + Hb[c]
A_{233}/A_{215}[d] (n = 4)		0.0	0.176 ± 0.102	0.149 ± 0.101	NA[e]	NA
TBARP (n = 4)		1.015[g] ± 0.035	1.385 ± 0.175	1.312 ± 0.117	ND[h]	ND
GC	16:0	0.9 %[j] ± 0.2	5.0	NM[k]	2.8	1.5
	18:0	39.9 % ± 0.9	38.8	NM	38.9	42.1
	18:1	32.6 % ± 11.9	38.3	NM	39.1	43.3
	22:6	8.5 % ± 3.1	0	NM	0	0
	20:4	2.9 % ± 0.9	1.3	NM	0	1.2
	20:1	1.9 % ± 0.1	3.0	NM	2.6	2.6
	others	13.3 %[l] ± 0.1	13.6	NM	16.6	9.3

[a]Sample as supplied by manufacturer. [b]See Method Section for SUV and LUV preparations. [c]SUVs and LUVs with about 2.3 ± 0.2 mg/ml lipid and oxyHb (about 2.3 ± 0.2 mg/ml), incubated at 37 °C for 30 min, a time period longer than those used in Hb oxidation. [d]See Methods sections for the methods used for lipid peroxidation measurements. [e]Sample not appropriate for assay, since Hb interferes with the absorbance readings. [g]in nm MDA/μmole lipid. [h]Assay not done since MDA binds to Hb (Kikugawa *et al.*, 1984). [j]Average values of 7 lots of BPS samples obtained from manufacturer's data sheet. [k]Not measured. [l]Consists of 14:0, 16:1, 18:2, 18:3, 20:0, 20:2, 20:3, 22:0 and 22:1; all less than 1 % each.

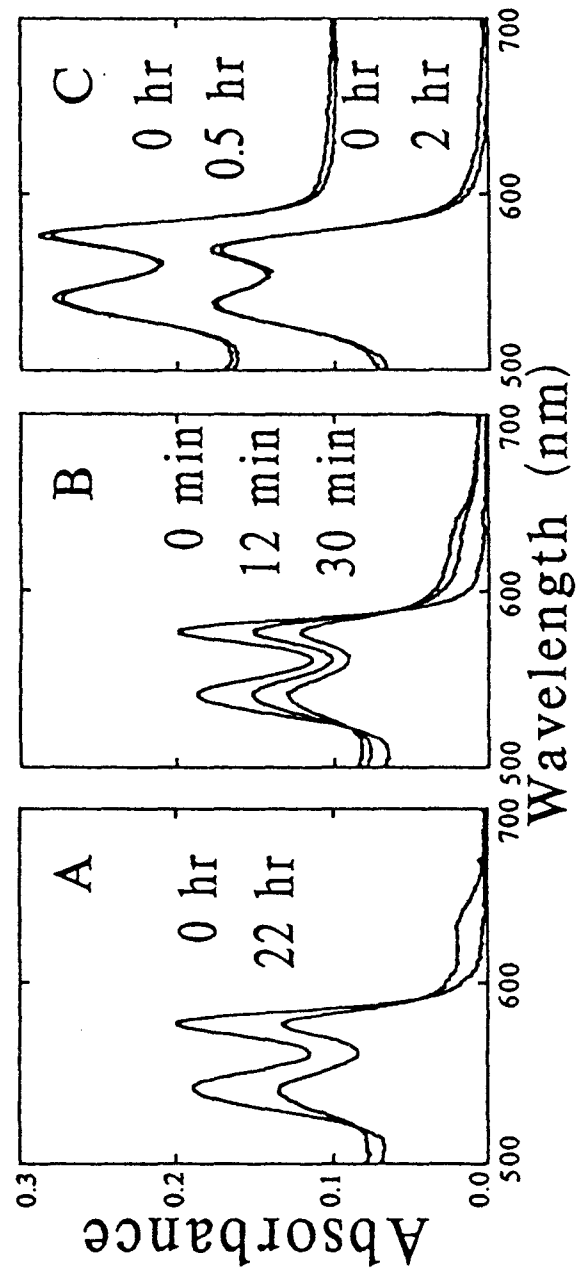
A
0 hr
22 hr
B
0 min
12 min
30 min
C
0 hr
0.5 hr
0 hr
2 hr
Absorbance
0.0
0.1
0.2
0.3
500
600
700
Wavelength (nm)

Figure 1

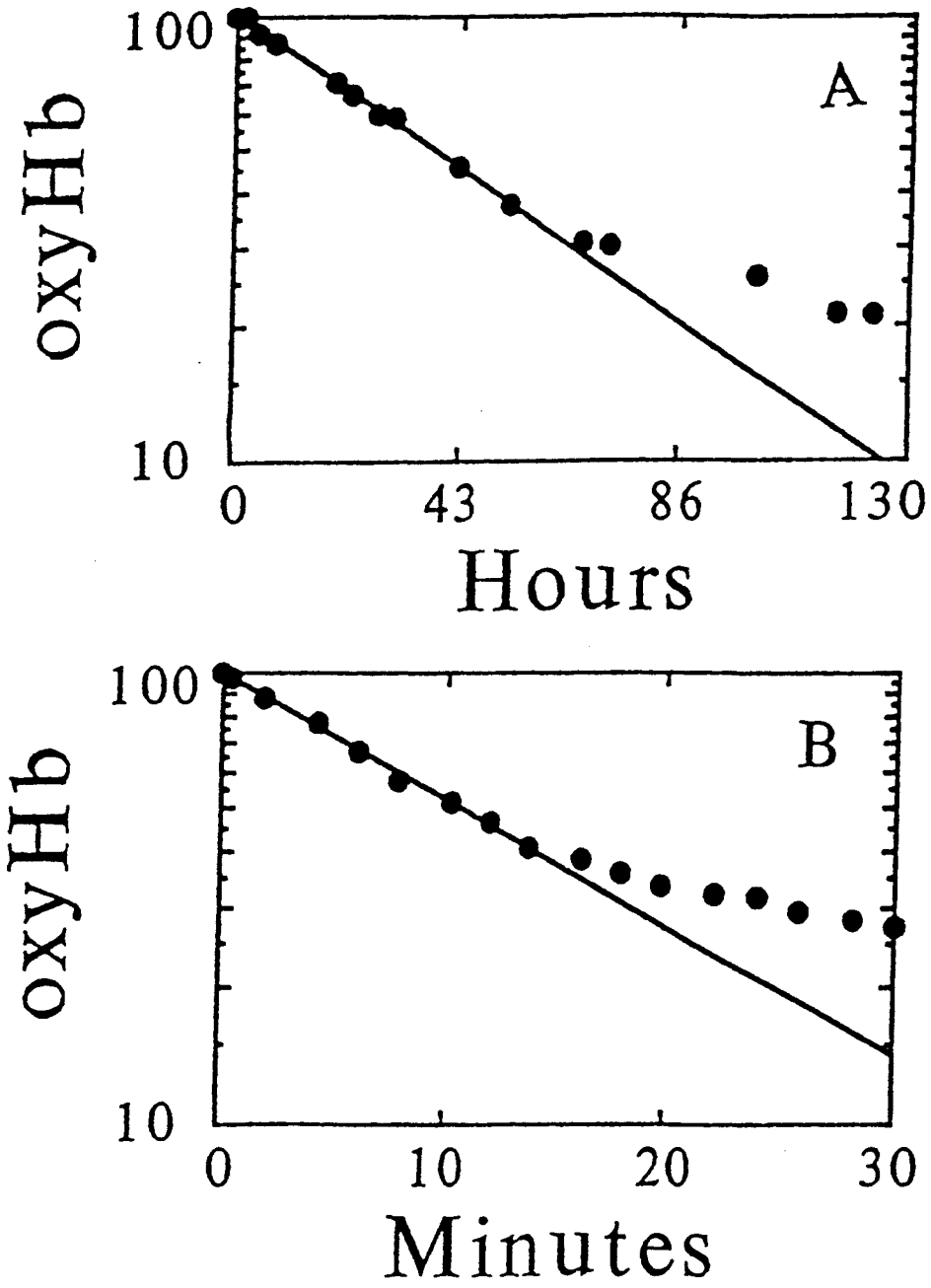

Figure 2

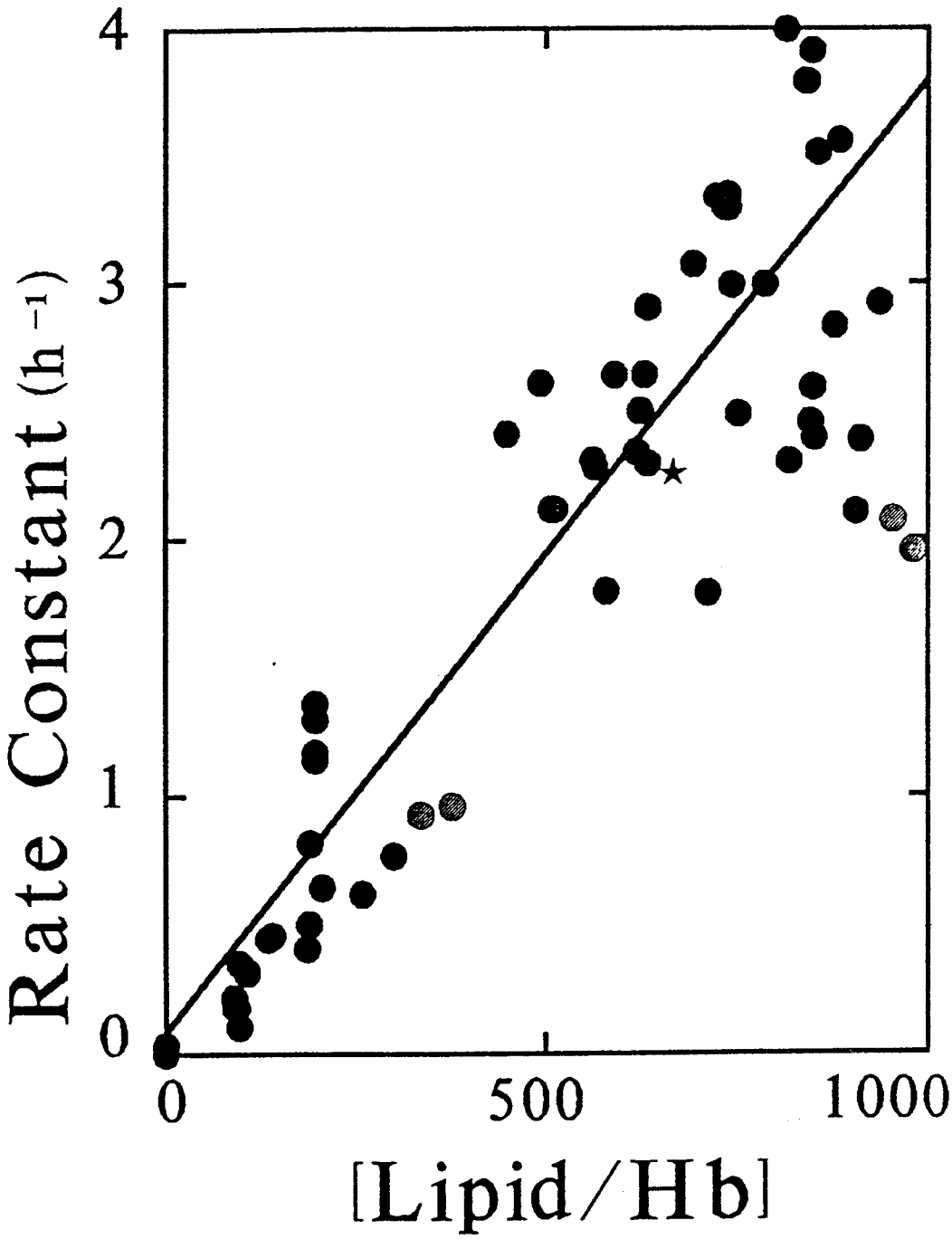

Figure 3

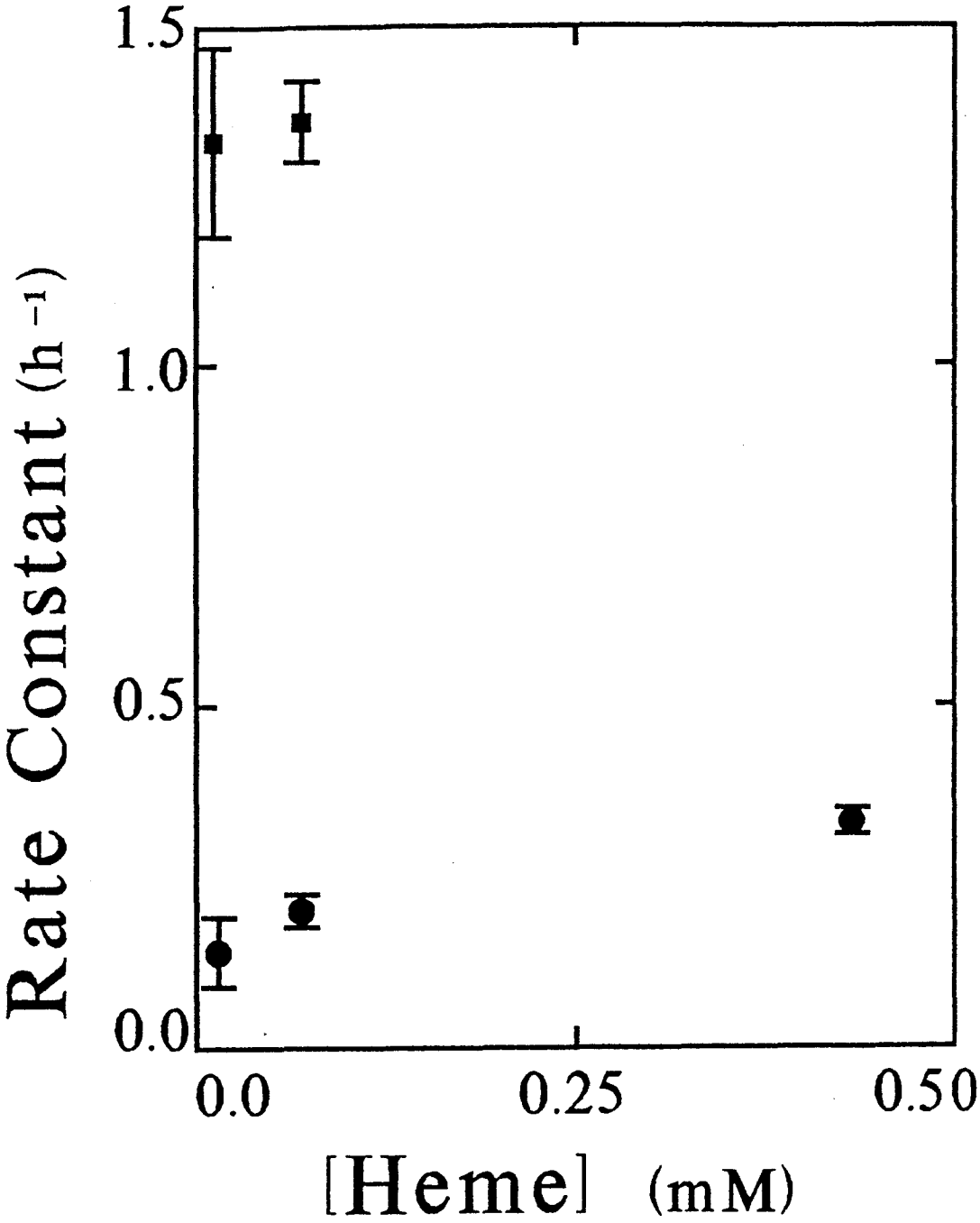

Figure 4

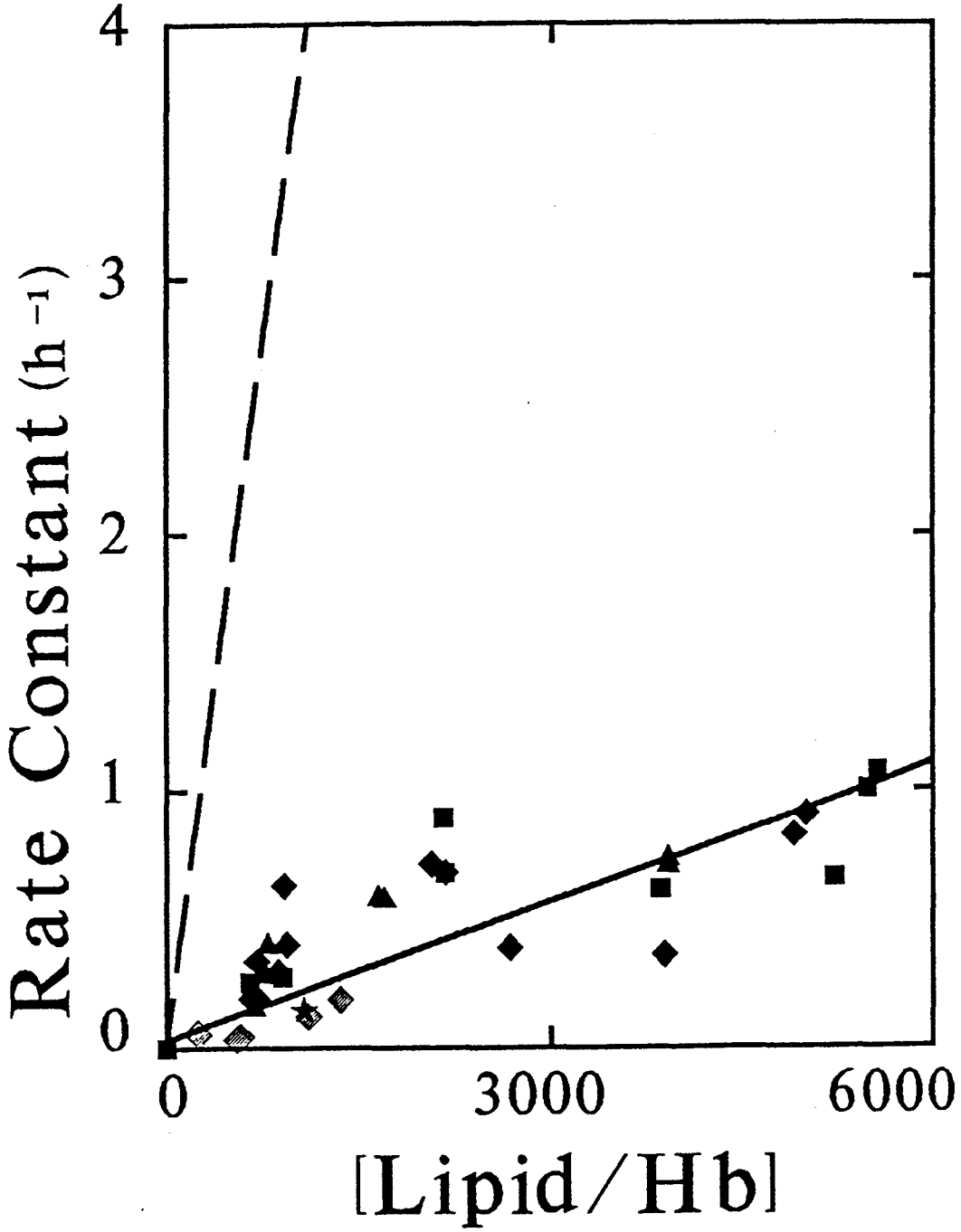

Figure 5

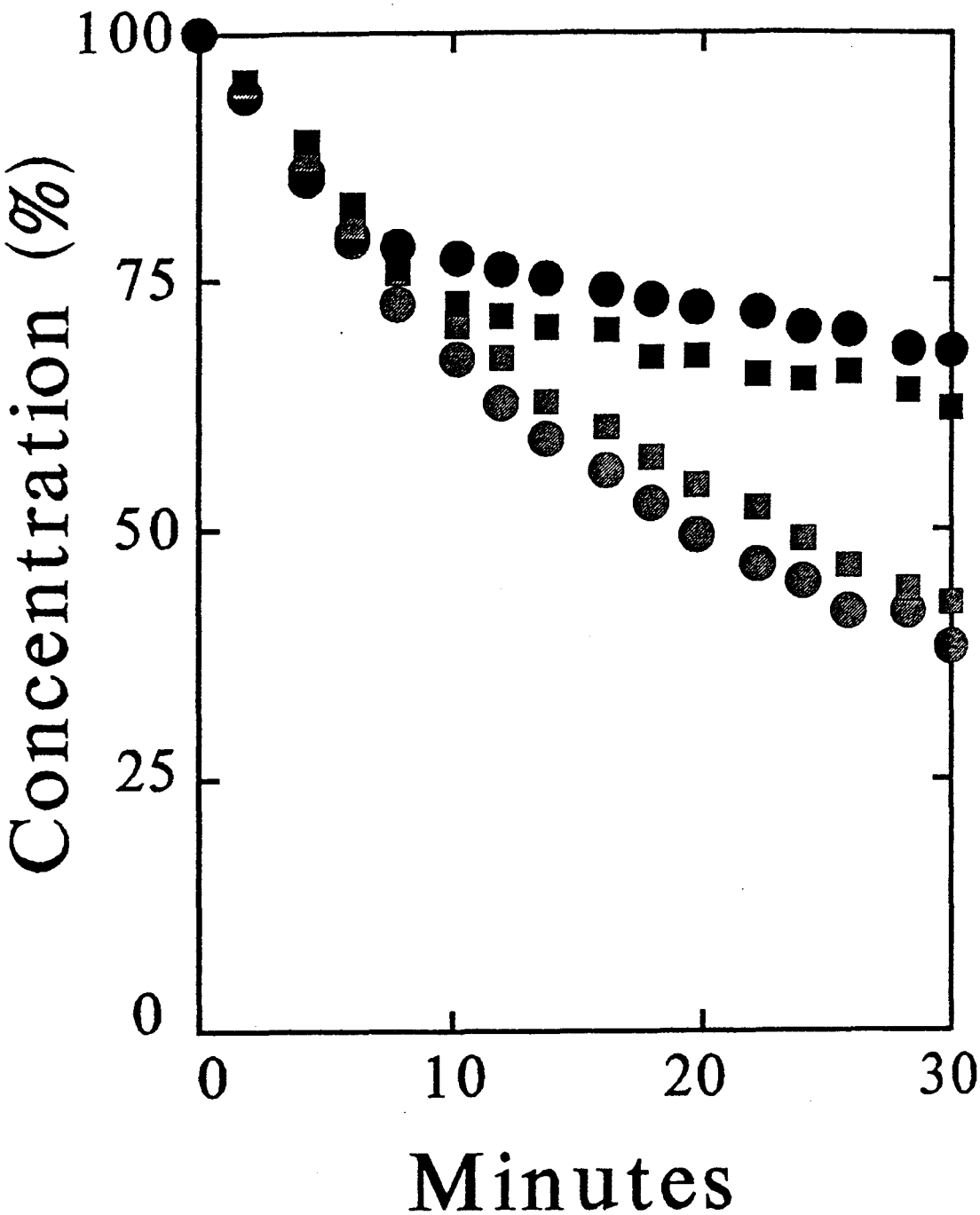

Figure 6

SUPPLEMENTAL MATERIAL

to

PHOSPHOLIPID VESICLES PROMOTE HUMAN HEMOGLOBIN OXIDATION

by

Cynthia C. LaBrake and Leslie W.-M. Fung

Department of Chemistry, Loyola University of Chicago, Chicago, IL 60626

I. MATERIALS AND METHODS

Unless stated otherwise, all experimental steps were carried out at 4 °C, and all chemicals were reagent grade from Fisher (Pittsburgh, PA), Sigma (St. Louis, MO) or Aldrich (Milwaukee, WI). HPLC-grade water was used for all buffers. All glassware was acid-washed.

Hemolysate Preparation. Human red blood cells were used within one week of withdrawal and washed with 5 mM sodium phosphate containing 150 mM NaCl, saturated with carbon monoxide (CO), at pH 7.4. The cells were lysed with 2 volumes of deionized water, followed by ammonium sulphate precipitation and desalting with a P6DG column (BioRad, Richmond, CA), equilibrated with 5 mM Tris buffer containing 150 mM NaCl at pH 7.5 to remove ammonium sulphate and other small molecules, including 2,3-bisphosphoglycerate, which affects hemoglobin autoxidation (Mansouri and Winterhalter, 1974; Kikugawa *et al.*, 1981), to give stripped hemolysate. The hemolysate solution was dialyzed against 23 mM sodium phosphate buffer with 2 mM EDTA and 127 mM NaCl at pH 7.4 (PEN7.4), saturated with CO. If not used immediately, the hemolysate was frozen drop-wise in liquid N_2 and stored at -80 °C. After thawing, the hemolysate was centrifuged at 38,000 g for 10 min before use.

Superoxide dismutase (SOD) and catalase activities were determined in the hemolysate samples. The SOD extraction methods of Winterbourn and coworkers (1975) and the reaction cocktail conditions of Fridovich (1985) were used. The catalase activity was determined by the method of Claiborne (1985). Full SOD and catalase activities were detected in the stripped hemolysate samples, with SOD activity about 1.3×10^3 units/gm-Hb, and catalase activity about 1.6×10^4 units/gm-Hb, similar to the activities published for erythrocytes (Das and Nair, 1980).

Hemoglobin Preparation. Hb was isolated from the stripped hemolysate solution according to a modified column chromatography procedure (Kawanishi and Caughey, 1985; Watkins *et al.*, 1985; Winterbourn, 1985a). The stripped hemolysate was dialyzed in 50 mM Tris buffer with 0.1 mM EDTA at pH 8.3 (TE8.3), followed by CO gassing. A DEAE-Sephadex A-50 (Pharmacia, Piscataway, NJ) column was used with a linear pH gradient made from buffer TE8.3 and a similar buffer at pH 7.0. The Hb fractions were concentrated, dialyzed against PEN7.4, and CO gassed to give carbon-monoxy Hb (COHb). This procedure removed all minor hemoglobin components, catalase, SOD, "adventitious" metals, and other red cell proteins to give "ultra-pure" HbA (Watkins *et al.*, 1985; Winterbourn, 1985a). No SOD or catalase activities were detected in these Hb samples, using assay methods noted above.

Some COHb samples were passed through a Chelex (BioRad, Richmond, CA) column to remove any residual trace metal (e.g., Cu and Fe) ions (Dunn *et al.*, 1980; Chiesi and Inesi,

1980).

Hb Concentration. The total Hb concentrations in the hemolysate and Hb solutions were determined by the cyano-met method (Riggs, 1981). In addition, at the beginning of each oxidation experiment, the concentration of the oxygenated Hb (oxyHb) solution was determined at 577 nm, using an extinction coefficient of 15.0 mM^{-1} cm^{-1} (Winterbourn, 1985a). No detectable absorbance at 630 nm was observed. The concentrations of oxyHb generally agreed to within 5 % with the values determined by the cyano-met method.

Lipid Vesicles. BPS was purchased from Avanti Polar Lipids (Alabaster, AL), and DPPC from Sigma. Both were used without further purification after verification of purity by thin-layer chromatography. Chloroform in lipid was removed with N_2 gas followed by pumping under vacuum. If necessary, the lipid films were stored, but no longer than 48 h, at -20 °C under a N_2 atmosphere. PEN7.4 buffer solution (5 ml) was saturated with N_2 gas, and added to the lipid film. Some buffer solutions were treated with Chelex. The solution was hand-swirled in the presence of glass beads to give multilamellar vesicles. For samples containing BHT, 0.5 to 1.5 mM BHT was added to the original lipid-chloroform solution.

SUVs. SUVs were prepared from the multilamellar vesicles by slightly modified procedures of Itabe and coworkers (1988). Multilamellar vesicles in PEN7.4 were sonicated to clearness, under N_2 at room temperature for BPS, and at 45 °C for DPPC, for about 20 min using a probe tip sonicator (Heat Systems-Ultrasonics Model W-10), and centrifuged at 38,000 g and 20 °C to remove any large multilamellar vesicles and titanium from the sonication probe. Sonication conditions were precisely controlled to obtain consistent SUV samples. Otherwise, irreproducible, but generally much faster, oxidation was observed. The SUV samples were used immediately for oxidation studies. Lipid concentrations in these samples ranged from 0.25 to 9 mg/ml, but were generally about 2.5 mg/ml. Freeze fracture electron micrographs of these SUVs, obtained by Lipex (Vancouver, Canada), showed typical SUVs with vesicle diameters ranging from 10 - 30 nm (Fig 1A-S). Some larger vesicles were also seen.

LUVs. LUVs were prepared from the multilamellar vesicle solutions (1 mg/ml to 14 mg/ml) by extrusion methods with a lipid extruder (Lipex) (Loughrey *et al.*, 1990). Polycarbonate filters (Nuclepore, Pleasanton, CA) with 30, 50 or 100 nm pore sizes were used. BPS vesicles were extruded at room temperature, and DPPC vesicles at 45 °C. Freeze fracture electron micrographs showed that the LUVs extruded with 100 nm filter exhibited diameters of about 100 nm (Fig 1B-S). These LUVs were also analyzed by a particle sizer (a service provided by Lipex), and exhibited an average diameter of 130 ± 30 nm, in good agreement with the published value of 138 nm for egg phosphatidylcholine (Mayer *et al.*, 1986), indicating that these vesicles are much larger than SUVs.

Lipid Concentration. Lipid concentrations of the vesicle samples were determined by the method of Stewart (1980), following extraction from the aqueous phase (Bligh and Dyer, 1959). Extinction coefficients of 1.99 mg^{-1} cm^{-1} for BPS, and 4.12 mg^{-1} cm^{-1} for DPPC were obtained experimentally, in good agreement with the published value (Stewart, 1980).

Lipid Peroxidation Products. The concentrations of lipid peroxidation products in SUVs and LUVs were estimated by three methods: conjugated diene assay, A_{233}/A_{215}, TBARP assay, and GC-mass spectrometry.

The conjugated diene assay followed the method of Klein (1970), using the ratios of the absorbances at 233 and 215 nm as an indication of the conjugated diene content.

MDA and other TBARP were determined using standard procedures (Buege and Aust,

1978; Aust, 1985). The extinction coefficient was determined from MDA solutions of known concentrations, and agreed well with the literature value of $1.56 \times 10^5\ M^{-1}\ cm^{-1}$ (Aust, 1985).

For GC-mass spectrometry measurements, the lipids were first converted to fatty acid methylesters (Van den Berg *et al.*, 1988). The fatty acid compositions were then determined using a GC-mass spectrometer (at the University of Illinois at Chicago) with a Supelco 2330 capillary column (Bellefonte, PA).

Heme Detection in Vesicles. In the heme assay, the heme or hemin was converted to porphyrin for fluorescence detection (Morrison, 1965; Shaklai *et al.*, 1985). A calibration curve was prepared using Hb solutions ranging from 0.31 μM to 3.13 μM in heme (0.005 to 0.05 mg/ml in Hb). Specifically, 50 μl of the standard Hb solution was added to 2 ml oxalic acid solution. The mixture was vortexed and incubated at 100 °C for 30 min. After cooling to room temperature, fluorescence intensity was measured using an excitation wavelength of 403 nm and an emission wavelength of 601 nm.

Hb (0.52 mg/ml) was mixed with BPS SUVs (4.2 mg/ml) and incubated at 37 °C for 2 h. The vesicles and Hb were then separated by gel filtration on a Sepharose 4B-CL (Pharmacia) column (41 cm x 1.5 cm) with a flow rate of 12 ml/h, similar to the method outlined by Szebeni *et al.* (1988). The vesicles eluted with the void volume. The Hb eluted about 3 h later, thus yielding a very clean separation of vesicles and Hb. The vesicle fractions were pooled and pelleted by centrifugation at 38,000 g for 90 min. The pellet was then taken up in a small volume of buffer (100 - 200 μl) and assayed for heme and lipid concentrations. Another portion of the Hb and vesicle mixture was loaded to the column immediately after mixing (t = 0) to serve as a control sample.

For the assay, 3 μl of Triton X-100 was added to a vesicle sample (25 μl) to solubilize the lipid, followed by 1 ml of oxalic acid solution for fluorescence measurements. It was found that if no Triton was added or if the Triton was added after the oxalic acid, a precipitate was formed causing light scattering.

Optical Measurements of Hb and Vesicle Mixtures. COHb was converted to oxyHb on ice under a flood light and O_2 atmosphere immediately before the experiment. Optical spectra were monitored from 500 to 700 nm to ensure complete conversion, and to ensure that there was no detectable oxidized Hb in the samples. Samples with detectable oxidized Hb were discarded. The concentration of Hb was adjusted to 17.5 ± 0.3 μM (1.12 ± 0.02 mg/ml) for most experiments. This cold oxyHb solution (120 μl) was introduced to a pre-warmed (37 ± 0.5 °C for about 5 min) solution of lipid vesicles (500 μl) of known concentration in the range from 0.25 mg/ml to 2.5 mg/ml for SUVs, or from 1 mg/ml to 14 mg/ml for LUVs, to give a final Hb concentration of 0.22 ± 0.02 mg/ml (3.4 ± 0.3 μM). Samples with higher final Hb concentrations, about 1.0 mg/ml and 7.0 mg/ml, were also used with SUVs (ranging from 1.25 mg/ml to 9 mg/ml) to give Lipid/Hb of 100 or 200 to study the potential Hb concentration effects. In the optical measurements, vesicle solutions with lipid concentrations the same as samples were used as blanks. The sample cuvettes (with 1 cm or 2 mm path lengths) were covered with parafilm, and maintained at 37 ± 0.5 °C. Spectra were collected from 500 to 700 nm every 2 min for 30 min. In experiments without lipid vesicles, buffer was used as a blank, and spectra were collected every 10 min for the first hour, and then periodically for 24 - 130 h, if necessary. In some experiments, COHb or oxygenated hemolysate was used instead of oxyHb.

Concentrations of Hb Species during Oxidation. In oxidized samples, oxyHb is oxidized to metHb, hemichrome, and choleglobin, following the definitions of Winterbourn (1985b). Thus the absorbance values at different wavelengths can be analyzed as a four-component (oxyHb, metHb, hemichrome and choleglobin) system at 560, 577, 630 and 700 nm to determine the concentrations of each Hb species in oxidized samples (Winterbourn, 1985a). The concentration of a component was set to zero if the analysis gave a negative value. The relative concentrations (percentages) for each component were then determined.

Rate Constant Determination. Rate constants for the disappearance of oxyHb or the appearance of oxidized Hb were obtained from linear regressions (Systat program, Systat Inc., Evanston, IL) of the linear portions of the logarithmic plots of percent Hb versus time.

II. POTENTIAL PROBLEMS IN OBTAINING KINETIC DATA FROM OPTICAL DATA

Spectral Baseline. The vesicle samples showed significant spectral absorption in the 500 to 700 nm region (Fig 2-S, Curve A) due to light scattering by vesicles. Thus vesicle solutions, critically matched in both lipid concentration and vesicle size were used as blanks for the oxidation experiments to compensate for light scattering induced baseline distortion. Since meta-stable vesicles fuse to give larger vesicles (Ohki, 1984), the spectra could still include signal from lipid vesicles as well as Hb species if the fusion process in both compartments were not the same. Analysis of Hb component concentrations from these spectra would then be subjected to systematic error. Our freeze-fracture electron micrograph (Fig 3-S) showed that, after incubation with oxyHb, the vesicles were substantially larger than those produced from spontaneous SUV fusion during the same time period (Fig 1A-S). Similar vesicle aggregation and fusion are observed in protein-liposome conjugates (Loughrey *et al.*, 1990) and BPS SUVs incubated with Ca^{++} (Wilschut *et al.*, 1981). Thus, a baseline rise was expected for a sample containing oxyHb and vesicle after 6 h incubation due to vesicle fusion and Hb oxidation, with the A_{700} reading increasing from 0.00 to about 0.06 (Fig 2-S, Curve C). The conversion of oxyHb to oxidized Hb species, especially choleglobin, also causes the baseline to increase (Winterbourn, 1985a; MacDonald and Charache, 1982). In the absence of lipid vesicles, an extensively oxidized Hb sample produced a readable A_{700} value, but the value was less than 0.01 (Fig 2-S, Curve B). Centrifugation (at 38,000 g for 10 min) of these extensively oxidized Hb samples did not change the absorbance readings. Thus we concluded that when $A_{700} > 0.01$, the vesicle fusion contribution to baseline was significant, and reliable Hb concentrations were not obtainable. It should be noted that this A_{700} cutoff value of 0.01 only applies to samples with total Hb concentrations of about 0.2 mg/ml.

Fig 1B in the main text indicates that, even for $t < 30$ min, a small increase in the baseline was observed for Hb samples containing SUVs, with A_{700} about 0.007. This could be interpreted as (a) SUV-induced formation of denatured Hb, including choleglobin, (b) Hb-induced vesicle fusion, or both (a) and (b). It is difficult to specifically delineate the cause of this slight increase in baseline at the beginning of the oxidation process. If the increase was due to Hb-induced vesicle fusion, the slight increase in baseline would give an overestimation of Hb concentration by about 3 - 4 %, since the maximum absorbance at 577 nm was about 0.20. As detailed below, our total Hb concentration determined from A_{577} agreed with the value determined by the cyano-met method, thus we believe that the slight increase in baseline observed in Fig 1B was due to either (a), or (a) and (b), but not due to (b) alone. Therefore the initial baseline increase may overestimate Hb concentration by about 3 % at most.

Under most of the conditions studied, oxidation appeared to proceed relatively faster than the process of induced vesicle fusion. Thus, during the time period to collect data for kinetic studies, A_{700} did not exceed 0.01, and reliable Hb concentrations can be obtained from the spectra. However, if oxidation proceeded slower than induced vesicle fusion, such as the case when hemolysate was added to SUVs, the A_{700} values would rise to above 0.01 before the entire linear portion of the data were collected (data not shown). The kinetic parameters for these systems could not be obtained with confidence.

Hb Concentration. Another potential problem comes from the Hb concentration analysis. The

sum of the concentrations of all Hb species, oxidized and not oxidized, obtained from spectral analysis should remain constant throughout the oxidation experiments. At the beginning of the experiment (t = 0), only one Hb component, namely the oxyHb, was present in the samples. The oxyHb concentrations determined from A_{577} for a set of samples with and without lipid vesicles were, for example, 0.211 and 0.194 mg/ml, respectively. The total Hb concentrations determined by the cyano-met method were 0.208 and 0.191 mg/ml, respectively. Thus for both samples with and without lipid vesicles at t = 0, the concentrations obtained by the A_{577} and the cyano-met method agreed to within 5 %.

At t > 0, the sum of the concentrations of Hb species obtained from two-component analysis, a method often used in autoxidation analysis (Winterbourn, 1985a), decreased from 0.208 mg/ml to 0.177 mg/ml, which represented a 16 % decrease, in samples containing SUVs. With four-component analysis, the sum of the concentrations of oxyHb, metHb, hemichrome and choleglobin remained constant, and agreed to within 5 % with the total Hb concentration determined by the cyano-met method. Thus inclusion of spectral contributions from hemichrome and choleglobin was necessary to accurately account for the relative concentration measurements of Hb species in solutions containing SUVs during oxidation.

These findings indicated that two-component analysis should not be used for these studies, due to significant amounts of hemichrome and choleglobin formation, but that the four-component analysis was adequate. Thus it was crucial to check the total Hb concentration to ensure that concentrations of the various Hb components in the samples were accurate.

Concentrations of Reduced and Oxidized Hb Species. With the spectra properly analyzed by the four-component method, the relative concentrations of various Hb components were obtained as a function of time. Fig 4-S shows the concentrations as a function of time in a typical sample with Hb and SUVs in PEN7.4. After incubation of Hb (0.19 mg/ml) with SUVs (2.1 mg/ml) at 37 °C for 30 min, less than 30 % oxyHb remained in solution. The majority of the Hb molecules had converted to metHb (about 40 %), hemichrome (about 20 %) and choleglobin (about 10 %). The concentrations of Hb species in the same buffer without SUVs are also shown. Only about 5 % of the Hb molecules oxidized during the same time period (30 min) in the samples without SUVs, yielding only low levels of metHb, hemichrome and choleglobin in samples without SUVs. These data also indicated that the time-dependent disappearance of oxyHb and the appearance of metHb, hemichrome and choleglobin were multiphasic. Thus the rate constants for the disappearance of oxyHb, or for the appearance of metHb, hemichrome or choleglobin provided a more informative description of the oxidation processes under different conditions.

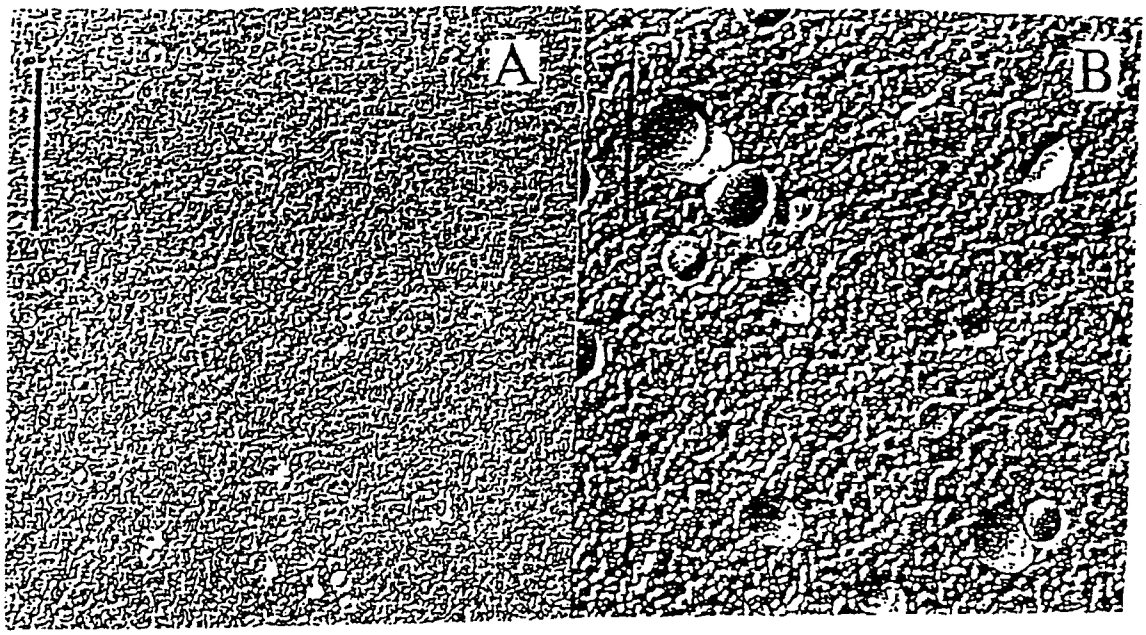

Fig 1-S: Freeze fracture electron micrographs of (A) BPS SUVs and (B) BPS LUVs. The scale bar is 200 nm. The SUVs were prepared by sonication and the LUVs were prepared by extrusion through a 100 nm polycarbonate filter in PEN7.4 buffer. The SUV diameters are about 10 - 30 nm. Some larger vesicles were also observed in SUV samples. The LUV diameters are about 100 - 130 nm. The micrographs were prepared, as a service, by Lipex (Vancouver, Canada).

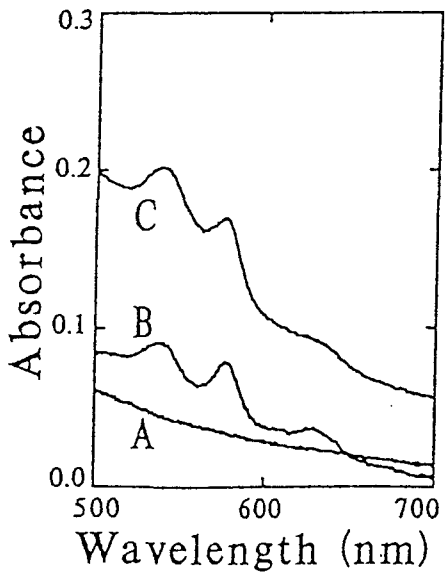

Fig 2-S: Spectra from 500 to 700 nm at 37 °C of (A) BPS SUVs (2.4 mg/ml) at t = 0; (B) Hb (0.21 mg/ml) at t = 4 days; (C) Hb (0.21 mg/ml) and BPS SUVs (2.0 mg/ml) mixture at t = 6 h. Buffer was used as blanks to obtain spectra in (A) and (B). BPS SUVs was used a blank for (C). PEN7.4 was the buffer in all samples.

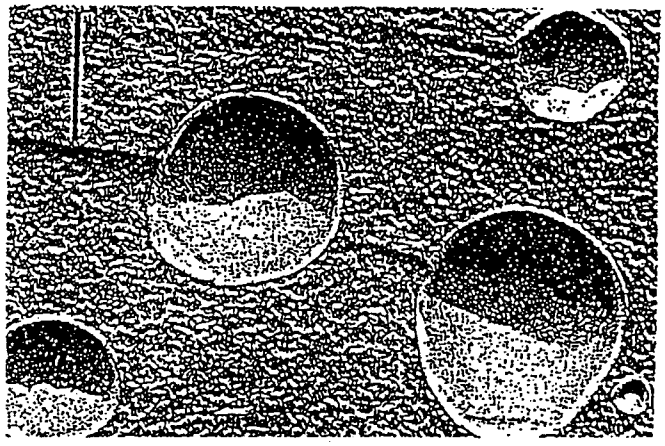

Fig 3-S: Freeze fracture electron micrograph of BPS LUVs (20 mg/ml) after incubation with Hb (0.21 mg/ml) overnight. The scale bar is 200 nm. Due to the presence of Hb, some of the LUVs with diameters about 100 - 130 nm fused to give very large vesicles.

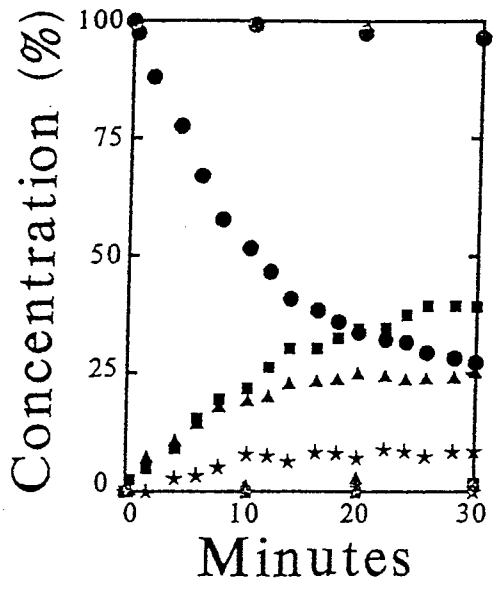

Fig 4-S: Comparison of oxyHb oxidation in the presence (filled symbols) and absence (shaded symbols) of BPS SUVs: % oxyHb (●), % metHb (■), % hemichrome (▲) and % choleglobin (★). OxyHb (0.19 mg/ml) was incubated at 37 °C in the presence of BPS SUVs (2.1 mg/ml) in PEN7.4 buffer. Spectra were collected every 2 min in the presence of BPS SUVs and every 10 min in the absence of BPS SUVs. The concentrations of Hb components were analyzed by a four-component analysis method, as discussed in text.

VITA

The author, Cynthia Carder LaBrake, was born on March 20, 1965 in Parkersburg, West Virginia. In August 1983 she entered West Virginia University and received a Bachelor of Science degree with honor's in Chemistry in May, 1987. Ms. LaBrake gained valuable industrial experience working the summers during her undergraduate tenure at Borg Warner Chemicals (Morgantown and Washington, WV facilities) as a research assistant. Following her marriage in the fall of 1987, she moved to Chicago to pursue her doctorate in Biophysical Chemistry at Loyola University of Chicago under the direction of Professor Leslie W.-M. Fung. She was supported with a teaching assistantship in 1988 and a research assistantship until the summer of 1991. In the fall of 1991 she received an Arthur J. Shmidt Fellowhip allowing her to complete her doctoral dissertation in June 1992.

Ms. LaBrake served the Chemistry Department at Loyola University of Chicago in the capacity of Secretary and President of the Graduate Student Organization in the academic years 1988/89 and 1989/90, respectively. She has also participated in several University sponsored research forums and won first prize for a Poster Presentation at the Sigma Xi 21st Annual Graduate Student Forum of Loyola University in May, 1991. Ms. LaBrake is a participating member of the Biophysical Society and has presented her research in the form of a poster at the annual meetings in 1990, 1991 and 1992. The author's formal publications include "Dynamic Light Scattering Investigations of Human Erythrocyte Spectrin" by Donna M. Budzynski, Albert S. Benight, Cynthia C. LaBrake and Leslie W.-M. Fung (1992) Biochemistry 31, 3653-3660 and "Phospholipid Vesicles Promote Human Hemoglobin Oxidation" by Cynthia C. LaBrake and Leslie W.-M. Fung (1992) The Journal of Biological Chemistry in press.

APPROVAL SHEET

The dissertation submitted by Cynthia LaBrake has been read and approved by the following committee:

Dr. Leslie W.-M. Fung, Director
Professor, Chemistry, Loyola

Dr. Daniel Graham
Assistant Professor, Chemistry, Loyola

Dr. Albert J. Rotermund
Associate Professor, Biology, Loyola

Dr. Patrick Henry
Professor, Chemistry, Loyola

Dr. Timothy Keiderling
Professor, Chemistry, University of Illinois, Chicago Campus

The final copies have been examined by the director of the dissertation and the signature which appears below verifies the fact that any necessary changes have been incorporated and that the dissertation is now given final approval by the Committee with reference to content and form.

This dissertation is therefore accepted in partial fulfillment of the requirements for the degree of Doctor of Philosophy.

June 30, 1992
Date

Director's Signature